Universidade Federal de Minas Gerais

Instituto de Ciências Biológicas

Departamento de Bioquímica e Imunologia

SEYI ELIJAH ELASORU

BIOPHYSICAL AND PHARMACOLOGICAL EVALUATION OF PROTECTIVE POTENTIALS OF ANDROGRAPHOLIDE AGAINST ISOPROTERENOL-INDUCED MYOCARDIAL INFARCTION IN RATS.

Belo Horizonte – MG

2021

SEYI ELIJAH ELASORU

BIOPHYSICAL AND PHARMACOLOGICAL EVALUATION OF PROTECTIVE POTENTIALS OF ANDROGRAPHOLIDE AGAINST ISOPROTERENOL-INDUCED MYOCARDIAL INFARCTION IN RATS.

Tese apresentada como parte dos requisitos para obtenção do título de Doctor em Bioquímica e Imunologia - Programa de Pós-graduação em Bioquímica e Imunologia da Universidade Federal de Minas Gerais.

Orientador: Prof. Dr. Jader dos Santos Cruz

Belo Horizonte – MG

2021

043 Elasoru, Seyi Elijah.
Biophysical and pharmacological evaluation of protective potentials of andrographolide against isoproterenol-induced myocardial infarction in rats. [manuscrito] / Seyi Elijah Elasoru. – 2021.
142 f. : il. ; 29,5 cm.

Orientador: Prof. Dr. Jader dos Santos Cruz.
Tese (doutorado) – Universidade Federal de Minas Gerais, Instituto de Ciências Biológicas. Programa de Pós-Graduação em Bioquímica e Imunologia.

1. Bioquímica e imunologia. 2. Infarto do Miocárdio. 3. Andrographis. I. Cruz, Jader dos Santos. II. Universidade Federal de Minas Gerais. Instituto de Ciências Biológicas. III. Título.

CDU: 577.1

Ficha catalografica elaborada por Fabiane C M Reis - CRB 6 2680

Universidade Federal de Minas Gerais
Curso de Pós-Graduação em Bioquímica e Imunologia ICB/UFMG
Av. Antônio Carlos, 6627 – Pampulha
31270-901 – Belo Horizonte – MG
e-mail: pg-biq@icb.ufmg.br (31)3409-2615

ATA DA DEFESA DA TESE DE DOUTORADO DE SEYI ELIJAH ELASORU. Aos dezoito dias do mês de março de 2021 às 14:00 horas, reuniu-se de forma "*on line*" na plataforma "*meet.google.com*" no Instituto de Ciências Biológicas da Universidade Federal de Minas Gerais, a Comissão Examinadora da tese de Doutorado, indicada "*ad referendum*" do Colegiado do Curso, para julgar, em exame final, o trabalho intitulado "*Biophysical And Pharmacological Evaluation Of Protective Potentials Of Andrographolide Against Isoproterenol-induced Myocardial Infarction In Rats*", requisito final para a obtenção do grau de Doutor em Ciências: Bioquímica. Abrindo a sessão, o Presidente da Comissão, Prof. Jader dos Santos Cruz, da Universidade Federal de Minas Gerais, após dar a conhecer aos presentes o teor das Normas Regulamentares do Trabalho Final, passou a palavra ao candidato para apresentação de seu trabalho. Seguiu-se a arguição pelos examinadores, com a respectiva defesa do candidato. Logo após a Comissão se reuniu, sem a presença do candidato e do público, para julgamento e expedição do resultado final. Foram atribuídas as seguintes indicações: Dr. Diego Santos de Souza (*University of Arizona*), aprovado; Dra. Liza Figueiredo Felicori Vilela (Universidade Federal de Minas Gerais), aprovado; Dra. Marília Martins Melo (Universidade Federal de Minas Gerais), aprovado; Dra. Darizy Flávia Silva Amorim de Vasconcelos (Universidade Federal da Bahia), aprovado; Dr. Jader dos Santos Cruz - Orientador (Universidade Federal de Minas Gerais), aprovado. Pelas indicações o candidato foi considerado:

(X) APROVADO
( ) REPROVADO

O resultado final foi comunicado publicamente ao candidato pelo Presidente da Comissão. Nada mais havendo a tratar, o Presidente da Comissão encerrou a reunião e lavrou a presente Ata que será assinada por todos os membros participantes da Comissão Examinadora. Belo Horizonte, 18 de março de 2021.

Dr. Diego Santos de Souza (University of Arizona)

Dra. Liza Figueiredo Felicori Vilela (UFMG)

Dra. Marília Martins Melo (UFMG)

Dra. Darizy Flávia Silva Amorim de Vasconcelos (Universidade Federal da Bahia)

Dr. Jader dos Santos Cruz - Orientador (UFMG)

DEDICATION

This research is dedicated to the helper of the helpless, the almighty God.

Also, to my beloved mother, Abigael Modupe Abike Eki (Onilegogoro). History will be kind to you that you supported me to the very pinnacle of academic qualification.

ACKNOWLEDGMENT

I am grateful to the Federal Republic of Brazil and my financiers, Coordenação de Aperfeiçoamento de Pessoal de Nível Superior (CAPES) and Conselho Nacional de Desenvolvimento Científico e Tecnológico (CNPq) for giving me the opportunity to advance my knowledge in the country.

I am indebted to my advisor, Prof. Dr. Jader dos Santos Cruz for his patience, guidance and unwavering support over these years. Also, I am grateful to his wife, Andrea for all the assistance she offered towards my documentation in the Federal data base when I arrived in Brazil.

I am as well thankful to Prof. Leda Quercia Vieira. As the chair of the graduate program in Biochemistry and Immunology, her compassion and love for international students from developing countries gave me the privilege of enrolling in the program.

Many thanks to all the staffs of the Department of Biochemistry and Immunology, UFMG, for their assistance and for the knowledge impacted on me during this period of four years.

To all my colleagues in Laboratory of Excitable Membranes and Cardiovascular Biology (LAMEX), words cannot describe how much I valued your assistance. Long live the spirit of LAMEX! We are simply the best.

Also, I will like to appreciate Prof. Marilia Martins Melo of the Department of Veterinary Clinic and Surgery for her assistance and collaborations.

I wish to place on record my appreciation to Mr Ashaolu Olalekan (Ashy) and Dr Ifeloju Folarin-Jonah. You guys are my angels.

Likewise, the contributions of my brothers, sisters, in-laws, friends and lecturers in Nigeria towards this journey of success are highly appreciated.

Most importantly, my appreciation goes to my wonderful wife, Taiwo Adebola and my beloved son, Gospel Campaigner for their sacrifices over the years. This success belongs to both of you.

ABSTRACT

Myocardial infarction (MI) is the irreversible injury of the myocardium caused by prolonged myocardial ischemia and is a major cause of heart failure and eventual death among ischemic patients. The current trend of mortality due to MI and shortcomings of available therapeutics informed the need for an alternative remedy that could make the heart more resistant to infarction. Andrographolide is the principal compound in *Andrographis paniculata,* an indigenous plant commonly included in herbal concoction indicated for cardiovascular diseases and chest pains. Therefore, the present study assessed the protective potentials of andrographolide against isoproterenol-induced myocardial infarction in rats. Animals were randomly divided into four groups: Control (Ctr) group received 0.9 % saline solution once daily for 21 days, Isoproterenol (Iso) group received 0.9 % saline solution once daily for 19 days followed by 80 mg/kg/day of isoproterenol hydrochloride solution on day 20 and 21, Andrographolide (Andro) group received 20 mg/kg/day of andrographolide for 21 days, and Andrographolide plus Isoproterenol (Andro + Iso) group received 20 mg/kg/day of andrographolide for 21 days with co-administration of 80 mg/kg/day of isoproterenol hydrochloride solution on day 20 and 21. At the end of all treatments, cardiac-specific parameters that define cardiac health and MI were evaluated in all groups. Likewise, the mechanical and electrical profiles that shapes the functions of the heart were assessed in cardiomyocytes isolated from each group using standard assay methods. In addition, effects of Andro on these mechanical and electrical profiles were further substantiated with *in-vitro* tests and compared to standard drug of MI. Iso caused: ST-segment elevation and significant ($p<0.05$) increases in heart rate, QRS, QT & QTc interval; significant ($p<0.05$) increases in cardiac mass indexes; significant ($p<0.05$) increases in systemic troponin I (cTnI), creatine kinase (CK), creatine kinase-MB fraction (CK-MB), aspartate transaminase (AST) & leukocyte levels; significant ($p<0.05$) increase of infarct size; cardiac histological alterations; significant ($p<0.05$) increases in myocytes shortening, maximal velocity of contraction (+dL/dt) & maximal velocity of relaxation (-dL/dt); significant ($p<0.05$) prolongation of action potential duration (APD); significant ($p<0.05$) increase in L-type calcium current ($I_{Ca,L}$) density and significant ($p<0.05$) decrease in transient outward potassium current (I_{to}) density typical of the onset of MI. Interestingly, pretreatment with Andro prevented and / or minimized these anomalies, notably, by reducing myocyte shortening, +dL/dt, -dL/dt, APD,

$I_{Ca,L}$ density and increasing I_{to} density significantly ($p<0.05$). Furthermore, *in-vitro* results supported the *in-vivo* effects of Andro on myocyte shortening, +dL/dt, -dL/dt, APD, $I_{Ca,L}$ density, and I_{to} density and indicated that the effects are concentration-dependent. Therefore, andrographolide could be seen as a promising therapeutic agent capable of making the heart resistant to infarction and it could be used as template for the development of semisynthetic drug(s) for cardiac protection against MI.

Keywords: Myocardial infarction, Andrographolide, Cardiac protection, Calcium current, Potassium current.

RESUMO

O infarto do miocárdio (IM) é a lesão irreversível do miocárdio causada por isquemia miocárdica prolongada e é uma das principais causas de insuficiência cardíaca e eventual morte entre pacientes isquêmicos. A tendência atual de mortalidade por IM e a deficiência da terapêutica disponível informaram a necessidade de um remédio alternativo que pudesse tornar o coração mais resistente ao infarto. Andrographolide é o principal composto da *Andrographis paniculata*, uma planta indígena comumente incluída na mistura de ervas indicada para doenças cardiovasculares e dores no peito. Portanto, o presente estudo avaliou o potencial protetor do andrographolide contra o infarto do miocárdio induzido por isoproterenol em ratos. Os animais foram divididos aleatoriamente em quatro grupos: o grupo controle (Ctr) recebeu solução salina 0,9% uma vez ao dia por 21 dias, o grupo isoproterenol (Iso) recebeu solução salina 0,9% uma vez ao dia por 19 dias seguido por 80 mg/kg/dia de cloridrato de isoproterenol solução nos dias 20 e 21, o grupo Andrographolide (Andro) recebeu 20 mg/kg/dia de andrographolide por 21 dias, e o grupo Andrographolide mais Isoproterenol (Andro + Iso) recebeu 20 mg/kg/dia de andrographolide por 21 dias com co-administração de 80 mg/kg/dia de solução de cloridrato de isoproterenol nos dias 20 e 21. No final de todos os tratamentos, parâmetros específicos do coração que definem a saúde cardíaca e IM foram avaliados em todos os grupos. Da mesma forma, os perfis mecânico e elétrico que moldam as funções do coração foram avaliados em cardiomiócitos isolados de cada grupo usando métodos de ensaio padrão. Além disso, os efeitos do Andro nesses perfis mecânicos e elétricos foram comprovados com testes *in-vitro* e comparados com a droga padrão de IM. Iso causou: elevação do segmento ST e aumentos significativos ($p<0,05$) na frequência cardíaca, intervalo QRS, QT e QTc; aumentos significativos ($p<0,05$) nos índices de massa cardíaca; aumentos significativos ($p<0,05$) na troponina I (cTnI), creatina quinase (CK), fração de creatina quinase-MB (CK-MB), aspartato transaminase (AST) e níveis de leucócitos; aumento significativo ($p<0,05$) do tamanho do infarto; alterações histológicas cardíacas; aumentos significativos ($p<0,05$) no encurtamento dos miócitos, velocidade máxima de contração (+dL/dt) e velocidade máxima de relaxamento (-dL/dt); prolongamento significativo ($p<0,05$) da duração do potencial de ação (DPA); aumento significativo ($p<0,05$) na densidade da corrente de cálcio tipo L ($I_{Ca,L}$) e diminuição significativa ($p<0,05$) na densidade da corrente de potássio externa transitória (I_{to}) típica do início do IM.

Curiosamente, o pré-tratamento com Andro evitou e / ou minimizou essas anomalias, notavelmente, reduzindo o encurtamento do miócito, +dL/dt, -dL/dt, DPA, densidade de $I_{Ca,L}$, e aumentando a densidade de I_{to} significativamente ($p<0,05$). Além disso, os resultados *in-vitro* apoiaram os efeitos *in-vivo* de Andro no encurtamento do miócito, +dL/dt, -dL/dt, DPA, densidade de $I_{Ca,L}$, e densidade de I_{to} e indicaram que os efeitos são dependentes da concentração. Portanto, o andrographolide pode ser visto como um agente terapêutico promissor capaz de tornar o coração resistente ao infarto e pode ser usado como modelo para o desenvolvimento de fármacos semissintéticos para proteção cardíaca contra IM.

Palavras-chave: Infarto do miocárdio, Andrographolide, Proteção cardíaca, Corrente de cálcio, Corrente de potássio.

LIST OF FIGURES

LIST OF ABBREVIATIONS

$[Ca^{2+}]i$	Intracellular Ca^{2+} concentration
+dL/dt	Maximal velocity of contraction
AAR	Area at risk
ACE	Angiotensin converting enzyme
AF	Atrial fibrillation
Andro + Iso	Andrographolide plus Isoproterenol
Andro	Andrographolide
ANOVA	Analysis of variance
AP	Action potential
APD	Action potential duration
ARF	Acute rheumatic fever
ASD	Atrial septal defect
AST	Aspartate transaminase
AVSDs	Atrioventricular septal defects
BMI	Body mass index
BW	Body weight
CABG	Coronary artery bypass grafting
CHD	Coronary heart disease
CHF	Chronic heart failure
CIB	Cell Isolation Buffer
CICR	Calcium-induced calcium release
CK	Creatine kinase
CK-MB	Creatine kinase - MB fraction
CNS	Central nervous system
cTnI	Cardiac troponin I
cTnT	Cardiac troponin T

Ctr	Control
CVDs	Cardiovascular diseases
-dL/dt	Maximal velocity of relaxation
DM	Diabetes mellitus
DORV	Double outlet right ventricle
DVT	Deep vein thrombosis
ECG	Electrocardiography
G_{max}	Maximal conductance
GPx	Glutathione peroxidase
GSH	Reduced glutathione
HF	Heart failure
HR	Heart rate
HW	Heart weight
$I_{Ca,L}$	L-type Ca^{2+} current
IHD	Ischemic heart disease
I_{Kr}	Rapidly activating delayed outward rectifying K^+ currents
I_{Ks}	Slowly activating delayed outward rectifying K^+ currents
I_{Kur}	Ultra-rapidly activating delayed outward rectifying K^+ currents
Iso	Isoproterenol
I_{to}	Transient outward K^+ current
LBBB	Left bundle branch block
LDH	Lactate dehydrogenase
LDL	Low-density lipoprotein
LVEF	Left ventricular ejection fraction
MDA	Malondialdehyde
MI	Myocardial infarction
MTD	Maximum tolerated dose

NCX	Na^{+}/Ca^{2+} exchanger
Nicard	Nicardipine
PAD	Peripheral arterial disease
PAF	Platelet-activating factor
PBS	Phosphate-buffered saline
PCI	Percutaneous coronary intervention
PE	Pulmonary embolism
PTA	Persistent truncus arteriosus
PVD	Peripheral vascular disease
RBC	Erythrocytes
RHD	Rheumatic heart disease
RyR	Ryanodine receptors
SEM	Standard Error of Mean
SERCA	SR Ca^{2+}-ATPase
SOD	Superoxide dismutase
SR	Sarcoplasmic reticulum
TGA	Transposition of the great arteries
TIA	Transient ischemic attack
TL	Tibia length
TOF	Tetralogy of fallot
TP	Total protein
TTC	Triphenyltetrazolium chloride
VSD	Ventricular septal defect
VTE	Venous thromboembolism
WBC	Leukocytes

SUMMARY

IV. MATERIALS AND METHODS

V. RESULTS

I. INTRODUCTION

Cardiovascular disease is a major cause of disability and premature death throughout the world, and contributes substantially to the escalating costs of health care. It represents a single family of diseases, linked by a common pathology of atherosclerosis with common risk factors, which develops over many years and is usually advanced by the time symptoms occur. The treatment of established cardiovascular disease is generally very expensive. Hence, prevention of cardiovascular disease is a rapidly evolving area.

Globally, ischemic heart disease has become the leading contributor to the burden of cardiovascular disease. Approximately half of all cardiovascular deaths were due to myocardial infarction (MI), an acute necrosis of the myocardium resulting from prolonged ischemia. Acute myocardial infarction (AMI) mostly occur suddenly, and are often fatal before medical care can be given. The high risk of morbidity and mortality following an episode of MI underlies the importance of instituting effective preventive regimens as part of the overall mitigation against MI occurrence and severity. Several interventions including, antiplatelet drugs, β-blockers, angiotensin-converting enzyme (ACE) inhibitors and lipid lowering drugs have been shown in clinical trials to reduce total and cardiovascular mortality in patients with coronary heart disease. Nevertheless, some of these interventions have been proven not to be suitable in some individuals for various reasons, such as co-morbidity, contraindications for some drugs and side effects.

Consequently, alternative remedies using bioactive constituents of plants are now gaining research interest as they are often considered effective and safer. One of such plants with suspected prospective anti-infarction bioactive constituents is *Andrographis paniculata* (Burm. f.) Wall. ex Nees, due to its ethnobotanical use as ingredient of herbal formulations indicated for chest pain and cardiovascular diseases. Here, andrographolide, a labdane diterpene lactone and the principal bioactive natural product isolated from the plant *Andrographis paniculata* (Burm. f.) Wall. ex Nees is evaluated for its protective potentials against experimental induced myocardial infarction in rats.

II. LITERATURE REVIEW

2.1 CARDIOVASCULAR PHYSIOLOGY

2.1.1 The Heart

The heart is a muscular organ about the size of a closed fist that functions as the body's circulatory pump. The heart lies in the center of the thoracic cavity and is suspended by its attachment to the great vessels within a fibrous sac known as the pericardium. A small amount of fluid is present within the sac (pericardial/serous fluid) which lubricates the surface of the heart and allows it to move freely during contraction and relaxation (Fig. 2.1). The human heart beats approximately 72 times per minute. It takes in deoxygenated blood through the veins and delivers it to the lungs for oxygenation before pumping it into the various arteries, which provide oxygen and nutrients to body tissues by transporting the blood throughout the body (Weinhaus and Roberts, 2009).

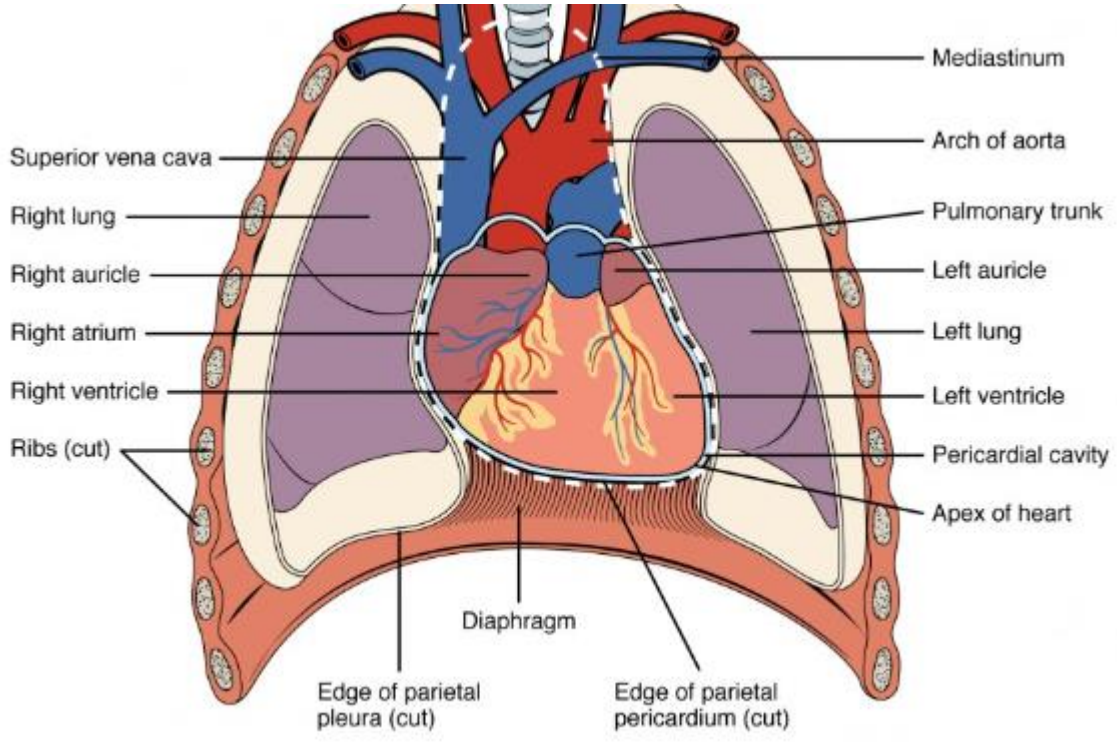

Figure 2.1. Pictorial Description of the Heart. The figure illustrates the architectural position, shape and size of the heart (Lumen Learning, 2021).

2.1.2 Structure and Function of the Heart

At the organ level, the heart is made up of four chambers: left atrium, right atrium, left ventricle, and right ventricle (Fig. 2.2). The upper two chambers (atria) are divided by a wall-like structure known as interatrial septum, while the lower two chambers (ventricles) are divided by a similar structure called the interventricular septum. Deoxygenated blood enters the heart through the right atrium from where the blood moves into the right ventricle first and then to the lungs through the pulmonary artery. The left atrium receives oxygenated blood from the lungs, which is then pumped into the left ventricle from where it moves into the aorta and then to the different parts of the body (Mesotten et al., 1998).

Likewise, the heart is made up of four important valves with primary function of regulating the blood flow through the heart (Fig. 2.2). These valves allow blood flow in one direction only. Tricuspid valve is located between the right ventricle of the heart and the right atrium, and allows the blood to move from the right atrium to the right ventricle. The pulmonary (semilunar) valve is between the pulmonary artery of the heart and its right ventricle. It opens up when the right ventricle contracts and allows the blood to move into the pulmonary artery. Mitral or bicuspid valve is located in a way that it causes a separation between the left ventricle of the heart and the left atrium of the heart. It pumps oxygenated blood into the left ventricle when the left atrium contracts. The aortic (semilunar) valve separates the aorta from the left ventricle and regulate the flow of blood from the ventricle to the rest of the body (Hinton and Yutzey, 2011).

Also, the heart consists of blood vessels which help transport blood to and from it. These vessels connect other organs in the body to the heart. The basic function of these vessels is to take deoxygenated blood from different organs, supply it to the heart, and then take oxygenated blood that comes from the lungs to the heart and to the rest of the body. The blood vessels of the heart are broadly classified into two: arteries and veins (Fig. 2.2). The arteries are quite tough on the outside but are smooth on the inside. There are three types of arteries in the heart: the aorta, the coronary artery and the pulmonary artery. The aorta is the main artery of the heart and help transports oxygenated blood to the rest of the body, the coronary arteries are attached to the heart and help transfer oxygen-rich blood to the heart muscles, while the pulmonary arteries are the only artery that takes deoxygenated blood from

the right side of the heart to the lungs. On the other hand, the veins are not as tough as the arteries because they don't transport blood at high pressure. The veins of the heart are also classified into three. The venae cavae takes deoxygenated blood from the rest of the body back to the heart, the cardiac veins receive deoxygenated blood from the myocardium and transfers it to the right atrium and the pulmonary veins transfer oxygenated blood from the lungs to the left side of the heart (Mesotten et al., 1998).

At the tissue level, the wall of the heart is made up of three different layers: pericardium, myocardium, and endocardium (Fig. 2.2). The pericardium is the sac that protects the heart from the outside. It is made up of four distinct layers (fibrous pericardium, serous pericardium, the space and epicardium) (Arackal and Alsayouri, 2020). The myocardium is a thicker layer right beneath the epicardium. This muscular middle layer of the heart wall contains cardiac muscle tissue. Most of the thickness and mass of the heart wall is made up of the myocardium. This layer is part of the heart that pumps blood through the body. The endocardium is a thin layer under the myocardium. This layer lines the inside of the heart and is usually very smooth. The main role of this smooth, thin layer is to prevent the blood from sticking into the sides of the heart and it also helps prevent the formation of deadly blood clots (Tran et al., 2020).

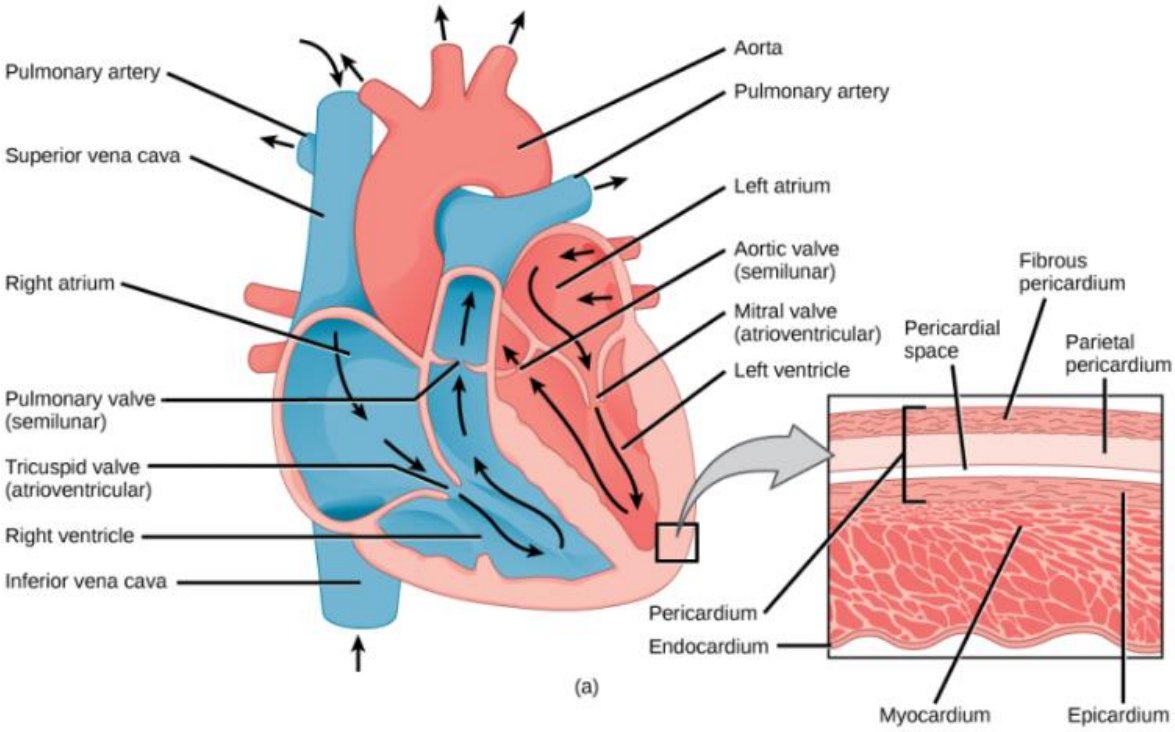

Figure 2.2. The Heart Structure. The figure shows the cardiac chambers, valves, arteries, veins and the heart wall (Molnar and Gair, 2015).

At the cellular level, the heart composed of several cell types that include smooth muscle cells, fibroblasts, and cardiomyocytes. Among all, cardiomyocytes are the fundamental contractile cell of the heart (Walker and Spinale, 1999). They possess unique structures and properties correlating to their contractile function. More importantly, they are striated, mostly uninucleate muscle cells and found exclusively in the heart muscle (Tran et al., 2020). A unique cellular and physiological feature of cardiomyocytes are intercalated discs, which contain three types of special structures (cell adhesions) including, fascia adherens, desmosomes, and gap junctions. The fascia adherens are bands of proteins that connect the actin filaments of the sarcomeres in each cardiac muscle fiber to the sarcomere in the neighboring cells, producing a single unified chain of sarcomeres. Desmosomes help to bind cardiac muscle cells together, but form smaller, tighter junctions compared to the fascia adherens. Intermediate fibers inside each muscle fiber are connected by a series of proteins in the desmosome, which form an interlocking protein chain. Finally, gap junctions serve as strong mechanical linkage between myocytes to facilitate cell-cell communication. Each gap junction is made of connexin proteins

that form a tunnel through the cell membranes of the cardiac muscle cells, allowing small molecules, including ions, to pass through (Fig. 2.3). These discs reduce internal resistance and allow action potentials to spread quickly throughout the entire heart muscle via the passage of charged ions (Walker and Spinale, 1999). Thus, cardiomyocytes within the heart contracts in unison in order to provide effective pump action that can ensure adequate blood perfusion of the various organs and tissues (Woodcock and Matkovich, 2005).

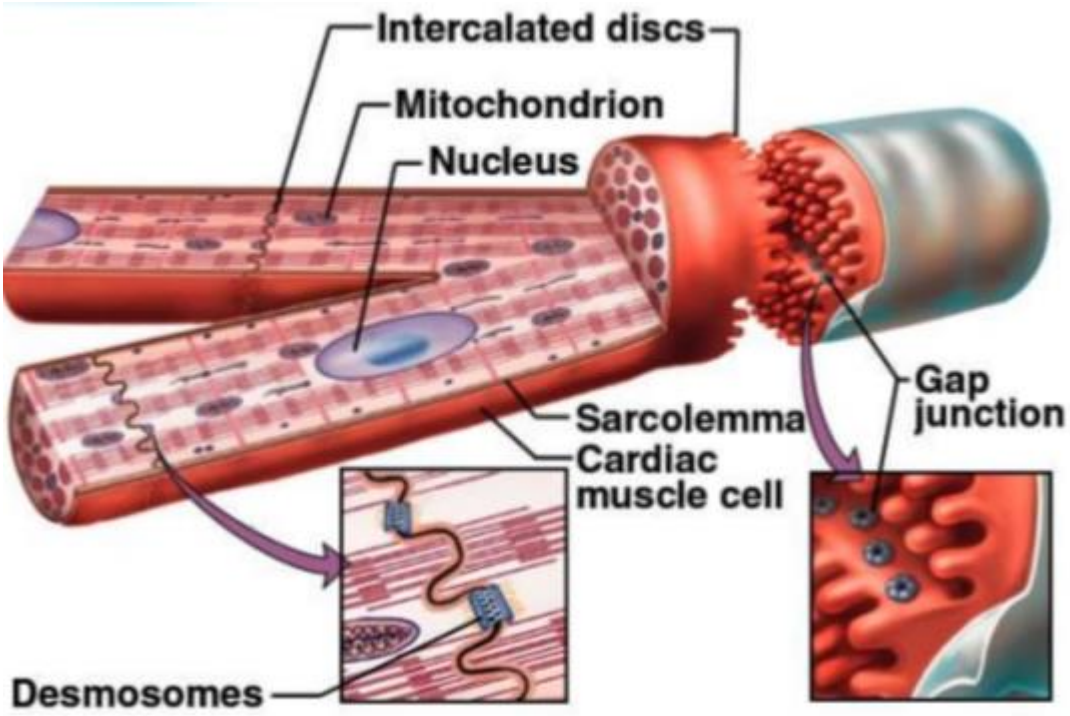

Figure 2.3. The Structure of Cardiomyocyte. The figure shows unique features of cardiac myocytes (Sadasivam, 2016).

2.1.3 Myocardial Excitability

The heart has an intrinsic system whereby the muscle is stimulated to contract without the need for nerve supply from the brain. This autonomous beating of cardiac muscle cells is regulated by the heart's internal pacemaker that uses electrical signals to time the beating of the heart (Fig. 2.4). The electrical signals and the resultant mechanical actions are intimately intertwined. The internal pacemaker begins at the sinoatrial node, a small mass of specialized

cells which lies in the wall of the right atrium near the opening of the superior vena cava. The impulses of contraction initiated by the sinoatrial node stimulate the myocardium of the atria to contract. This wave of contraction stimulates the atrioventricular node to produce impulses that pass to the apex of the heart through the Purkinje fibers before being transmitted to the ventricular muscle. In this way the ventricular contraction begins at the apex of the heart and blood is forced into the pulmonary artery and the aorta that leave the heart near its base (Mesotten et al., 1998).

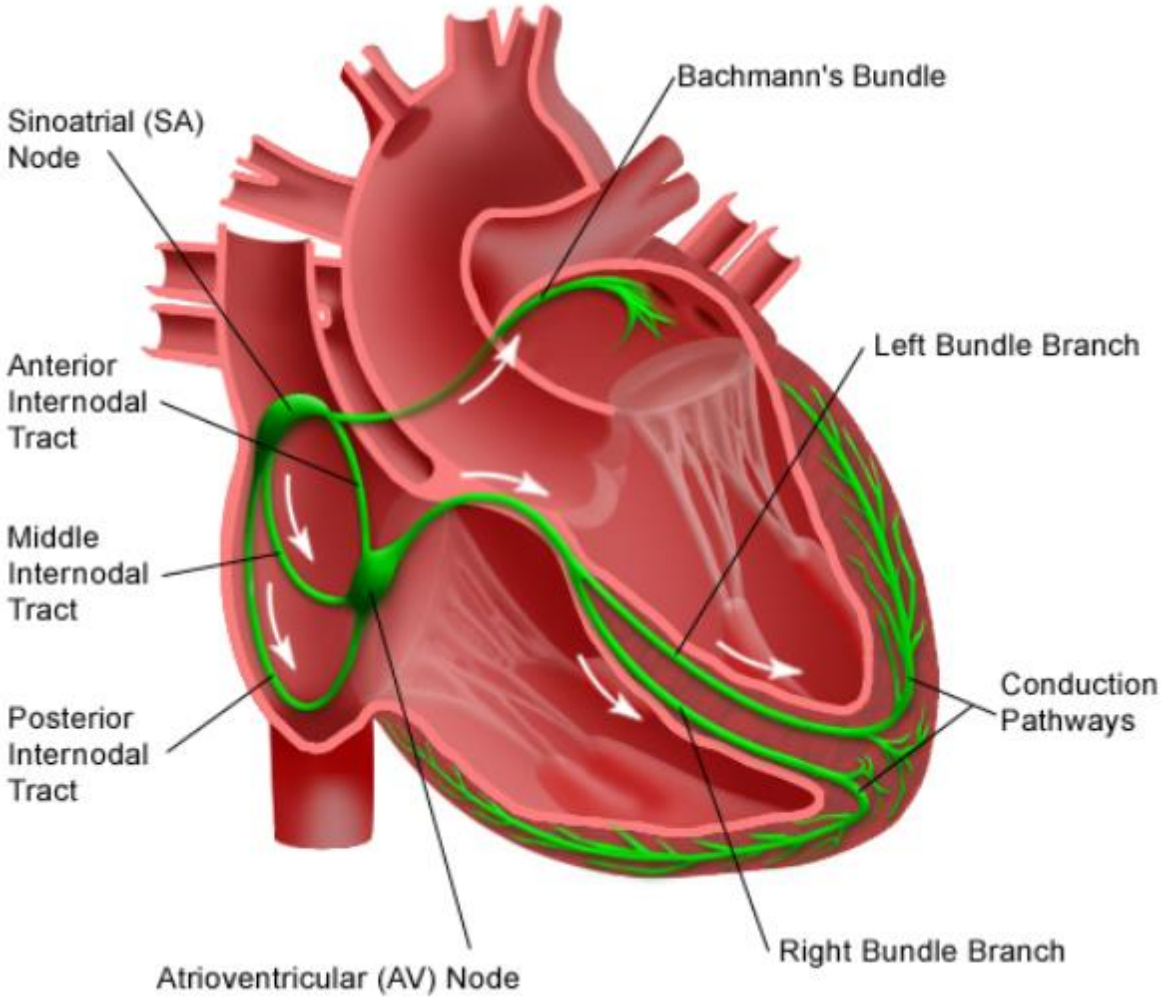

Figure 2.4. The Heart Conduction System. The figure illustrates the pathway of impulse generation and impulse conduction system of the heart (mdmedicine, 2011).

2.1.4 Cardiac Ion Channels and Action Potentials

Ion channels are viewed as narrow, water-filled, macromolecular pores permeable to certain specific ions (Hille, 2001). Cardiac ion channels have two fundamental properties, ion permeation and gating. Ion permeation describes the movement ionic current through the open channel. The selective permeability of ion channels to specific ions is the basis of classification of ion channels, e.g. (as Na^+, K^+, and Ca^{2+} channels). Gating is the mechanism of opening and closing of ion channels and is their second major property. Ion channels are also subclassified by their mechanism of gating: voltage-dependent, ligand-dependent, and mechano-sensitive gating. Among these, voltage-dependent gating is the commonest observed in cardiac myocytes, as majority of ion channels open in response to depolarization (Grant, 2009).

Functionally, ion channels reduce the activation energy required for ion movement across the lipophilic cell membrane (Grant, 2009) and help maintain ionic concentration gradients and charge differentials between the inside and outside of the cardiomyocytes (Amin et al., 2010). Essentially, in cardiac myocytes, ions are distributed in such a way that there is a higher concentration of potassium (K^+) on the inside of cells than outside, and a higher concentration of sodium (Na^+) outside cells than on the inside. The combination of these ionic concentration differences and selective permeability of the membrane brings about generation of voltage - a measure of electrical energy that has the potential to do work. In other words, membrane potential (V_m) is the voltage measured when the inside of a cell is compared to the outside (Egri and Ruben, 2012).

The electrical stimulation created by a sequence of ion fluxes through ion channels in membrane of cardiomyocytes that leads to cardiac contraction is known as Action Potential (Nerbonne and Kass, 2005). That is, action potential generation and propagation occurs through, and is regulated by, the function of voltage-gated ion channels (Egri and Ruben, 2012). Action potential in typical cardiomyocytes is composed of 5 phases (0-4), beginning and ending with phase 4 (Fig. 2.5A). Phase 4 or the resting state is generally attributed with stable and negative resting membrane potential (-85 mV to -90 mV) in normal working myocardial cells due to the high conductance for K^+ of the I_{K1} channels. Phase 0 is the phase of rapid depolarization. During this phase, membrane potential shifts to the positive voltage

range due to activation of voltage-gated Na^+ channels which permit an inward Na^+ current (I_{Na}). In addition, this phase is central to the rapid propagation of the cardiac impulse. Phase 1 is the phase of early repolarization, accomplished by the transient outward K^+ current (I_{to}). This phase sets the potential for the next phase of the action potential. Phase 2 or plateau phase, is the longest phase. This phase marks the phase of calcium entry into the cell and represents a balance between the depolarizing L-type inward Ca^{2+} current ($I_{Ca,L}$) and the repolarizing ultra-rapidly (I_{Kur}), rapidly (I_{Kr}), and slowly (I_{Ks}) activating delayed outward rectifying currents. Phase 3 is the phase of rapid repolarization that restores the membrane potential to its resting value. It reflects the predominance of the delayed outward rectifying currents after inactivation of the L-type Ca^{2+} channels. Final repolarization during phase 3 is due to K^+ efflux through the I_{K1} channels (Amin et al., 2010; Grant, 2009; Hoffman and Cranefield, 1960; Nerbonne and Kass, 2005). In addition, the sum durations of all of these phases gives the overall duration of a particular action potential. Technically, this duration can also be captured on the ECG (Fig. 2.5B). For instance, the average duration of a ventricular action potential is reflected in the QT interval on the ECG (Grant, 2009).

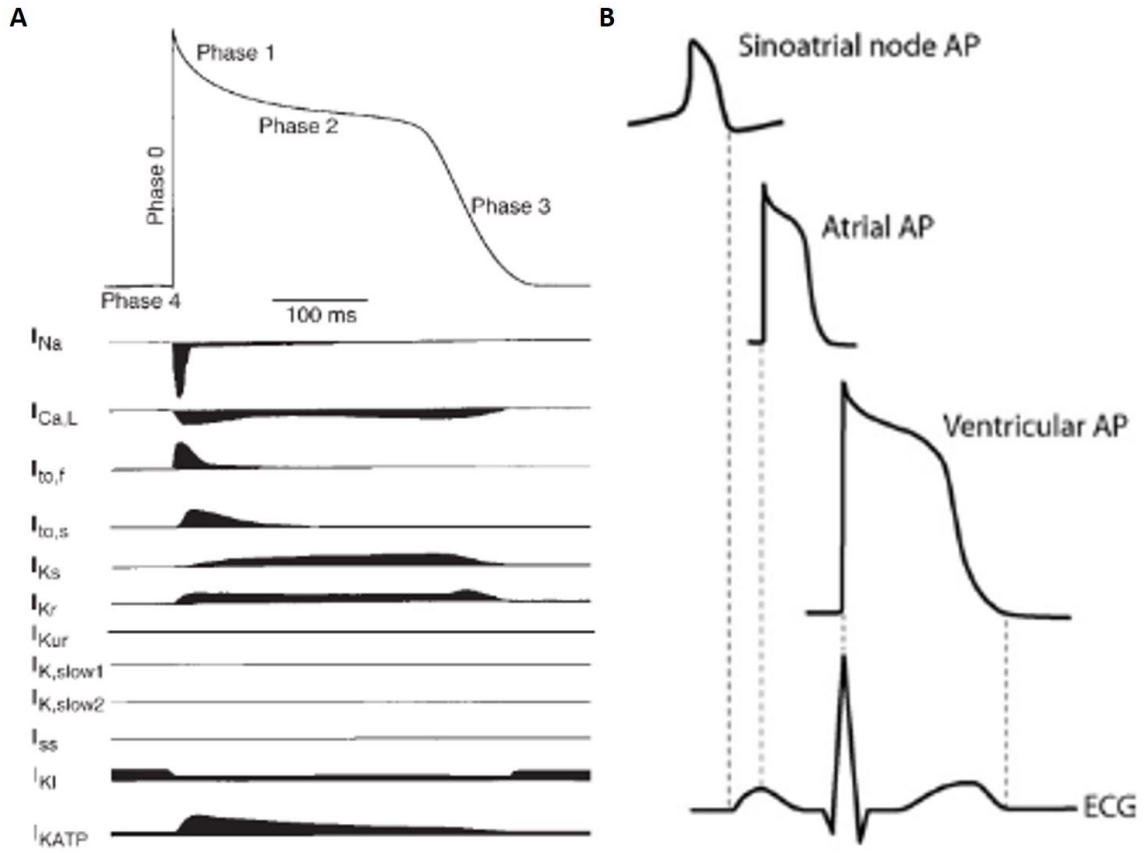

Figure 2.5. Cardiac Electrical Activity. (A) Action potential waveform and underlying ionic currents (Nerbonne and Kass, 2005). (B) Relationship between ECG and action potentials (APs) of cardiac myocytes from different cardiac regions (Amin et al., 2010).

2.1.5 Cardiac Excitation-Contraction Coupling

Cardiac excitation-contraction (E-C) coupling is the process that links the electrical excitation of the surface membrane (action potential) to myocyte contraction (Fig. 2.6). Action potentials traveling along the sarcolemma and down into the transverse tubule (T-tubule) system depolarize the cell membrane. The depolarization produced by the action potential caused the voltage-gated L-type (also called dihydropyridine-sensitive) Ca^{2+} channels situated in the surface membrane and transverse tubules to open (Eisner et al., 2017). This opening of the L-type Ca^{2+} channel in response to membrane depolarization allows the passage of Ca^{2+} into the myocyte, mainly into a restricted subspace called the dyad, a region bounded by the t-tubule and sarcoplasmic reticulum (SR) (Jafri, 2012). The resulting entry of small amount of Ca^{2+} results in a large increase of intracellular Ca^{2+}

concentration ([Ca^{2+}]i) in the dyadic space. This increase of [Ca^{2+}]i makes the SR Ca^{2+} release channels (ryanodine receptors (RyR)) open thereby releasing a much larger amount (10-20 fold) of Ca^{2+} from the SR in a process termed calcium-induced calcium release (CICR) (Jafri, 2012). The combination of Ca^{2+} influx and this SR Ca^{2+} release raises the free [Ca^{2+}]i, allowing Ca^{2+} to bind to the myofilament protein troponin-C (Bers, 2002). The binding of cytosolic Ca^{2+} to Troponin-C induces conformational changes in the regulatory complex such that troponin-I leading to the so-called activated state, in which myosin-binding sites on actin are exposed (Y. Wang et al., 1999). Then, the formation of cross-bridges produces the sliding of myofilaments one over the other, eventually resulting in muscle contraction (Piazzesi and Lombardi, 1996). For relaxation to occur, [Ca^{2+}]i must decline, allowing Ca^{2+} to dissociate from troponin-C. This requires that the RyRs close and then that Ca^{2+} is pumped back into the SR, by the SR Ca^{2+}-ATPase (SERCA) and out of the cell, largely by the sarcolemmal Na^{+}/Ca^{2+} exchanger (NCX) (Eisner et al., 2017).

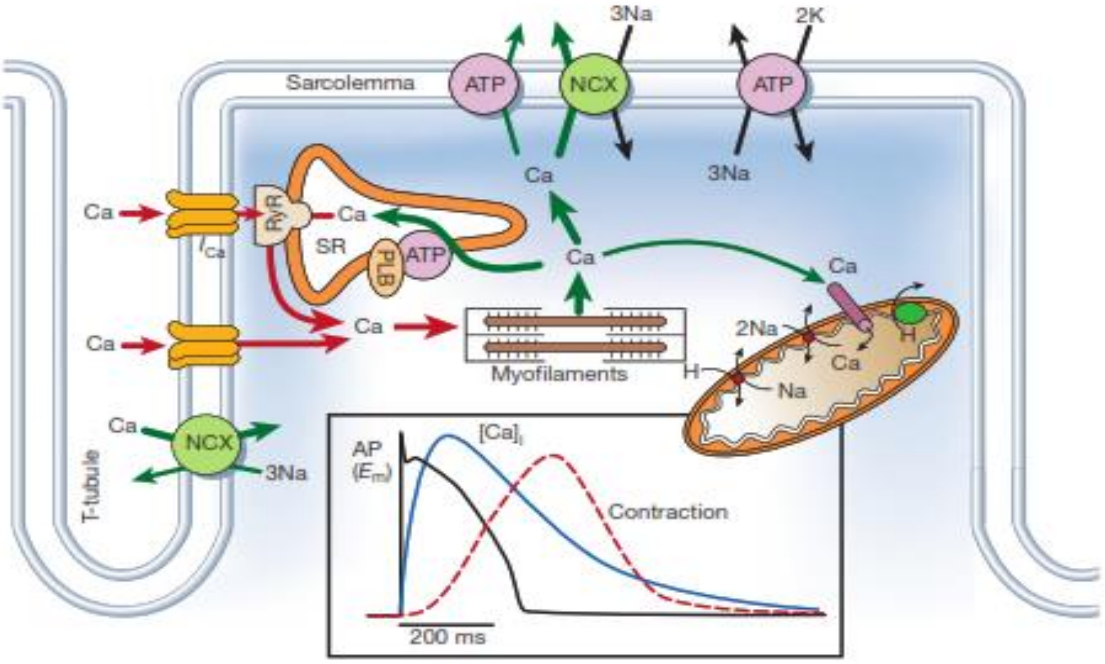

Figure 2.6. Excitation-Contraction Coupling in a Cardiac Myocyte. The figure shows surface membrane, transverse tubule, sarcoplasmic reticulum (SR), and mitochondria, as well as the various channels and transporters involved in cardiac excitation-contraction coupling. Inset shows the time course of an action potential, Ca^{2+} transient and contraction (Bers, 2002).

2.2 CARDIOVASCULAR DISEASES

Cardiac refers to the heart and vascular refers to the blood vessels. Therefore, cardiovascular diseases (CVDs) can be defined as a group of disorders that affects the heart and blood vessels (Olas and Bryś, 2018). That is, the spectrum of CVDs encompasses many different conditions which share risk factors, some of which are modifiable (Conte and Vale, 2018).

2.2.1 Types of Cardiovascular Diseases

2.2.1.1 Coronary Heart Disease

Coronary heart disease (CHD) refers to disease of the blood vessels supplying the heart muscle, caused by the narrowing of the coronary arteries. Coronary arteries supply the heart with oxygen and when narrowing occurs, the flow of oxygen is reduced. A mild shortage of oxygen causes pain in the chest and arm, while a severe shortage may result in a heart attack, otherwise known as myocardial infarction (MI), a permanent damage or death of part of the heart muscle.

2.2.1.2 Heart Rhythm Disorders

Heart rhythm disorders or cardiac arrhythmias, refers to changes in heart rhythm or rate due to abnormal generation or conduction of electrical impulses in the heart. The abnormal electrical activity in arrhythmias is commonly due to dysfunction and/or structural disruption of the electrical conduction system of the heart (S. C. Wang et al., 2018). These abnormal rhythms sometimes are classified according to their origin as either ventricular arrhythmias (originating in the ventricles) or supraventricular arrhythmias (originating in heart areas above the ventricles, typically the atria). They also can be classified according to their effect on the heart rate, with bradycardia indicating a heart rate of less than 60 beats per minute and tachycardia indicating a heart rate of more than 100 beats per minute. Combining these classifications, supraventricular tachyarrhythmias are diverse family of cardiac arrhythmias that begins in parts of the heart above the ventricles and causes rapid heartbeats (S. C. Wang et al., 2018). Atrial fibrillation (AF) is the most common supraventricular tachyarrhythmia that accounts for 0.5% all emergency visits (Go et al., 2014). Ventricular tachyarrhythmias is an abnormal heart rhythm that begins in either the right or left ventricle and causes rapid heartbeats. It may last for a few seconds (non-sustained) or for many minutes or even hours

(sustained). A sustained ventricular tachyarrhythmias often progresses to ventricular fibrillation. A bradyarrhythmia is a slow heart rhythm that is usually caused by disease in the heart's conduction system, types include sinus node dysfunction and heart block (S. C. Wang et al., 2018).

2.2.1.3 Heart Valve Diseases

Heart valve diseases or valvular heart diseases are characterized by damage to or a defect in any of the four heart valves. When it affects more than one heart valve, it is called multiple valvular heart disease (Zamorano et al., 2020). There are two main classifications of valvular heart diseases: stenosis and insufficiency. Valvular stenosis results from narrowing of the valve orifice, usually caused by thickening and increased rigidity of the valve leaflets, often accompanied by calcification (Nishimura, 2002). When this occurs, the valve does not open completely as blood flows across it, thereby resulting in a high resistance to flow and the development of a large pressure gradient across the valve when blood is flowing through the valve (Zamorano et al., 2020). Valvular insufficiency occurs when the valve leaflets do not completely seal when the valve is closed; sometimes, the valve bulges back into the previous chamber of the heart, a phenomenon called valve prolapse (Zamorano et al., 2020). This causes regurgitation of blood into the proximal chamber. For example, in aortic valve insufficiency blood regurgitates from the aorta into the left ventricle after ventricular ejection (Nishimura, 2002). These two conditions can affect any of the four main valves, however, the mitral and aortic valves are the two valves which are commonly affected (Zamorano et al., 2020).

2.2.1.4 Congenital Heart Defects

Congenital heart defects are a group of structural defects of the heart or the great vessels which are present at birth, and can often severely affects cardiac function (Sharma, 2019). Besides, they are the most common of all human birth defects and are the leading cause of neonatal and infant morbidity and mortality (Snider and Conway, 2011). There are many types of congenital heart defects, some are simple while others are combinations of simple defects, and to a greater extent, the level of complexity of the defect determines the severity of the condition. The most common congenital heart defects are ventricular septal defect (VSD) and atrial septal defect (ASD). However, the most severe congenital heart defects

include: double outlet right ventricle (DORV), persistent truncus arteriosus (PTA), transposition of the great arteries (TGA), tetralogy of fallot (TOF), atrioventricular septal defects (AVSDs), and large VSDs (Sharma, 2019).

2.2.1.5 Rheumatic Heart Disease

Rheumatic heart disease (RHD) refers to the long-term cardiac damage (mostly valvular damage) caused by either a single severe episode or multiple recurrent episodes of acute rheumatic fever (ARF), an abnormal autoimmune reaction to group A streptococcal infection in genetically susceptible individuals (Marijon et al., 2012; Sika-Paotonu et al., 2017). The valves most commonly affected are the mitral and aortic. The most serious permanent cardiac damage usually caused by ARF is endocarditis, characterized by swelling, edema, and deformity of the heart valves. When the valvulitis heals it may lead to fibrous thickening and adhesion of chordae tendineae and valve commissures, resulting in stenosis and/or regurgitation (Ueland, 1985).

2.2.1.6 Heart Failure

Heart failure (HF) describes an acute or chronic situation in which the heart cannot pump blood properly to meet the body's demands at a normal cardiac filling pressure due to weakness or stiffness of the heart muscle, causing symptoms such as decreased energy, troubled breathing, weight gain, and swelling of the legs or abdomen (Baman and Ahmad, 2020; Ponikowski et al., 2017). Chronic heart failure (CHF) is a common late phase in the natural history of many cardiovascular diseases (Drozd et al., 2020). HF is broadly classified into two based on the left ventricular ejection fraction (LVEF). It is classified as systolic heart failure when the left ventricle is unable to contract normally and is unable to pump enough blood into circulation, that is the LVEF is < 40 %. Systolic heart failure is the most common type of heart failure. Diastolic heart failure occurs when the left ventricle stiffens or bulks up and as a result, causing the heart an impaired relaxation during diastole but with a preserved LVEF (≥ 50 %) (Ponikowski et al., 2017).

2.2.1.7 Stroke

Stroke is defined as a neurological deficit attributed to an acute focal injury of the central nervous system (CNS) by a vascular cause. That is, a sudden death of brain cells due to lack

of oxygen, caused by blockage of blood flow or rupture of an artery to the brain. Strokes are classified into three main categories including; transient ischemic attack (TIA), ischemic stroke, and hemorrhagic stroke. A transient ischemic attack or ministroke occurs when blood flow to the brain is blocked temporarily. By definition, a stroke would be classified as a TIA if all symptoms resolved within 24 hours. A stroke is classified as an ischemic stroke when the arteries supplying blood to the brain is blocked by blood clots, causing a permanent damage to a part of the brain. The two most common types of ischemic strokes are thrombotic and embolic. A thrombotic stroke occurs when blood clots (thrombus) caused a blockage to an artery in the brain. An embolic stroke is when a blood clot or a piece of atherosclerotic plaque forms in another part of the body (often the heart or arteries in the upper chest and neck) and then moves through the bloodstream and lodges in an artery in the brain. A hemorrhagic stroke happens when an artery in the brain breaks open and leaks blood into the surrounding brain tissue, causing swelling and severe damage to the brain cells and tissues. The two types of hemorrhagic strokes are intracerebral and subarachnoid. An intracerebral hemorrhagic stroke happens when the tissues surrounding the brain fill with blood after an artery burst. Whereas, in a subarachnoid hemorrhage stroke, blood accumulates in the space beneath the arachnoid membrane that lines the brain (Campbell and Khatri, 2020; Sacco et al., 2013).

2.2.1.8 Aneurysm

Aneurysm is an abnormal bulge or a morbid dilation of the wall of a blood vessel, usually an artery, due to a weakened vessel wall. It has been reported that hemodynamic stress initiates early stage aneurysm formation, making it to be found mostly at sites of constant hemodynamic stress (Yokoi et al., 2015). Aneurysms can occur in any artery of the body, but the most common and most serious ones are those that occurs in the brain (cerebral aneurysm) or along the body's largest blood vessel, the aorta (aortic aneurysm). The aorta starts on the left side of the heart and runs down the chest to the abdomen and the rest of the body. When the bulge occurs in the chest region, it is called a thoracic aortic aneurysm and when it occurs in the abdomen, it is called an abdominal aortic aneurysm. However, abdominal aortic aneurysms are much more common than thoracic aortic aneurysms (Isselbacher, 2005).

2.2.1.9 Peripheral Arterial Disease

Peripheral arterial disease (PAD) or peripheral vascular disease (PVD) is defined as narrowing and obstruction of antegrade flow of major systemic arteries other than those of the cerebral and coronary circulations. It occurs most commonly in the lower limbs and is caused mostly by atherosclerosis (Conte and Vale, 2018; Kullo and Rooke, 2016). PAD is strongly an age-dependent condition, as its prevalence increases with age in both genders. Similarly, PAD has been found to contribute significantly to morbidity and healthcare expenditures in the elderly (Golomb et al., 2006). The condition itself has since been recognized as an independent risk factor for both myocardial infarction and stroke. Thus, PAD affects both quality of life and life expectancy (Abdulhannan et al., 2012).

2.2.1.10 Deep Venous Thrombosis and Pulmonary Embolism

Deep vein thrombosis (DVT) is the formation of a blood clot, or thrombus, in a deep vein, most commonly the lower leg. The blood clot restricts blood circulation through the blocked area, leading to symptoms that can include pain, swelling, redness of the leg, and dilation of the surface veins. Pulmonary embolism (PE) happens when a part of the blood clot breaks off and travels through the circulation to the heart and into the lungs, completely or partially blocking a pulmonary artery, leading to manifestation of symptoms like pain in the chest while breathing, circulatory instability, and difficulty breathing (Galson, 2008). Because both illnesses share a common pathogenesis, they are collectively referred to as venous thromboembolism (VTE) (Van Neste et al., 2009). Among life-threatening cardiovascular diseases, VTE is the third most common after myocardial infarction and stroke, indicating that it is associated with substantial morbidity and mortality (Di Nisio et al., 2016). For instance, VTE has been reported to be the leading causes of morbidity and mortality following surgical procedures (Ali et al., 2015). In addition, VTE disproportionately affect the elderly, as incidence increases exponentially with age to up to one case per hundred people older than 80 years (Di Nisio et al., 2016).

2.2.2 Prevalence and Burden of Cardiovascular Diseases

Cardiovascular diseases (CVDs) are one of the most serious problems in modern medicine. They are the most common non-communicable diseases and leading cause of death

worldwide (Roth et al., 2018). Overall, the crude prevalence of CVDs was 485.6 million cases in 2017, an increase of 28.5% from 2007 (Virani et al., 2020). In 2017, approximately 17.8 million deaths were attributed to CVDs globally, which amounted to an increase of 21.1% from 2007 (Roth et al., 2018; Virani et al., 2020). On the basis of the 2017 National Health Interview Survey, the age-adjusted prevalence of all types of heart disease was 10.6% of the population in the United States (Virani et al., 2020). Each year CVDs causes 3.9 million deaths in Europe and over 1.8 million deaths in the European Union (EU) (Wilkins et al., 2017). The burden of CVDs remains disproportionately larger in low-income and middle-income countries compared to high-income countries, as more than 80% of CVD deaths occur in low-income and middle-income countries (Alwan and MacLean, 2009; Bovet and Paccaud, 2011). Particularly, sub-Saharan Africa has witnessed unprecedented increase in cases of CVDs over the past two decades and it is now a public health problem throughout the Region. In 2013, an estimated 1 million deaths were attributed to CVDs in sub-Saharan Africa, constituting about 5.5% of global CVD deaths and 11.3% of total deaths in Africa (Amegah, 2018). Besides, CVDs affects working age populations much more in sub-Saharan Africa. For instance, young adults in this region have tendency of developing CVDs at least two decades earlier than their counterparts in more developed regions (Yuyun et al., 2020) and cardiovascular deaths occurs among matured adults of the region at least 10 years earlier than their counterparts in high-income countries (Baingana and Bos, 2006).

The global burden of CVDs is not only a health issue, but also a financial and economic challenge to healthcare systems (Anand and Yusuf, 2011). This is because, cardiovascular healthcare constitutes a significant proportion of total healthcare expenditure across the world and is expected to grow exponentially in future years (Timmis et al., 2020). The average annual direct and indirect cost of CVDs and stroke in the United States (over the period of 2014 – 2015) was estimated to be $351.3 billion (Virani et al., 2020). CVDs was estimated to cost the European Union (EU) economy €210 billion a year in 2015, of which 53% (€111 billion) is due to healthcare costs, 26% (€54 billion) to productivity losses and 21% (€45 billion) to the informal care of people with CVD. Out of this, the total costs of ischemic heart disease (IHD) amounted to approximately €59 billion (Timmis et al., 2020; Wilkins et al., 2017). Stevens and colleagues reported that heart conditions including hypertension, myocardial infarction, atrial fibrillation and heart failure imposed significant financial and

wellbeing impacts across Brazil, with the four conditions costing R$56.2 billion in 2015 alone (Stevens et al., 2018). The World Health Organization (WHO) projected the economic loss due to CVDs in low-income and middle-income countries combined, to be $3.76 trillion over the period of 2011 – 2025 (World Health Organization, 2011).

2.2.3 Risk Factors for cardiovascular Diseases

Epidemiological studies have demonstrated a marked association between certain factors and the development of CVDs (Olas and Bryś, 2018). These factors are broadly classified as behavioral risk factors and intermediate risk factors. The most important behavioral risk factors for CVDs are unhealthy diet, physical inactivity, tobacco use and harmful use of alcohol. Intermediate risk factors include; dyslipidemia, hypertension, diabetes, overweight/obesity and inflammation. These intermediate risks factors are direct consequences of the behavioral risk factors and they indicate an increased risk of developing CVDs (Timmis et al., 2020).

2.2.3.1 Unhealthy Diet

Unhealthy dietary patterns are major risk factor for cardiovascular morbidity and mortality. Reports indicates that excessive intake of sodium and refined carbohydrates increases the probability of developing CVDs (Casas et al., 2018).

2.2.3.2 Physical Inactivity

Physical inactivity, as manifested by a sedentary lifestyle, is considered to be one of the major risk factors of coronary heart disease. Equally, it has been found to be associated with reduced functional capacity of the cardiovascular system (Halar, 1995).

2.2.3.3 Tobacco Use

Tobacco use is one of the avoidable risk factors for CVDs. It has been reported that smoking reduces the activities of nitric oxide synthase and causes coronary artery spasm (Choi et al., 2016). Teo et al reported a linear relationship between number of cigarette smoked and the magnitude of risk of acute myocardial infarction (Teo et al., 2006).

2.2.3.4 Harmful Use of Alcohol

Chronic alcohol use has been linked with adverse cardiac outcomes including; hypertension, coronary heart disease, stroke, peripheral arterial disease, and cardiomyopathy (Piano, 2017). A study noted that endothelial functions are impaired in individuals with history of long-term harmful use of alcohol even years after withdrawing from the habit (Di Gennaro et al., 2007).

2.2.3.5 Dyslipidemia

Dyslipidemia is recognized as a prominent risk factor for CVDs (Hedayatnia et al., 2020). Lipid abnormalities, including high levels of low-density lipoprotein cholesterol (LDL-C), elevated triglycerides and low levels of high-density lipoprotein cholesterol (HDL-C), are associated with an increased risk of cardiovascular events (Miller, 2009). The importance of low-density lipoprotein (LDL) cholesterol in the development of atherosclerosis has long been recognized, and LDL cholesterol remains the primary target of therapy for the prevention of coronary heart disease (Carmena et al., 2004).

2.2.3.6 Hypertension

Hypertension is the strongest risk factor for almost all different CVDs acquired during life, including coronary heart disease, left ventricular hypertrophy and valvular heart diseases, cardiac arrhythmias including atrial fibrillation, cerebral stroke and renal failure (Kjeldsen, 2018). Hypertension accounts for an estimated 54 percent of all strokes and 47 percent of all ischemic heart disease events globally (Lawes et al., 2008). The management and control of hypertension are important to the prevention of these diseases (Kokubo and Iwashima, 2015).

2.2.3.7 Diabetes

Diabetes has long been recognized to be an independent risk factor for CVDs (Dokken, 2008). Leon and Maddox reported a close link between diabetes mellitus (DM) and CVDs (Leon and Maddox, 2015). As such, DM appears to contribute directly to the development of cardiomyopathy, rather than solely via coronary atherosclerosis and hypertension (Asghar et al., 2009). Diabetes also affects the heart muscle, causing both systolic and diastolic heart failure (Dokken, 2008).

2.2.3.8 Overweight and Obesity

In adults, overweight is defined as a body mass index (BMI) of 25.0 to 29.9 Kg/m^2 and obesity is defined as a BMI $\geq$ 30.0 Kg/m^2 (Poirier et al., 2006). Both overweight and obesity has been reported to be strong risk factors for the development of CVDs, particularly heart failure and coronary heart disease (Carbone et al., 2019). In fact, a linear relationship has been found between adiposity and cardiovascular outcomes (Wilson et al., 2002).

2.2.3.9 Inflammation

Chronic inflammation, exemplified by elevated C-reactive protein, has been added to the risk factors for CVD as non-traditional risk factor (Katsiari et al., 2019; Lüscher, 2018). Current scientific evidence shows that chronic inflammation plays a key role in the pathogenesis of coronary artery disease, including the initiation/progression of atheroma plaque and rupture, post-angioplasty and restenosis. Consequently, the expression of mediators such as C-reactive protein (CRP), interleukin (IL)-1, IL-6, IL-8, IL-1β, IL-18, monocyte chemoattractant protein (MCP)-1, and tumor necrosis factor (TNF)-α has been reported to correlate with CAD severity (Zakynthinos and Pappa, 2009).

2.3 MYOCARDIAL INFARCTION

Myocardial infarction (MI) is the medical term for a heart attack, a life-threatening and most lethal manifestation of coronary artery diseases. It was first described patho-physiologically in 1912 by American physician, James B. Herrick (Herrick, 1912). Myocardial infarction occurs when blood flow to the heart muscle is abruptly cut off, usually due to blockage in one or more of the coronary arteries, and subsequent myocardial ischemia results in damage to the surrounding heart muscle. The blockage can be as a result of a blood clot or buildup/rupture of a plaque, a substance mostly made of fat, cholesterol, and cellular waste products, in the vessels (Torpy et al., 2008).

2.3.1 Types of Myocardial Infarction

Myocardial infarction is classified into five types based on the etiology and pathogenesis of the disease (Thygesen et al., 2007, 2012a, 2019). These classifications were first introduced in 2007 as an important component of the universal definition of MI (Thygesen et al., 2007).

2.3.1.1 Type 1 MI

Type 1 MI, otherwise known as spontaneous MI, involves thrombotic occlusion of the coronary artery (Thygesen et al., 2007, 2012a, 2019). This thrombotic event occurs when a pre-existing atherosclerotic plaque ruptures or fissures and or eroded, thereby exposing underlying thrombogenic material to the circulation (Alpert, 1989). Consequently, the intact endothelium of the coronary artery which has vasodilatory and antiplatelet-aggregating effects loses its functions, leading to platelets activation and clotting cascade initiation (Pepine, 1989). The endothelium being sensitive to trauma, becomes damaged by high shear stress exerted on it as a result of narrowing of the coronary artery, leading to total occlusion of the coronary artery in that part of the myocardium (Pepine, 1989). Finally, the lack of blood supply to such part of myocardium brings about the myocardial tissue damage (Fig. 2.7).

2.3.1.2 Type 2 MI

This type refers to MI secondary to an ischemic imbalance, originating from a condition other than coronary artery disease that contributes to an acute imbalance between oxygen demand and supply (Thygesen et al., 2007, 2012a). The myocardial oxygen supply/demand imbalance attributable to acute myocardial ischemia here may be multifactorial (Fig. 2.7), related either to: reduced myocardial perfusion due to fixed coronary atherosclerosis without plaque rupture, vasospasm, coronary microvascular dysfunction, coronary embolism, coronary artery dissection with or without intramural hematoma, or other mechanisms that reduce oxygen supply such as severe bradyarrhythmia, respiratory failure with severe hypoxemia, severe anemia, and hypotension/shock; or to increased myocardial oxygen demand due to sustained tachyarrhythmia or severe hypertension with or without left ventricular hypertrophy (Thygesen et al., 2019).

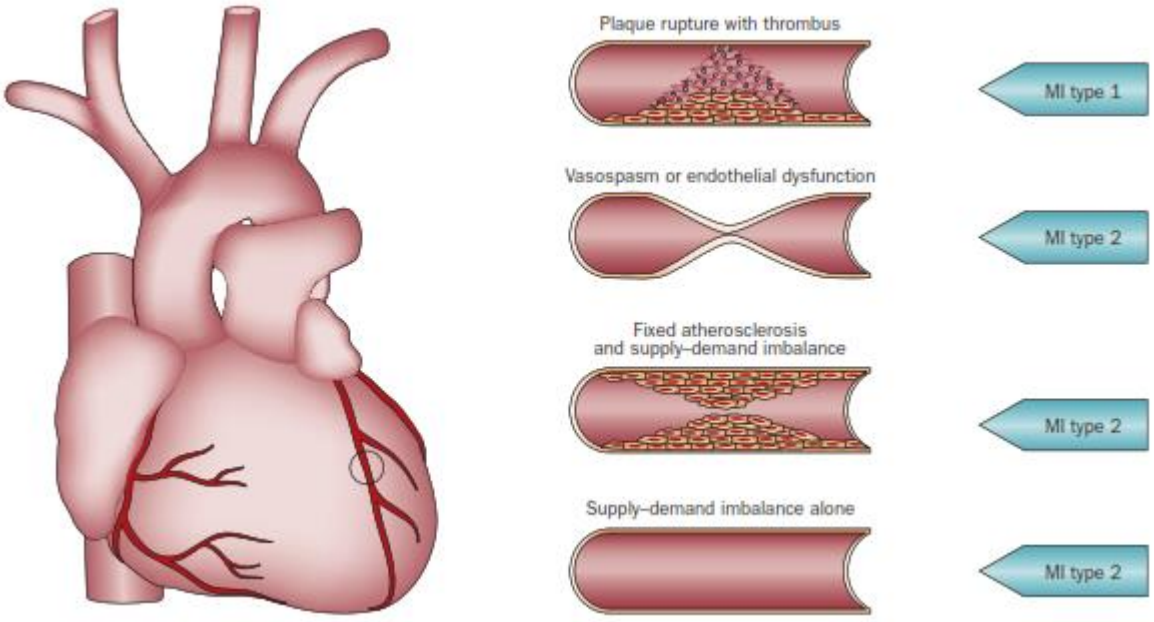

Figure 2.7. Pictorial Illustration of Type 1 and Type 2 Myocardial Infarction. The figure illustrates the distinction between MI types 1 and 2 from the perspectives of the condition of the coronary arteries (Thygesen et al., 2012b).

2.3.1.3 Type 3 MI

Type 3 MI refers to any sudden cardiac death, including cardiac arrest, often with symptoms suggestive of myocardial ischemia, accompanied by presumed new ischemic ECG changes or new left bundle branch block (LBBB) or ventricular fibrillation that resulted in death before blood samples for biomarkers can be obtained, or before cardiac biomarker could rise in the blood (Thygesen et al., 2007, 2012a, 2019).

2.3.1.4 Type 4 / Type 5 MI

Type 4 and type 5 MI refers to cardiac procedural myocardial injuries, related to coronary revascularization procedures. For instance, type 4 MI are associated with percutaneous coronary intervention (PCI), while type 5 MI are secondary to coronary artery bypass grafting (CABG) (Thygesen et al., 2007, 2012a, 2019).

2.3.2 Symptoms of Myocardial Infarction

The most common manifestation of MI in men and women is chest pain (Pilote, 2014). However, the symptoms can be quite varied in some individuals to include pressure or tightness in the chest, shortness of breath, sweating, nausea, vomiting, anxiety, cough, dizziness, fast heart rate, jaw pain, upper back pain and lightheadedness among others (Passinho et al., 2018).

2.3.3 Detection and Identification of Myocardial Infarction

Myocardial infarction can be recognized by clinical features, including electrocardiographic (ECG) findings, elevated values of biochemical markers (biomarkers) of myocardial necrosis, and by imaging, or may be defined by pathology (Thygesen et al., 2012a).

2.3.3.1 Electrocardiographic Detection of Myocardial Infarction

Electrocardiography (ECG) is an integral part of the diagnostic workup of individuals with suspected MI (Thygesen et al., 2007, 2012a, 2019). This is because MI is often associated with dynamic changes in ECG waveform (Thygesen et al., 2012a). The hallmarks of a MI on an ECG are; ST segment elevation, T wave inversion, and Q wave formation, occurring in that succession. This sequence of events is termed as the electrocardiographic evolution of an infarction (Gavaghan, 1999). A normal heart rhythm displays a P wave, QRS complex, and T wave. However, a profound ST-segment shift or T wave inversions involving multiple leads are associated with a greater degree of myocardial ischemia, and a worse prognosis (Thygesen et al., 2012a, 2019). On a normal ECG, the Q wave is a negative deflection, but not remarkable. The development of a Q wave that is about one-third the height of an R wave indicates irreversible myocardial damage or necrosis (Gavaghan, 1999). Other ECG abnormalities associated with MI include: PR segment depression (Jim et al., 2006), short PR interval and prolongation of QRS complex (Goldbloom and Dumanis, 1946).

2.3.3.2 Biomarker Detection of Myocardial Infarction

A variety of cardiac proteins and enzymes are used to evaluate myocardial cell death including: creatine kinase - total (CK), creatine kinase - MB fraction (CK-MB), troponin I (cTnI), troponin T (cTnT), Myoglobin, Lactate dehydrogenase (LDH) and Aspartate transaminase (AST) (Danese and Montagnana, 2016; Thygesen et al., 2007), but the most

specific for MI are; cardiac cTnI, cTnT, CK-MB (Ibrahim et al., 2014) and lactate dehydrogenase-1 isoenzyme (LDH-1) (Paloheimo and Pitkänen, 1964). Acute myocardial infarction (AMI) is detected when levels of these sensitive and specific biomarkers are increased in the blood (Thygesen et al., 2007).

cTnI and cTnT are structural components of cardiac muscle. They are cardiac contractile proteins which are released into the bloodstream following myocardial injury. The nearly absolute myocardial tissue specificity as well as high clinical sensitivity makes them the preferred biomarker for myocardial necrosis than CK-MB, and helps to exclude elevations of CK caused by skeletal muscle trauma (Thygesen et al., 2007).

Creatine kinase acts as a regulator of high-energy phosphate production and utilization within contractile tissues (Bessman and Carpenter, 1985). Cytoplasmic creatine kinase is a dimer composed of M and B subunits which associate to form CK-MM, CK-MB and CK-BB isoenzymes (Kemp et al., 2004). CK-MB is the main isoenzyme found in cardiac muscle while CK-MM is predominantly found in striated muscle and CK-BB is found mostly in brain, colon, ileum, stomach and urinary bladder (Lott and Abbott, 1986). Serum total CK and CK-MB activities rise in parallel following myocardial infarction, however, serum CK-MB is considerably more specific for MI than serum total CK because serum total CK may be elevated in many conditions especially where skeletal muscle is damaged (Hamburg et al., 1991). Specific quantitation of CK-MB is made possible by immunoinhibition technique using antibodies that inhibit M-subunit activity, with residual enzyme activity being derived from B-subunits only (Jockers-Wretou and Pfleiderer, 1975).

Since LDH is present in nearly all human tissues, measurement of LDH-1 isoenzyme is necessary for greater specificity for cardiac injury (Danese and Montagnana, 2016). Sometimes, LDH-1 activities are corrected for in vivo or in vitro hemolysis by measuring the ratio of LDH-1&2. Ideally, the level of isoenzyme 2 is greater than isoenzyme 1 in healthy individuals, but with MI, the pattern changes and isoenzyme 1 is higher than isoenzyme 2, making the ratio to be > 1.0 in MI subjects, whereas it is usually < 1.0 in samples of subjects with hemolysis (Galbraith et al., 1990).

2.3.3.3 Histopathological Characteristics of Myocardial Infarction

Histologically, the first ultrastructural changes detectable few minutes after the onset of myocardial injury are diminished cellular glycogen, relaxed myofibrils, sarcolemma disruption (Jennings and Ganote, 1974) and mitochondrial abnormalities (Virmani et al., 1990). Coagulative necrosis is observed between 4-12 hours after infarction (Fishbein et al., 1978). Pathologically, AMI is characterized by cellular infiltrations and so detection and identification of MI is done based on the presence of polymorphonuclear leukocytes (Thygesen et al., 2007), including neutrophils at about 12-24 hours after the onset of infarction (Fishbein et al., 1978).

2.3.4 Prevalence and Burden of Myocardial Infarction

Myocardial infarction is a key component of the burden of cardiovascular diseases and therefore occupies a central role in the assessment of the burden of heart disease (Roger, 2007). It has been reported to be one of the most frequent causes of hospitalization in persons 65 years of age and above in Brazil in recent years (Alves and Polanczyk, 2020). Thygesen and colleagues reported that MI is a major cause of death and disability worldwide (Thygesen et al., 2007, 2012a). Although, recent epidemiological data suggests that the incidence of MI is decreasing in developed countries due to improved health care systems and effective implementation of public health strategies (Jayaraj et al., 2018), nevertheless the incidence of MI is on the upsurge in the developing countries (Gaziano et al., 2010; Jayaraj et al., 2018). Furthermore, the prevalence of MI has been reported to be higher among men of all age groups than women (Jayaraj et al., 2018) and ethnic minority groups are disproportionately affected (Van Oeffelen et al., 2015). The reason for these disparities is not known. However, sex disparities in cardiovascular risk factors and the protective effect of female hormones in premenopausal women are considered the most likely explanatory factors (Jousilahti et al., 1999; Kalin and Zumoff, 1990).

2.3.5 Experimental Models of Myocardial Infarction

After the onset of myocardial ischemia, cell death is not immediate but takes a finite period to develop (Thygesen et al., 2007, 2012a). However, it can be developed in some animal models within a short period of time. Jennings and Ganote reported an irreversible

histological cell death (20 to 60 minutes after the onset of ischemia) following experimental acute occlusion of a major branch of a coronary artery in dog (Jennings and Ganote, 1974).

Prominently, Rona and others reported an infarct-like myocardial necrosis of uniform severity which resembled closely human myocardial infarction after two consecutive (24 h interval) acute doses (85 mg/kg/day) of isoproterenol were administered subcutaneously in rats (Rona et al., 1959). Isoproterenol, otherwise known as Isoprenaline is a synthetic catecholamine that acts on beta adrenergic receptors as agonist. Originally, it is used to increase the heart rate in conditions such as severe bradycardia that is unresponsive to atropine (Siddiqui et al., 2016). It is known to accelerate the sinus node and enhance atrioventricular node conduction (Vargas et al., 1975). According to Rona et al, a relative ischemia, elicited by exaggerated beta-adrenergic stimulation and reduced coronary blood flow, is responsible for the infarct-like character of the myocardial necrosis induced by isoproterenol in rats (Rona et al., 1959). This pharmacologic technique developed by Rona and colleagues does have an advantage over the occlusion method in that it requires no surgical procedures and so reduces fatality before experimental assessments. Thus, after confirmation of their observations by a number of other groups (Beznak, 1962; Handforth, 1962; Hill et al., 1960), it has since been adopted as a reliable non-surgical animal model of myocardial infarction (Rona et al., 1963).

2.4 MEDICINAL PLANTS

Medicinal plant refers to all plants with specific ethnobotanical claims of capacity to treat or prevent certain illnesses (Heinrich, 2018). Others defined medicinal plants as plants which, in one or more of its organs, contains substance that can be used for therapeutic purposes, or which are precursors for chemo-pharmaceutical semi-synthesis (Karunamoorthi et al., 2013). Since ancient times, when there was no commercial and synthetically-manufactured drugs, people have used plants and plant extracts to ameliorate diseases and foster healing. Historically, human beings came to the awareness of medicinal plants usage as a result of many years of struggles against illnesses (Petrovska, 2012). Medicinal properties derived from plants can come from many different parts of a plant including leaves, roots, bark, fruit, seeds and flowers. In fact, until the mid-nineteenth century nature's pharmaceuticals, in the form of herbs, plants, roots, vines and fungi, were all that were

available to relieve man's pain and suffering (Jones, 2011). It was only in 1869 that the first synthetic drug, chloral hydrate, was discovered and introduced as a sedative-hypnotic (Jones, 2011), followed by creation of aspirin out of the salicylic acid extracted from willow barks in 1897 (Carmona and Pereira, 2013). These discoveries led to an era dominated by synthetic drug development, making herbal medicines to be seen as obsolete. Undoubtedly, this development greatly improved medical care, human health, thus extending human life (Carmona and Pereira, 2013). However, due to decreasing efficacy of synthetic drugs and the increasing contraindications of their usage (Petrovska, 2012), the interest in phytopharmaceutical products and herbal medicines has been a trend in recent years (de Oliveira et al., 2017).

2.4.1 *Andrographis paniculata* (Burm. f.) Nees

Andrographis paniculata (Burm. f.) Wall. ex Nees (Fig. 2.8), popularly known as Kalmegh or king of bitters, is an annual herbaceous plant belonging to the family Acanthaceae (Mishra et al., 2007). The plant is commonly used as ingredient of herbal formulations indicated for chest pain and cardiovascular diseases in India, China, Hong Kong, Philippines, Malaysia, Indonesia, Thailand (Akbar, 2020; C. Y. Zhang and Tan, 1997) and many regions of Africa (Okhuarobo et al., 2014). Other ethnobotanical used of *Andrographis paniculata* includes; treatment of snake bite, bug bite, diabetes, dysentery, fever, and malaria (Hossain et al., 2014). The commonly utilized parts of the plant include whole plant, aerial part, leaves and the root (Akbar, 2011).

Figure 2.8. Picture of *Andrographis paniculata*. The mature plant (Hossain et al., 2014).

Several studies have investigated the activities of crude and fractional extracts of this plant against cardiovascular diseases. Zhang and Tan reported that aqueous extract of *Andrographis paniculata* produced a dose-dependent fall in systolic blood pressure in both spontaneously hypertensive rats and normotensive rats, with a corresponding significant decrease in plasma angiotensin converting enzyme (ACE) activity and that the decrease in ACE activity was not significantly altered in normotensive rats, an indication that suggests its hypotensive effect (C. Y. Zhang and Tan, 1996). In addition, Ojha et al investigated the protective effects of hydroalcoholic extract of *Andrographis paniculata* on ischemia reperfusion-induced myocardial injury in rats and reported favorable modulation of hemodynamic and left ventricular contractile function, restoration of the myocardial antioxidants and prevention of myocytes injury similar to the effects of standard drug

(benazepril) treatment (Ojha et al., 2012). Moreover, the cardioprotective activities of both methanolic and alcoholic extracts of *Andrographis paniculata* against experimentally-induced myocardial infarction has also been reported (Adeoye et al., 2019; Sah and Nagarathana, 2016). Similarly, Guo et al reported that extracts of *Andrographis paniculata* protected against Ca^{2+}-overloading in the process of myocardial ischemic reperfusion through significant augmentations in activities of sarcolemma Ca^{2+}-ATPase and Na^{+}-K^{+} ATPase (Z. Guo et al., 1995).

Importantly, Hossain et al reviewed the ethnobotany, phytochemistry, and pharmacology of *Andrographis paniculata*, and pointed out that the existing reports on the crude and fractional extracts of the plant indicated that it could be used as alternative source for the treatment of cardiovascular diseases. More importantly, they suggested that pharmacological investigation using the bioactive constituents of the plant will provide more specific evidence to substantiate the veracity of the ethnobotanical claims and to unravel the possible mechanisms of action (Hossain et al., 2014).

2.5 BIOACTIVE NATURAL PRODUCTS

The term "natural products" encompasses all materials and or substances that are produced by biological sources, including biotic materials, bio-based materials, bodily fluids and other natural materials that were once found in living organisms. However, within the fields of medicinal chemistry**,** natural products are often defined as secondary metabolites (Krause and Tobin, 2013). Secondary metabolites are organic compounds that typically do not have direct involvement in the normal growth, development and or reproduction of the organism producing them, but are in the correct chiral configuration to exert extrinsic biological activity or function that mainly affects other organisms outside of their producer (Zähner, 1979).

Plants are an important source of secondary metabolites (Kourkoutas et al., 2018). The pharmacologically important plant secondary metabolites are often referred to as bioactive natural products (Brahmkshatriya and Brahmkshatriya, 2013; Velu et al., 2018). These bioactive natural products are structurally and chemically diverse molecules (Pham et al., 2019) and have provided chemical leads for the development of many drugs for diverse

indications (Beutler, 2009). Over the past few decades, a lot of studies have focused on the protective effect of bioactive natural products obtained from plants against various diseases such as cardiovascular, diabetes, reproductive, cancer, and neurodegenerative diseases (Kourkoutas et al., 2018; Sairazi and Sirajudeen, 2020).

Plant bioactive natural products can be classified on the basis of their chemical structure, composition, aqueous solubility, and based on the pathway by which they are synthesized. A simple classification includes three main groups: terpenes, phenolics, and alkaloids. Among these, terpenes are the most abundant and most structurally diverse, constituting about 55 % of all plant bioactive natural products (Brahmkshatriya and Brahmkshatriya, 2013).

2.5.1 Terpenes

Terpenes are naturally occurring hydrocarbons produced by a wide variety of plants and animals. The term "terpene" was originally coined from turpentine (resin of pine trees) to describe a mixture of isomeric hydrocarbons found in several pine tree species (Brahmkshatriya and Brahmkshatriya, 2013). Terpenes predominantly shapes the properties of plants such as conifer wood, balm trees, citrus fruits, coriander, eucalyptus, lavender, lemon grass, lilies, carnation, caraway, peppermint species, roses, rosemary, sage, thyme, violet and many other plants or parts of those (roots, rhizomes, stems, leaves, blossoms, fruits, seed) which are well known to smell pleasantly, to taste spicy, or to exhibit specific pharmacological activities (Breitmaier, 2006). They are classified based on the number of isoprene (C_5H_8) units incorporated in their basic molecular skeleton (Croteau, 1998), which include hemiterpenes (one isoprene units), monoterpenes (two isoprene units), sesquiterpenes (three isoprene units), diterpenes (four isoprene units), sesterterpenes (five isoprene units), triterpenes (six isoprene units), tetraterpenes (eight isoprene units) and polyterpenes (many isoprene units) (Breitmaier, 2006). Among these classes, diterpenes has been recognized as fulfilling the definition of a pharmacological preconditioning class of compounds and give hope for the therapeutic use in cardiovascular diseases (Tirapelli et al., 2008).

Consequently, several diterpenes has been studied for their cardiovascular effects. Cuadrado et al reported cardioprotective effects of labdane diterpenes derived from hispanolone, isolated from *Ballota hispanica* (L.) Benth against anoxia/reperfusion-induced injury in

isolated cardiomyocytes (Cuadrado et al., 2011). Also, Garcia et al reported that neo-clerodane and ent-clerodane diterpenes from *Baccharis trimera* (Less.) reduced the maximal contractions induced by $CaCl_2$ in KCl depolarized rat portal vein preparations, via blockade of the voltage-dependent calcium channels (Garcia et al., 2014). Similarly, Jin and Li reported the cardioprotective effects of tanshinone, a lipophilic diterpene quinone from *Salvia miltiorrhiza* (Danshen) (Jin and Li, 2016). Most recently, Monteiro et al reported that manool, a labdane diterpene isolated from the plant *Salvia officinalis*, mediated antihypertensive effects through mechanism involving nitric oxide pathways (Monteiro et al., 2020).

2.5.1.1 Andrographolide

Andrographolide (Fig. 2.9), molecular formula: $C_{20}H_{30}O_5$ and molecular weight: 350.4 g/mol, is a labdane diterpene lactone compound extracted from the plant *Andrographis paniculata* (Burm. f.) Wall. ex Nees. Actually, a number of active principles are reported from the plant, which mainly include diterpene lactones, flavonoids, and polyphenols (Chao and Lin, 2010; Li et al., 2007; Rao et al., 2004). However, andrographolide has been established to be the major constituent and has been found to be mostly responsible for its key therapeutic properties (Brahmachari, 2011; Chao and Lin, 2010). This prime constituent is mainly concentrated in leaves of the plant and can easily be isolated from the crude plant extracts as crystalline solid (Kulyal et al., 2010; Lomlim et al., 2003; Rajani et al., 2000).

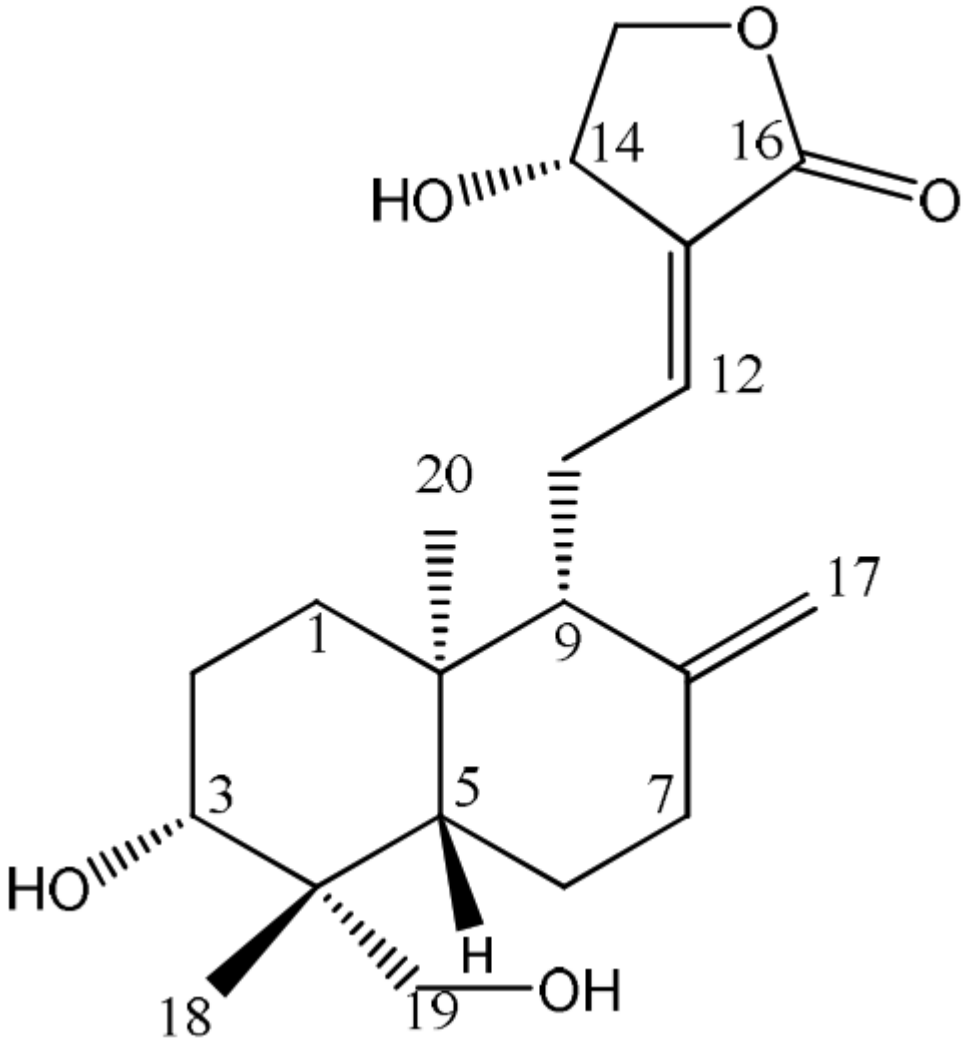

Figure 2.9. Structure of Andrographolide. The figure shows the chemical structure of andrographolide with carbon atoms in the compound numbered accordingly (Chao and Lin, 2010).

2.5.1.1.1 Pharmacokinetics and Bioavailability of Andrographolide

Andrographolide has been found to be quickly absorbed and extensively metabolized both in rats and humans. Panossian et al reported that andrographolide was quickly and almost completely absorbed into the blood following oral administration of the compound at a dose of 20 mg/kg body weight in rats, and that in human, maximum plasma levels of approximately 393 ng/ml (~1.12 μM) were reached after 1.5 - 2 hours following oral administration of 80 mg of the compound (Panossian et al., 2000). Similarly, Chen et al reported that after a single intragastric administration of andrographolide (50mg/kg) in rats,

maximum plasma concentration of 1 μM was recorded in 30 min, indicating a bioavailability of 1.19% (H. Chen et al., 2014). Likewise, Pholphana et al reported that andrographolide was completely dissolved in the simulated pH of gastrointestinal tract within 60 min of dissolution (Pholphana et al., 2016).

2.5.1.1.2 Pharmacological activities of Andrographolide

Andrographolide has been reported to exhibit diverse pharmacological activities in isolation. For instance, it has been shown in some experimental studies that andrographolide may help in liver protection and regeneration (Roy et al., 2014; Trivedi et al., 2007; Ye et al., 2011). Similarly, the effectiveness of andrographolide against viral infections has been described in a number of studies (J. X. Chen et al., 2009; Wintachai et al., 2015). Also, there are scientific evidences suggesting andrographolide as an anti-inflammatory agent (Abu-Ghefreh et al., 2009; Bao et al., 2009). Furthermore, Yu et al studied the ameliorative effects of andrographolide against streptozotocin-induced diabetes in rat, their results indicated that oral administration of andrographolide reduced plasma glucose concentration in diabetic rats in a dose-dependent manner and that andrographolide at the effective dose of 15 mg/kg significantly attenuated the increase of plasma glucose induced by an intravenous glucose challenge test in normal rats (Yu et al., 2003). Other pharmacological effects documented for andrographolide in the literature include antineoplastic activity (Rajagopal et al., 2003; Varma et al., 2011) and immunomodulatory activity (W. Wang et al., 2010).

2.5.1.1.3 Previous Reports on The Cardiovascular effects of Andrographolide

Earlier, there are a number of hints in the literature suggesting andrographolide as the cardioprotective principle in *Andrographis paniculata* and also suggesting the protective potentials of the compound against cardiac and vascular damages. Amroyan et al reported the inhibitory effect of andrographolide against platelet-activating factor (PAF)-induced platelet aggregation and linked the effect to the cardiovascular and antithrombotic activity described of *Andrographis paniculata* (Amroyan et al., 1999). Also, Woo et al investigated the cardioprotective effects of andrographolide and several other diterpene lactones derived from *Andrographis paniculata* against hypoxia/reoxygenation injury in neonatal rat cardiomyocytes; they discovered that it was only pretreatment with andrographolide that protected the cardiomyocytes against hypoxia/reoxygenation injury and concluded that

andrographolide is the cardioprotective principle in *Andrographis paniculata* (Woo et al., 2008). In addition, Zhi-Tao et al reported that andrographolide inhibited intimal hyperplasia in a rat model of autogenous vein grafts through suppression of p65, E-selectin and MMP-9 at the transcriptional level (Zhi-Tao et al., 2011). More recently, Zeng et al reported that andrographolide inhibited aconitine-induced arrhythmias in rabbits (Zeng et al., 2017). Likewise, Wu et al reported that andrographolide protected against aortic banding-induced cardiac hypertrophy in mice through inhibition of MAPKs signaling (Wu et al., 2017).

III. JUSTIFICATION AND OBJECTIVES

3.1 JUSTIFICATION

Cardiovascular diseases are the leading cause of death globally (Mc Namara et al., 2019). Notable among these diseases is myocardial infarction (an acute condition of necrosis of myocardium) owing to its relative irreversibility (Ferrari, 2001; Kumar et al., 2017) and higher percentage of mortality among the affected patients (Roth et al., 2018). Myocardial infarction results from myocardial ischemia and is a serious problem for the ischemic patients as it compromises the ability of the heart to pump blood efficiently (Thygesen et al., 2012a). In addition, platelet-dependent thrombus formation has been identified as a key event in the pathogenesis of this disease (Gawaz, 2004). In the first place, arterial microthrombus formation results in hypoxia (Evans, 2019), chronic intermittent of which promotes myocardial ischemia-related ventricular arrhythmias and sudden cardiac death (Morand et al., 2018). Though, it is very difficult to define symptoms of myocardial infarction, it has been reported that myocardial infarction accounted for up to 14.7 % of hospital visits because of chest pain (Goldman et al., 1996). Over the past three decades, there have been concerted efforts in cardiology to identify interventions that could make the heart more resistant to infarction. These include thrombolytics, beta blockers and calcium antagonists but either not very effective or with serious side effects (Genoni et al., 1996; Hollenberg, 2005; Russell, 1988). Given these hitches, alternative remedies using bioactive constituents of plants are now gaining popular research interest as they are often considered effective and safer.

Andrographis paniculata (Burm. f.) Wall. ex Nees (family: Acanthaceae), popularly known as Kalmegh or king of bitters is a common ingredient of herbal formulations indicated for chest pain and cardiovascular diseases in some parts of Asia (C. Y. Zhang and Tan, 1997) and many regions of Africa (Okhuarobo et al., 2014). In a review on ethnobotany, phytochemistry and pharmacology of *Andrographis paniculata*, Hossain et al concluded that the existing reports on the crude and fractional extracts of the plant indicated that it could be used for the treatment of cardiovascular diseases. They however suggested that pharmacological investigation using the principal bioactive compound in the plant will provide a more specific knowledge about the veracity of the ethnobotanical claims and the possible mechanism of action (Hossain et al., 2014).

Among the single compounds isolated from *Andrographis paniculata*, andrographolide ($C_{20}H_{30}O_5$, MW: 350.4 g/mol), a diterpene lactone is the principal one in terms of abundance and bioactivity (Jayakumar et al., 2013). Andrographolide has been reported to have diverse pharmacological potentials in isolation (Bao et al., 2009; Chan et al., 2010; Rajagopal et al., 2003; Wintachai et al., 2015). Much earlier, Amroyan et al reported its dose-dependent antithrombotic activity (Amroyan et al., 1999) and recently, Woo and colleagues also reported its protective effects against hypoxia and reoxygenation injury (Woo et al., 2008). Considering the roles of thrombosis and hypoxia in the pathogenesis of myocardial infarction, we hypothesized that andrographolide could confer protective effects on the heart against myocardial infarction. Hence, this study assessed the protective potentials of andrographolide against isoproterenol-induced myocardial infarction in rats.

3.2 OBJECTIVES

3.2.1 General Objective

This study had as general objective to investigate the protective potentials of andrographolide against isoproterenol-induced myocardial infarction in rats.

3.2.2 Specific Objectives

i. Evaluate the effects of andrographolide administration on cardiac electrocardiography (ECG) profiles in comparison with the positive and negative controls.

ii. Evaluate the effects of andrographolide administration on cardiac biometrical indexes in comparison with the positive and negative controls.

iii. Evaluate the effects of andrographolide administration on the systemic cardiac biochemical markers and hematological profiles in comparison with the positive and negative controls.

iv. Evaluate the effects of andrographolide administration on cardiac antioxidant status in comparison with the positive and negative controls.

v. Examine the effects of andrographolide administration on the gross morphology and histological structure of the heart tissue in comparison with the positive and negative controls.

vi. Evaluate the effects of treatments on the mechanical and electrical activities of cardiac myocytes isolated from each experimental group to unravel the mode of actions of andrographolide.

vii. Validate the mode of actions of andrographolide obtained from the *in-vivo* study with an *in-vitro* test of andrographolide (at different concentrations) on freshly isolated cardiomyocytes in comparison with standard drug.

IV. MATERIALS AND METHODS

4.1 MATERIALS

4.1.1 Chemicals and Reagents

Andrographolide (Catalog number: 33684, purity: 95%) was purchased from AstaTech Inc (Bristol, PA, USA). Isoproterenol hydrochloride (Product number: 15627), bovine insulin, porcine pancreas trypsin, Streptomyces griseus protease, bovine serum albumin, L-aspartic acid, ATP disodium trihydrate, Evans blue, NaCl, $CaCl_2.2H_2O$, HCl, EGTA, Na_2HPO_4, TEA-Cl, CsCl, TEA-OH, CsOH, $CdCl_2$ and NMDG were purchased from Sigma-Aldrich (St. Louis, Missouri, USA). Glucose, NaOH, KOH and NaH_2PO_4 were purchased from Labsynth (SP, Brazil). HEPES free acid and KCl were purchased from Amresco LLC (Solon, Ohio, USA). $MgCl_2.6H_2O$ was purchased from Merck (Darmstadt, Germany). Collagenase (type 2) was purchased from Worthington Biochemical Corporation (Lakewood, NJ, USA). TTC was purchased from GFS Chemicals (Powell, Ohio, USA). Formalin was purchased from Cromoline Quimica Fina Ltda (SP, Brazil). Heparin was purchased from Blau Farmaceutica (SP, Brazil).

4.1.2 Experimental Animals

Male Wistar rats of body weight 250-300 g were used for the experiments. Animals were housed in polypropylene cages lined with husk, allowed free access to water and standard pellet diet and maintained under standard laboratory conditions (12 h light/dark cycle at 22 ± 5^0C with 60 ± 10 % relative humidity) in the departmental animal house. All animal procedures were approved by the Committee on Ethical Use of Animals (CEUA) of the Federal University of Minas Gerais, Brazil. The study was carried out in compliance with recommendations in the Guide for the Care and Use of Laboratory Animals of the National Institute of Health (NIH Pub. No. 85-23, revised 1985).

4.2 METHODS

4.2.1 Preparation of Drugs

Drug solutions (andrographolide and isoproterenol hydrochloride) were prepared in 0.9 % normal saline solution under sterile condition and used within 10 min of preparation.

4.2.2 Experimental Induction of Myocardial Infarction

Myocardial infarction was induced in rats with two consecutive doses of Isoproterenol hydrochloride (80 mg/kg) injected subcutaneously at an interval of 24 h (B. Y. Guo et al., 2011; Rona et al., 1959; Saroff and Wexler, 1970).

4.2.3 Evaluation of Maximum Tolerated Dose (MTD)

Healthy male Wistar rats (250-300g) were randomly divided into 6 groups (n = 5 per group) and then received graded doses of andrographolide formulated in 0.9 % saline solution with one dose daily by subcutaneous administration for a period of 21 days (3 weeks). The control group was given only 0.9 % saline solution and the remaining groups were injected with andrographolide at 10, 20, 40, 80, and 160 mg/kg body weight. The body weight, clinical signs of distress, behavioral change and mortality of rats were observed daily during 3 weeks of study. Animals were anesthetized with isoflurane and humanely euthanized by decapitation when displayed signs of compound-related intolerance such as skin swollen and severe unrelieved distress. At the end of the study, all animals were anesthetized with isoflurane and humanely euthanized by decapitation.

4.2.4 Experimental Design

Animals were randomly divided into four groups: Control (Ctr), Isoproterenol (Iso), Andrographolide (Andro), and Andrographolide plus Isoproterenol (Andro + Iso). Ctr group received 0.9 % normal saline solution once daily for 21 days. The Iso group received 0.9 % normal saline solution once daily for a period of 19 days, and on day 20 and 21 received 80 mg/kg/day of isoproterenol hydrochloride solution. Andro group received 20 mg/kg/day of andrographolide for 21 days. Likewise, Andro + Iso group were pretreated with 20 mg/kg/day of andrographolide for a period 21 days and in addition received 80 mg/kg/day of isoproterenol hydrochloride solution on day 20 and 21 respectively (Fig. 4.1). All treatments

were administered subcutaneously. Experimental assessments of the animals were done 24 h after the last administration, beginning with non-invasive assessments after which the animals were sacrificed and samples were collected for analysis of various parameters of interest to the study.

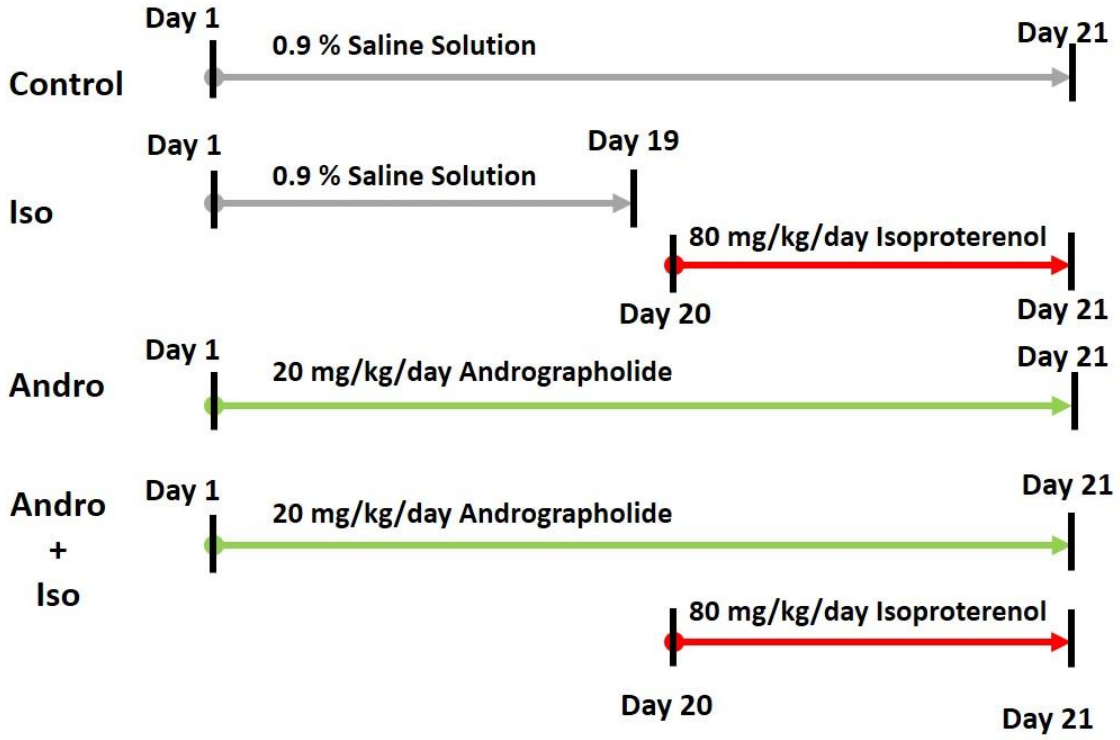

Figure 4.1. Schematic Illustration of Experimental Design for *in-vivo* Studies. All treatments were administered through subcutaneous route and experimental assessment of impacts of all treatments were done 24 h after the last administration.

4.2.5 Electrocardiography Experiments

Real-time monitoring, acquisition and analysis of ECG pattern was performed using a simultaneous 12-channel ECG module for veterinary (ECG-PC TEB, São Paulo, Brazil) as previously described (Costal-Oliveira et al., 2016). Briefly rats were anaesthetized with isofluranol using Brasmed veterinary anaesthetic inhaler (Brasmed, São Paulo, Brazil). Animals were then placed in supine position and electrodes were attached underneath the forelimbs and the hindlimbs. The ECG tracings were recorded at speed of 50 mm/s and

sensitivity of 2 N. Then, parameters of interest to the study; heart rate (HR), PR interval (PRi), QRS complex duration, QT interval (QTi), corrected QT interval (QTc) and S wave amplitude were all analyzed on the lead II channel.

4.2.6 Biometrical Indexes Measurement

Cardiac hypertrophy was assessed by measuring biometrical indexes including the heart weight/body weight ratio and heart weight/tibia length ratio as previously described (Yin et al., 1982). Body weight of animals was measured prior to sacrifice. After sacrifice, the heart was removed and immediately placed in cold phosphate-buffered saline (PBS) (1X) solution for cleaning of blood remnants in the heart chambers. After which the heart was blotted dry and weighed. One leg was severed above the knee joint from each animal, and the muscle and skin of the tibia were removed by mechanical stripping. Then the length of the tibia from the condyles to the tip of the medial malleolus was measured using Vernier caliper.

4.2.7 Cardiac Biochemical Markers' Assay

Blood sample was collected from the animals 24 h after the last administration through cardiac puncture. The blood was centrifuged at 4500 rpm for 15 min; the serum was aspirated and used for the assays. Aspartate transaminase (AST), lactate dehydrogenase (LDH), creatine kinase (CK) and creatine kinase-MB fraction (CK-MB) activities were determined in the serum by enzymatic method using commercial kit (Kovalent, RJ, Brazil) and quantified by spectrophotometry at 340 nm using COBAS MIRA random access biochemistry analyser (Roche Diagnostic Corporation, Branchburg, NJ). Troponin I (cTnI) concentration was determined in the serum by rapid chromatographic immunoassay using commercially available kit (Biocon, BH, Brazil).

4.2.8 Hematological Analysis

Whole blood was aliquoted into an EDTA-tube for hematological analysis. For total erythrocytes (RBC) and leukocytes (WBC) count, 20 µL of total blood was diluted in 3.98 mL of Gower solution and 0.38 mL of Turk solution, respectively. Neubauer chamber was used for RBC and WBC count and the content of cells per microliter of sample was calculated from the equations:

$$Erythrocytes/mm^3 of\ blood = Counted\ cells \times 10.000$$

$$Leukocytes/mm^3 of\ blood = Counted\ cells \times 50$$

Blood slides were made and rapid panoptic staining (NewProv, Brazil) was used for differential leukocytes count. 100 leukocytes were counted in different sites and results were expressed in percentage.

4.2.9 Oxidative Stress Assessment

4.2.9.1 Tissue Preparation and Total Protein Determination

Animals were sacrificed by decapitation 24 hours after the last administration and the heart was excised. Heart (0.2g) were weighed and homogenized (Euro Turrax T20b IKA LABORTECHNIK) in 1ml of PBS (pH 7.2) on ice, the homogenates were centrifuged at 10,000g for 15min and the supernatant was used for malondialdehyde (MDA) concentration, superoxide dismutase (SOD) and catalase activities analysis. For glutathione peroxidase (GPx) activity analysis, the tissues were homogenized in ice-cold Tris·HCl buffer (50mM, pH 7.5, containing 5mM EDTA) and centrifuged at 10,000g (4°C) for 20min, and the supernatant was used for the experiment. Total protein (TP) concentrations in the samples were determined by Lowry method with bovine serum albumin used as standard (Lowry et al., 1951).

4.2.9.2 Antioxidant Enzymes' Assay

4.2.9.2.1 Superoxide Dismutase Activity

SOD activity was measured as described by Dieterich et al (Dieterich et al., 2000), with some modifications (Gioda et al., 2010). Briefly, aliquots of the homogenate were added in phosphate-buffered saline (pH 7.2), MTT (1.25mM) and pyrogallol (100mM). After 5 minutes, the reaction was stopped by the addition of DMSO. The absorbance was read at 570nm. The activity of the enzyme was determined from the ability of superoxide dismutase to inhibit autoxidation of pyrogallol and expressed in U/µg protein. Where 1U = 50% inhibition of autoxidation of pyrogallol.

4.2.9.2.2 Catalase Activity

Catalase activity was assayed following the protocol described by Nelson and Kiesow (Nelson and Kiesow, 1972). Briefly, the supernatant (0.05ml) was added in 50mM sodium

phosphate buffer (2ml, pH 7.0, 25°C). The reaction was started by adding H_2O_2 (6mM) and the reaction proceeded for 1min at room temperature. Decomposition of H_2O_2 by catalase was quantified at absorbance of 240nm and expressed in millimoles of H_2O_2 decomposed per minute per milligram of protein ($\Delta E \cdot min^{-1} \cdot mg^{-1}$ protein).

4.2.9.2.3 Glutathione Peroxidase Activity

GPx activity was measured in the supernatants as described by Paglia and Valentine (Paglia and Valentine, 1967), with some modifications (Gioda et al., 2010). Briefly, supernatant (0.004ml) was added to 0.2ml of potassium phosphate buffer (100mM, pH=7.5), contained 2mM reduced glutathione (GSH), 0.1U/ml glutathione reductase, 0.12mM NADPH, 2mM H_2O_2 and 1mM sodium azide. Glutathione peroxidase activity was quantified at absorbance of 340 nm and expressed in mmol $NADPH \cdot min^{-1} \cdot mg^{-1}$ protein.

4.2.9.3 Malondialdehyde Assay

MDA concentration was measured in the supernatants as described by Ohkawa and colleagues (Ohkawa et al., 1979), with some modifications (Janero, 1990). Briefly, supernatant (0.05 ml) was added to mixture containing 0.5 ml of thiobarbituric acid reactive substance (0.67%) and 0.25ml tricloroacetic acid (20%). The reaction mixture was incubated at 100°C for 20 min, after which the absorbance was measured at 532nm and the MDA concentration in the sample expressed in nanomoles per milligram of protein (nmol/mg protein).

4.2.10 Tissue Necrosis Assessment

Tissue Necrosis was assessed using Evans blue/triphenyltetrazolium chloride (TTC) tissue enzyme double staining technique as described previously by others (Bohl et al., 2009; Nachlas and Shnitka, 1963). Briefly, freshly excised heart was cannulated at the aorta, perfused with 200 µL of 1 % Evans blue solution and freezed in a small plastic bag at -20^0C without washing. After 2 h, five transverse sections (about 2mm slice thickness each) were harvested from the tissue using a sharp scalpel and incubated for 20 min in 1 % TTC solution at 37^0C. Thereafter, the sections were fixed in 10 % formalin for another 20 min and then transferred to glass microscope slides for photograph. Infarcted region was objectively differentiated from viable region of the tissue through color threshold mode (healthy/less at-

risk myocardium as dark blue color, healthy/more at-risk myocardium as deep red color and infarcted/most at-risk myocardium as whitish color) using ImageJ software (ImageJ, Version 1.44p, NIH, USA). Infarct size was calculated by dividing infarcted area of each tissue section by their respective total area at risk (AAR) (i.e., the total volume of the tissue section) and expressed as percentage.

4.2.11 Histological Assessment

Hearts were excised immediately after sacrifice, quickly rinsed in ice-cold PBS solution (pH 7.2), dried with blotting paper and fixed in 10 % formaldehyde solution. The fixed hearts were then dehydrated in graded alcohol (70-100 %), embedded with paraffin and cuts were made 4µm thick. Some sections were stained with hematoxylin and eosin (H&E), and others with Masson's trichrome. Examinations were done under light microscope for histopathological changes and photomicrographs were taken.

4.2.12 Cardiomyocytes Isolation

Cardiomyocytes were enzymatically isolated as previously described by others (Shioya, 2007). Animals were given 200 U of heparin (i.p.) for anticoagulation before decapitation. The heart was excised, cannulated through the aorta and immediately mounted on a temperature controlled (37^{o}C) perfusion system. The heart was then retrogradely perfused with Cell Isolation Buffer (CIB) supplemented with 0.4 mM EGTA. The CIB contained 130 mM NaCl, 5.4 mM KCl, 0.5 mM $MgCl_2.6H_2O$, 0.33 mM NaH_2PO_4, 22 mM glucose, 25 mM HEPES free acid and 50 µU/ml bovine insulin (pH set to 7.4 with NaOH). After few minutes of stabilization, the perfusate was switched to enzyme solution made up of CIB supplemented with 0.3 mM $CaCl_2$, 1mg/ml collagenase, 0.06 mg/ml trypsin and 0.06 mg/ml protease for 6 min. The digested heart was then excised, shredded into several pieces and further digested by incubation at 37^{o}C in fresh enzyme solution for 20 min. After which the digested tissue was briefly subjected to gentle mechanical agitation and filtered. The filtrate containing the cardiomyocytes was then centrifuged at 14 x g for 3 min. The cell pellet was resuspended in CIB supplemented with 1.2 mM $CaCl_2$ and 2 mg/ml BSA, incubated at 37^{o}C for 10 min, centrifuged (14 x g, 3 min) and then resuspended in tyrode solution (in mM) 140 NaCl, 5.4 KCl, 0.5 $MgCl_2.6H_2O$, 0.33 NaH_2PO_4, 11 glucose, 5 HEPES free acid, 1.8 $CaCl_2.2H_2O$ (pH

set to 7.4 with NaOH) supplemented with 2 mg/ml BSA. The isolated cardiomyocytes were used for experiments within 8 h after isolation.

4.2.13 Cardiomyocytes Contractile Analysis

The contractile properties of isolated cardiomyocytes from various groups were assessed using a video-based edge-motion detection system (Ionoptix, MA, USA) as previously described (Roman-Campos et al., 2009). Cells were placed in a coverslip chamber with lumini glass base, mounted on the stage of an inverted microscope (Nikon Eclipse TS100, Tokyo, Japan) and superfused with Tyrode solution. The cells were field stimulated with suprathreshold voltage at a frequency of 1 Hz and duration of 3 ms with the aid of a pair of platinum electrodes connected to an SD9 stimulator (GRASS Tech., Austin, Texas). Cells were visualized on a PC monitor with an NTSC camera (MyoCam, Ionoptix, MA, USA) attached to the microscope. Myocyte lengths at maximal contraction and relaxation were electronically captured as contractile traces by the edge motion detector. The contractile traces were then sampled (at least 50 consecutive contractions for each cell), analyzed with IonWizard software (Ionoptix, MA, USA) and the obtained cell shortening and derivatives indexes of contractility averaged.

4.2.14 Patch Clamp Experiments

Whole-cell recordings were obtained using an EPC-10plus patch clamp amplifier (HEKA Electronics, Rheinland-Pfalz, Germany) at room temperature (23-25^{0}C). After the establishment of the whole-cell configuration, the cells were maintained for 3-5 min at rest to give room for ionic equilibrium between the pipette solution and the intracellular medium. The patch pipettes were fabricated from 1.5 mm diameter thin-walled glass capillaries (Perfecta Ltda, SP, Brazil), using a vertical puller (PP-830, Narishige, Tokyo, Japan), and had a 1-4 MΩ resistance when filled with internal solution.

4.2.14.1 Action Potential (AP) Recording

For the recording of action potential, cardiomyocytes were maintained in external solution containing (in mM) 140 NaCl, 5.4 KCl, 0.5 $MgCl_2.6H_2O$, 0.33 NaH_2PO_4, 11 glucose, 5 HEPES free acid and 1.8 $CaCl_2.2H_2O$ (pH set to 7.4 with NaOH). Pipettes were filled with an internal solution containing (in mM) 130 L-aspartic acid, 20 KCl, 5 NaCl, 2 $MgCl_2.6H_2O$,

10 HEPES free acid and 5 EGTA (pH set to 7.4 with KOH). Action potentials were evoked by applying a test pulse of 1 nA current for a duration of 5 ms at 1 Hz frequency.

4.2.14.2 L-type Calcium Current ($I_{Ca,L}$) Recordings

To record L-type Ca^{2+} current, cardiomyocytes were maintained in external solution containing (in mM) 150 TEA-Cl, 0.5 $MgCl_2.6H_2O$, 1.8 $CaCl_2.2H_2O$, 10 HEPES free acid and 11 glucose (pH set to 7.4 with TEA-OH). Pipette solution contained (in mM) 120 CsCl, 20 TEA-Cl, 5 NaCl, 10 HEPES free acid, 10 EGTA and 1 $MgCl_2.6H_2O$ (pH set to 7.4 with CsOH). The holding potential was set at -80 mV, prepulse was applied from -80 mV to -40 mV for 50 ms to inactivate any remnants Na^+ channels and then pulses were applied from -50 mV to +40 mV in 10 mV increments for 400 ms.

4.2.14.3 Total Potassium Current (I_K+) Recording

To record whole-cell potassium current, cardiomyocytes were maintained in external solution containing (in mM) 140 NMDG, 5.4 KCl, 1.8 $CaCl_2.2H_2O$, 0.1 $CdCl_2$, 0.5 $MgCl_2.6H_2O$, 5.5 glucose and 5 HEPES free acid (pH set to 7.4 with HCl). Pipette solution contained (in mM) 130 KCl, 1 $MgCl_2.6H_2O$, 2 ATP disodium trihydrate, 10 HEPES free acid and 5 EGTA (pH set to 7.4 with KOH). The holding potential was set at -80 mV from which depolarizing pulse was applied to raise the membrane potential to +60 mV in 10 mV increments for 3 s and the transient outward potassium current (I_{to}) was measured at the peak of the depolarized test potential (+60 mV).

4.2.15 Concentration-Response Assessments

To validate the cardioprotective mode of action of andrographolide, effects of andrographolide on the mechanical and electrical properties of cardiac myocytes were further assessed *in vitro* in reference to a standard drug of MI (nicardipine). Briefly, cardiomyocytes were isolated from hearts excised from healthy male Wistar rats (that was not given any treatments) and the cardiomyocytes were used for the experiments.

To investigate the concentration-response impacts of andrographolide on cardiac mechanical activities, cardiomyocytes were incubated in andrographolide (10^{-5} M, 10^{-4} M & 10^{-3} M) and nicardipine (10^{-5} M) for 10 minutes. Unincubated cardiomyocytes were used as control. Then,

the contractile analysis of cardiomyocytes from each group were analyzed as described earlier.

To investigate the concentration-response impacts of andrographolide on cardiac action potential, time course of AP was recorded before and after exposure to andrographolide (10^{-5} M, 10^{-4} M & 10^{-3} M) in comparison with nicardipine (10^{-5} M). To do this, AP was evoked by applying a test pulse of 1 nA current for a duration of 5 ms at 1 Hz frequency. With this protocol, 30 consecutive sweeps of AP (4s between each) were recorded for the control, followed by another 30 consecutive sweeps (4s between each) for the test in each case.

To investigate the concentration-response impacts of andrographolide on the cardiac L-type Ca^{2+} current, time course of $I_{Ca,L}$ peak current was recorded before and after exposure to andrographolide (10^{-5} M, 10^{-4} M & 10^{-3} M) in comparison with nicardipine (10^{-5} M). To do this, prepulse was applied from holding potential of -80 mV to -40 mV for 50ms, from which test pulse was applied to raise the membrane potential to 0 mV for 400ms to directly measure $I_{Ca,L}$. With this protocol, 6 consecutive sweeps of $I_{Ca,L}$ (20s between each) were recorded for the control, followed by another 6 consecutive sweeps (20s between each) for the test in each case.

To investigate the concentration-response impacts of andrographolide on the cardiac transient outward potassium current, time course of I_{to} peak current was recorded before and after exposure to andrographolide (10^{-5} M, 10^{-4} M & 10^{-3} M) in comparison with nicardipine (10^{-5} M). To do this, holding potential was set at -80 mV and then depolarized to +60 mV for 600ms to directly measure I_{to}. With this protocol, 6 consecutive sweeps of I_{to} (20s between each) were recorded for the control, followed by another 6 consecutive sweeps (20s between each) for the test in each case.

4.2.16 Statistical Analysis

Most data were analyzed by one-way analysis of variance (ANOVA), followed by Bonferroni's multiple comparisons test, others were analyzed by paired t-test using GraphPad Prism 8.0 (GraphPad Software, CA, USA). Results are presented as Mean ± Standard Deviation (SD). For all comparisons, p values lower than 0.05 were considered statistically significant.

V. RESULTS

5.1 Maximum Tolerated Dose of Andrographolide in Rats

A maximum tolerated dose (MTD) test was performed to determine the amount of andrographolide which could be administered in rats (Fig. 5.1). The animals tolerated a dose up to 80 mg/kg with no significant changes in animal behavior and no clinical signs of distress. However, an animal in the group subjected to the highest dose of andrographolide (160 mg/kg) showed clinical signs of distress including skin swollen on day 17 of treatments and was euthanized. Thus, the MTD study indicated that the maximum tolerated dose of andrographolide is between 80 and 160 mg/kg in male Wistar rats. Therefore, informed the choice of 20 mg/kg/day dose for the *in-vivo* efficacy assays in agreement with previous scientific evidences (Al Batran et al., 2014; Liang et al., 2018).

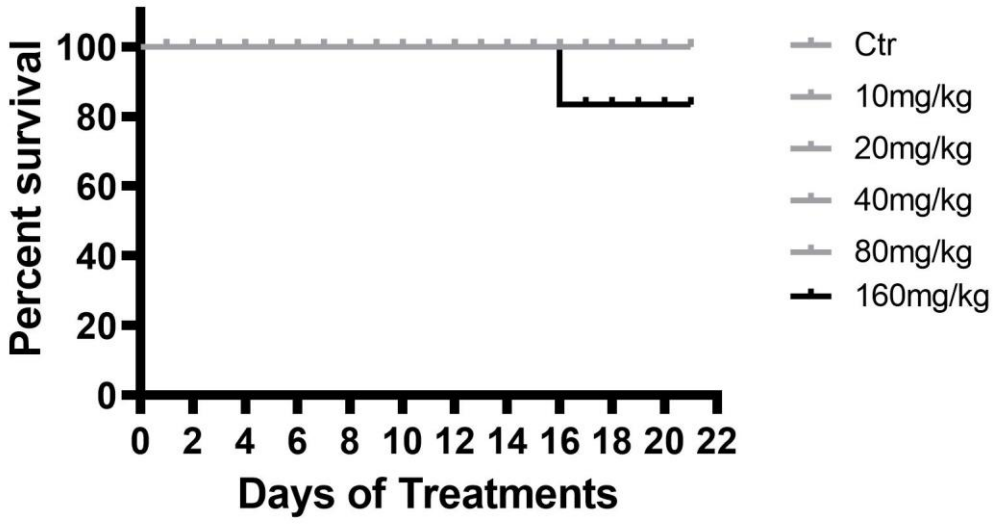

Figure 5.1. Rats Survival Curves from Maximum Tolerated Dose Study. All animals (n = 5 per group) received one dose daily for 21 days (3 weeks). 0.9% saline solution was used as the vehicle of administration and also served as negative control.

5.2 Andrographolide Pretreatment Prevents Infarction-like Changes in ECG Profiles

To assess the impacts of andrographolide on the electrical activities of the heart, ECG profiles were measured in each experimental group. Twenty (20) complete cycles were sampled for each experimental group, results show unambiguous ST-segment elevation in Iso group compared to the Ctr, while both Andro and Andro + Iso group exhibited normal ST-segment similar to the Ctr when compared to the Ctr and Iso group (Fig. 5.2). In addition, results show a significant ($p < 0.05$) increase in heart rate (HR) in Iso group compared to the Ctr, while both Andro and Andro + Iso group exhibited a Ctr level HR when compared to Iso group (Fig. 5.3A). There was no significant change recorded in the PR interval across all experimental groups, indicating no signaling blockage from the atria to the ventricle (Fig. 5.3B). On the other hand, QRS, QT and QTc were in similar fashion increased significantly ($p < 0.05$) in Iso group compared to the Ctr, suggesting ventricular dysfunction typical of MI. Interestingly, almost all of these parameters were maintained significantly ($p < 0.05$) at Ctr levels and near Ctr levels in Andro and Andro + Iso group respectively (Fig. 5.3C-E). A remarkable increase was also recorded in S wave amplitude in Iso group which further confirms the ST-segment elevation, whereas, andrographolide kept the S wave amplitude slightly below the isoelectric line in Andro and Andro + Iso group (Fig. 5.3F).

Figure 5.2. Representative ECG Records for All Experimental Groups. It shows 20 complete cycles sampled from each experimental group with distinct ST-segment elevation in Iso group typical of MI while other groups exhibited normal ST-segments.

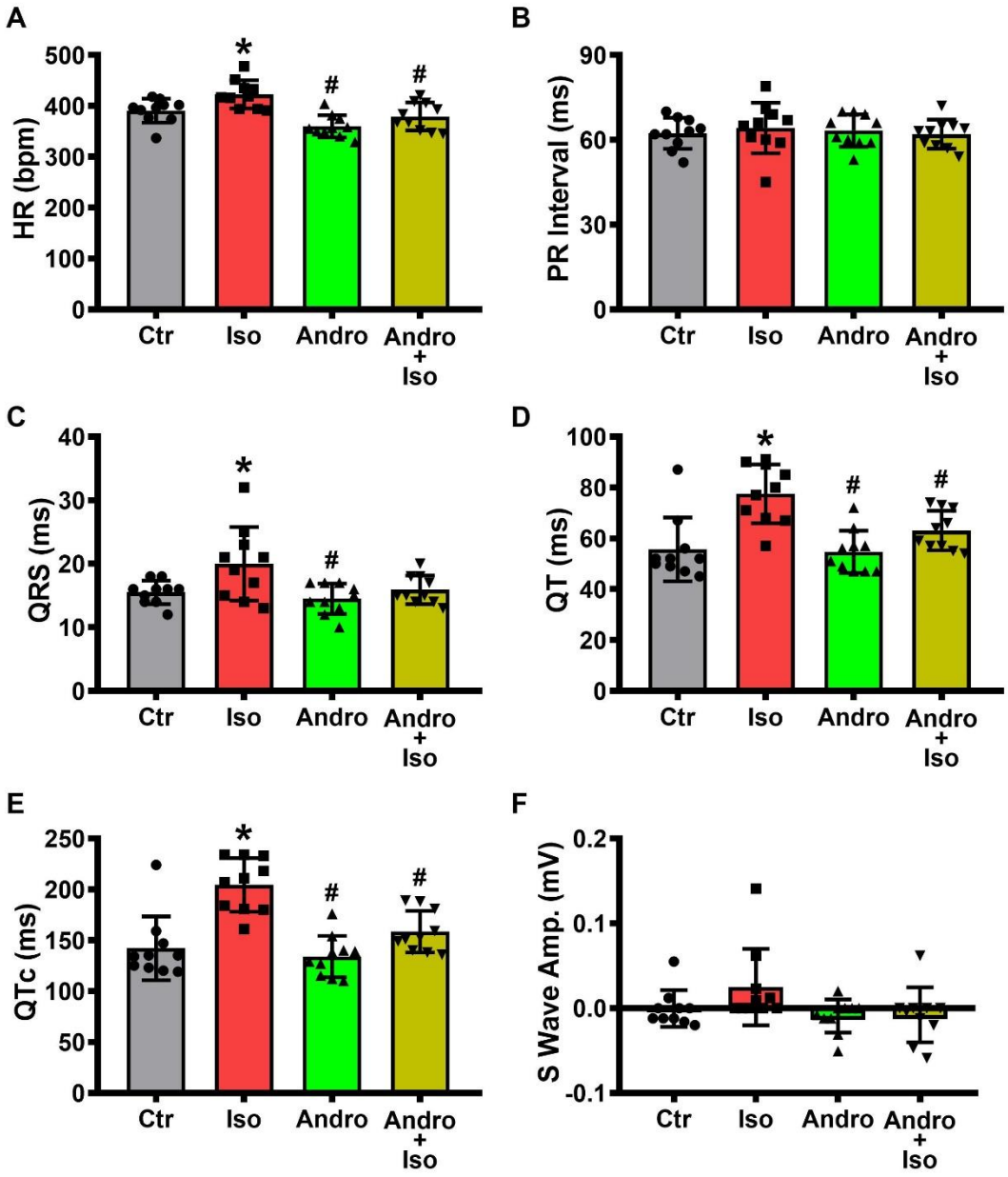

Figure 5.3. Effects of Andrographolide on Cardiac ECG Profiles. (A) Heart rate (HR). (B) PR interval. (C) QRS complex. (D) QT interval. (E) Corrected QT interval (QTc). (F) S wave amplitude. HR, QRS, QT and QTc were all increased markedly in Iso group as against Andro group and Andro + Iso group where the parameters were maintained at control levels. Data are presented as Mean ± SD, n = 10 per group and analysed by one-way ANOVA followed by Bonferroni's multiple comparisons test. *$p < 0.05$ vs Ctr and $^{\#}p < 0.05$ vs Iso.

5.3 Andrographolide Pretreatment Minimizes MI-associated Cardiac Hypertrophy

To assess the effects of andrographolide on the heart tissue intrinsic compensatory response to myocardial damage (cardiac hypertrophy) usually accompanied MI, biometrical indexes including body weight (BW), tibia length (TL), heart weight (HW), HW/BW ratio and HW/TL ratio were measured for each experimental group. There were no statistically significant differences recorded in BW (Fig. 5.4A) as well as TL (Fig. 5.4B) across all experimental groups. Thus, validates that animals used for the study were indeed of the same age and weight range. However, the HW, HW/BW ratio and HW/TL ratio were significantly ($p < 0.05$) increased in Iso group compared to the Ctr, while the indexes were maintained at Ctr levels in Andro group. Consequently, the indexes were significantly ($p < 0.05$) reduced to near Ctr levels in Andro + Iso group when compared to Iso group (Fig. 5.4C-E). Hence, suggesting that andrographolide minimized ventricular wall stress, a major event required for the induction of cardiac hypertrophy in MI.

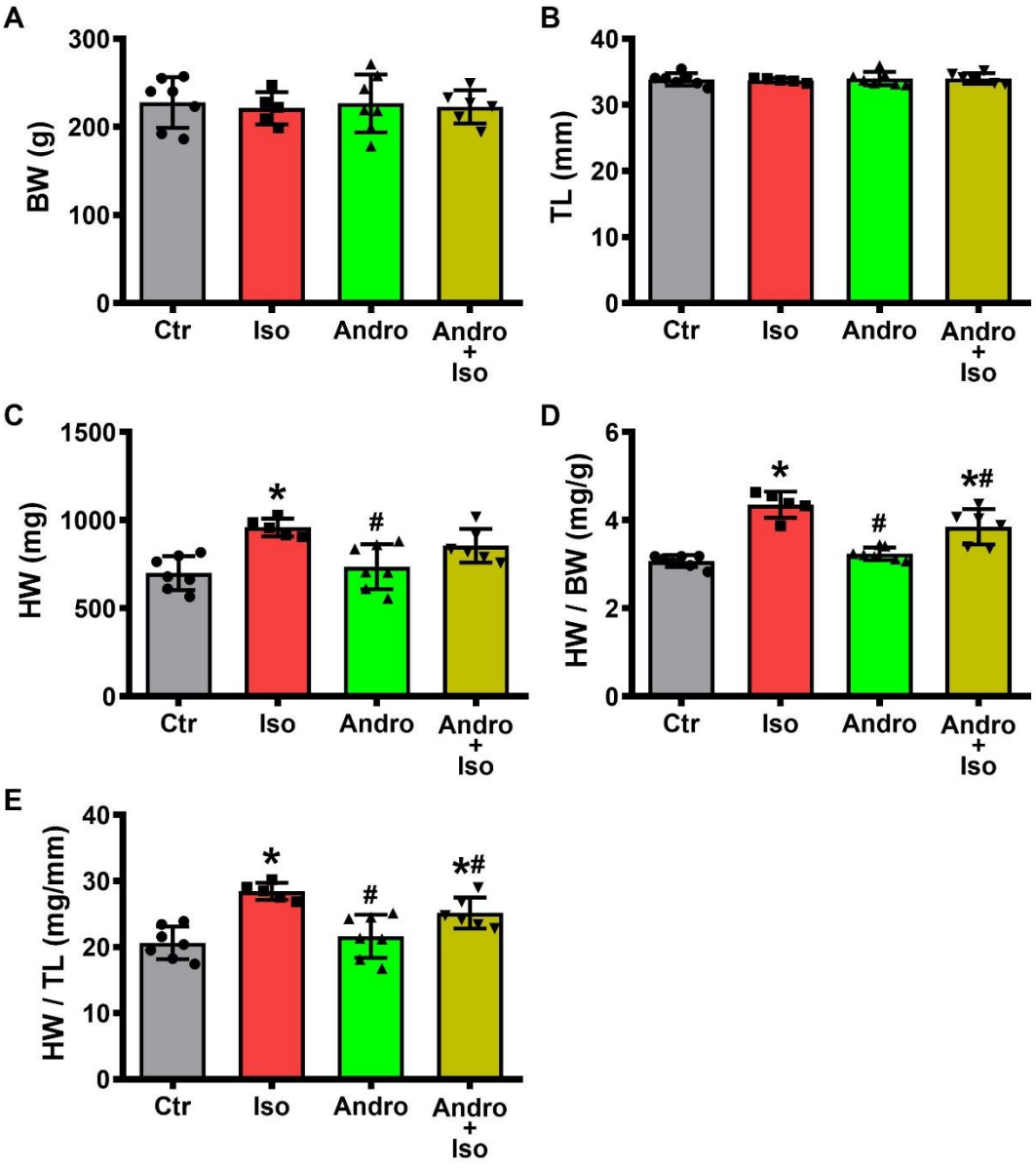

Figure 5.4. Effects of Andrographolide on MI-Associated Cardiac Hypertrophy. (A) Body weight (BW). (B) Tibia length (TL). (C) Heart weight (HW). (D) Heart weight/body weight ratio (HW/BW). (E) Heart weight/tibia length ratio (HW/TL). BW as well as TL were maintained at relatively the same range in all experimental groups. HW, HW/BW and HW/TL were remarkably increased in Iso group while the indexes were maintained at control levels in Andro group and near control levels in Andro + Iso group. Data are presented as Mean ± SD, n = 7 for Ctr and Andro, while n = 5 for Iso and n = 6 for Andro + Iso group, analysed by one-way ANOVA followed by Bonferroni's multiple comparisons test. *$p < 0.05$ vs Ctr and $^{\#}p < 0.05$ vs Iso.

5.4 Andrographolide Pretreatment Prevents MI-associated Increases in Systemic Cardiac Markers

To determine the impacts of andrographolide on systemic myocardial injury markers, serum levels of CK, CK-MB, LDH, AST and cTnI were measured in all experimental groups (Fig. 5.5A-E). A significant ($p < 0.05$) increase was recorded in the levels of CK, CK-MB, AST, and a remarkable increase in the level of cTnI, as well as a slight increase in the level of LDH in Iso group compared to the Ctr. Whereas, levels of these parameters were maintained almost at the Ctr levels in Andro group as well as Andro + Iso group when compared to the Iso group. Indicating astonishing prevention of MI-associated myocardial membrane leakages by andrographolide.

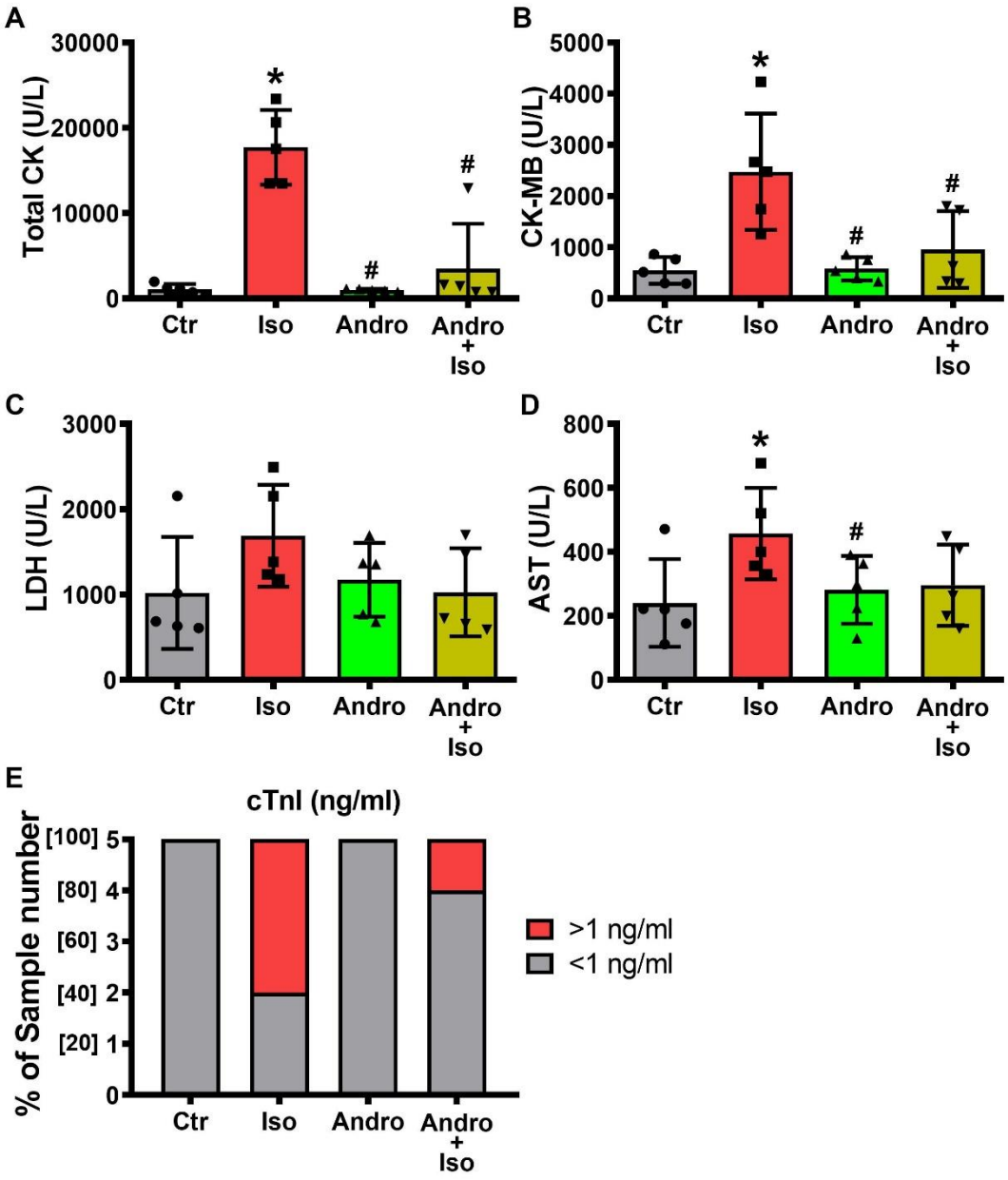

Figure 5.5. Effects of Andrographolide on Systemic Cardiac Markers. (A) Total creatine kinase (CK). (B) Creatine kinase-MB (CK-MB). (C) Lactate dehydrogenase (LDH). (D) Aspartate transaminase (AST). (E) Cardiac troponin I (cTnI). Levels of these serum markers of myocardial injury were markedly increased in Iso group as against Andro group and Andro + Iso group where they were maintained almost at the control levels. Data are presented as Mean ± SD, n = 5 per group and analysed by one-way ANOVA followed by Bonferroni's multiple comparisons test. *$p < 0.05$ vs Ctr and $^{\#}p < 0.05$ vs Iso.

5.5 Andrographolide Pretreatment Minimizes MI-associated Increase in Systemic Leukocytes

To determine the effects of andrographolide on abnormal changes in hematological profiles that usually accompanied MI, levels of key systemic blood cells (RBC and WBC) were measured in each experimental group. There was no significant difference recorded in the RBC counts across various experimental groups (Fig. 5.6A). On the other hand, while WBC count was maintained at the Ctr level in Andro group, same was significantly ($p < 0.05$) increased in Iso group when compared to the Ctr. However, in Andro + Iso group the WBC count was slightly reduced to a near control level when compared to the Iso group (Fig. 5.6B).

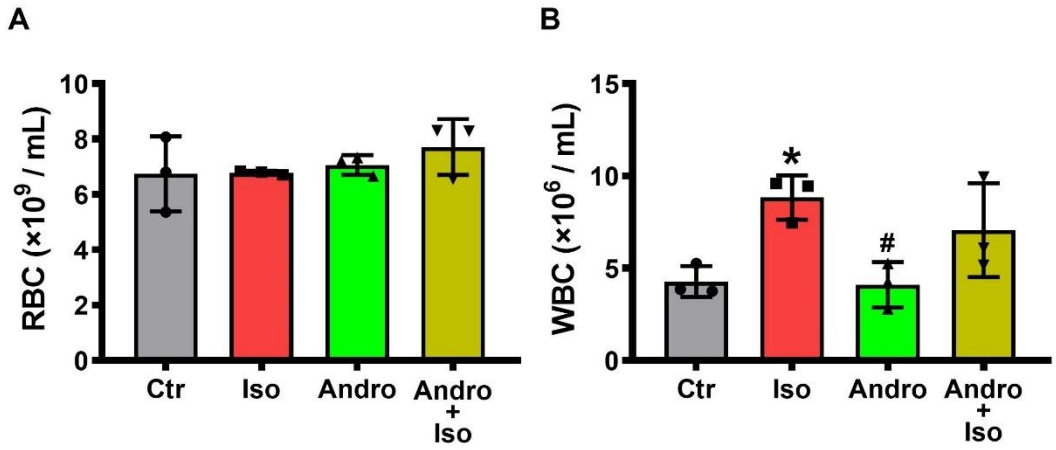

Figure 5.6. Effects of Andrographolide on MI-associated Abnormal Variation in Blood Cells. (A) Red blood cell (RBC) count. There was no significant variation recorded in RBC counts across all groups. (B) White blood cell (WBC) count. WBC counts was markedly increased in Iso group, whereas, same was reduced to a near control level in group pretreated with andrographolide (Andro + Iso). Data are presented as Mean ± SD, n = 3 per group and analysed by one-way ANOVA followed by Bonferroni's multiple comparisons test. *$p < 0.05$ vs Ctr and $^{\#}p < 0.05$ vs Iso.

5.6 Andrographolide Pretreatment Prevents Myocardial Oxidative Stress

To assess the effects of andrographolide on cardiac oxidative stress commonly associated with MI, levels of cardiac antioxidant enzymes (SOD, catalase & GPx) and product of lipid peroxidation (MDA) were measured in all experimental groups. Result shows no significant difference in the SOD activity across all the experimental groups (Fig. 5.7A). However, decreases were recorded in catalase ($p < 0.05$) and GPx activities (Fig. 5.7B&C) in Iso group when compared to the Ctr group, indicating substantial oxidative stress in this group. In contrast, significant increases ($p < 0.05$) were recorded in the activities of both enzymes in Andro + Iso group when compared to the Iso group. This observation could be attributed to the antioxidant effects of andrographolide. Hence, indicative of its ability to protect cardiac tissue against oxidative stress. On the other hand, no evidence of lipid peroxidation was obtained as indicated by no significant changes in the level of MDA across all experimental groups (Fig. 5.7D).

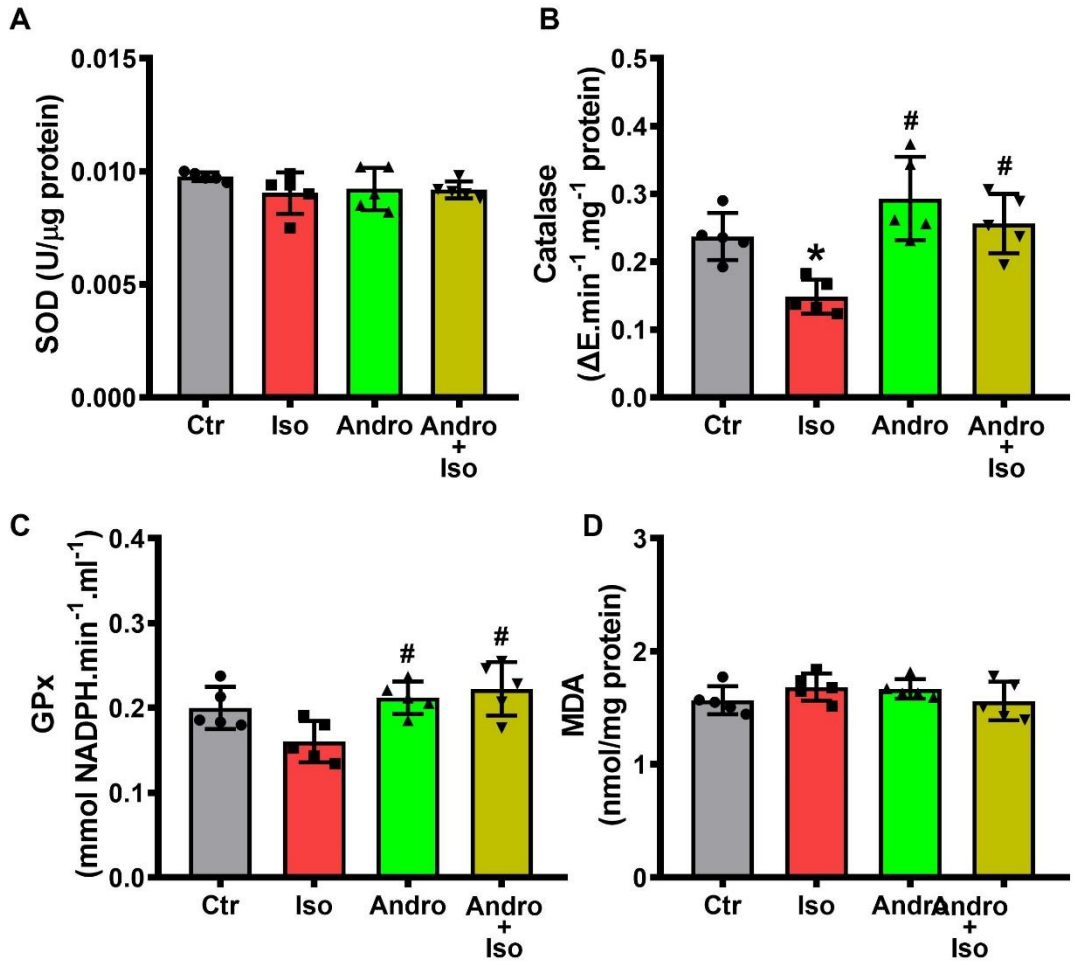

Figure 5.7. Effects of Andrographolide on MI-associated Cardiac Oxidative Stress. (A) Superoxide dismutase (SOD). (B) Catalase. (C) Glutathione peroxidase (GPx). Malondialdehyde (MDA). While levels of SOD and MDA were not significantly changed in all groups, the activities of catalase and GPx were considerably decreased in Iso group as against Andro + Iso group where activities of both enzymes were significantly maintained at the control levels. Data are presented as Mean ± SD, n = 5 per group and analysed by one-way ANOVA followed by Bonferroni's multiple comparisons test. *$p < 0.05$ vs Ctr and $^{\#}p < 0.05$ vs Iso.

5.7 Andrographolide Pretreatment Prevents Infarction-like Ventricular Necrosis

Microscopic images of whole heart tissue taken for each group shows that heart tissues belonging to Ctr, Andro and Andro + Iso maintained the normal healthy heart morphology and color (deep red). Whereas, heart tissues belonging to Iso group appeared pale tan colors, indicating unprecedented levels of injuries and cell death (Fig. 5.8A). Furthermore, a substantial degree of Evans blue/TTC-negative area (whitish color) was observed in the ventricular subendocardial region of tissue sections belonging to Iso group in consistency with the original report of Rona et al that infarct-like necrosis was located most frequently in the apex and subendocardial portion of the ventricles (Rona et al., 1959, 1963). Thus, suggesting a reduced level of dehydrogenase enzymes and cofactors in the tissue sections and by implication the presence of infarction. In contrast, tissue sections from Ctr, Andro and Andro + Iso were mostly Evans blue/TTC-positively stained (dark blue and deep red colors), suggesting higher levels of dehydrogenase enzymes and cofactors which signifies vast area of viable myocardium (Fig. 5.8B). Infarct size quantification in the tissue sections shows that Iso induced significant ($p < 0.05$) increase in infarct size while pretreatment with Andro significantly maintained it at the Ctr level (Fig. 5.8C).

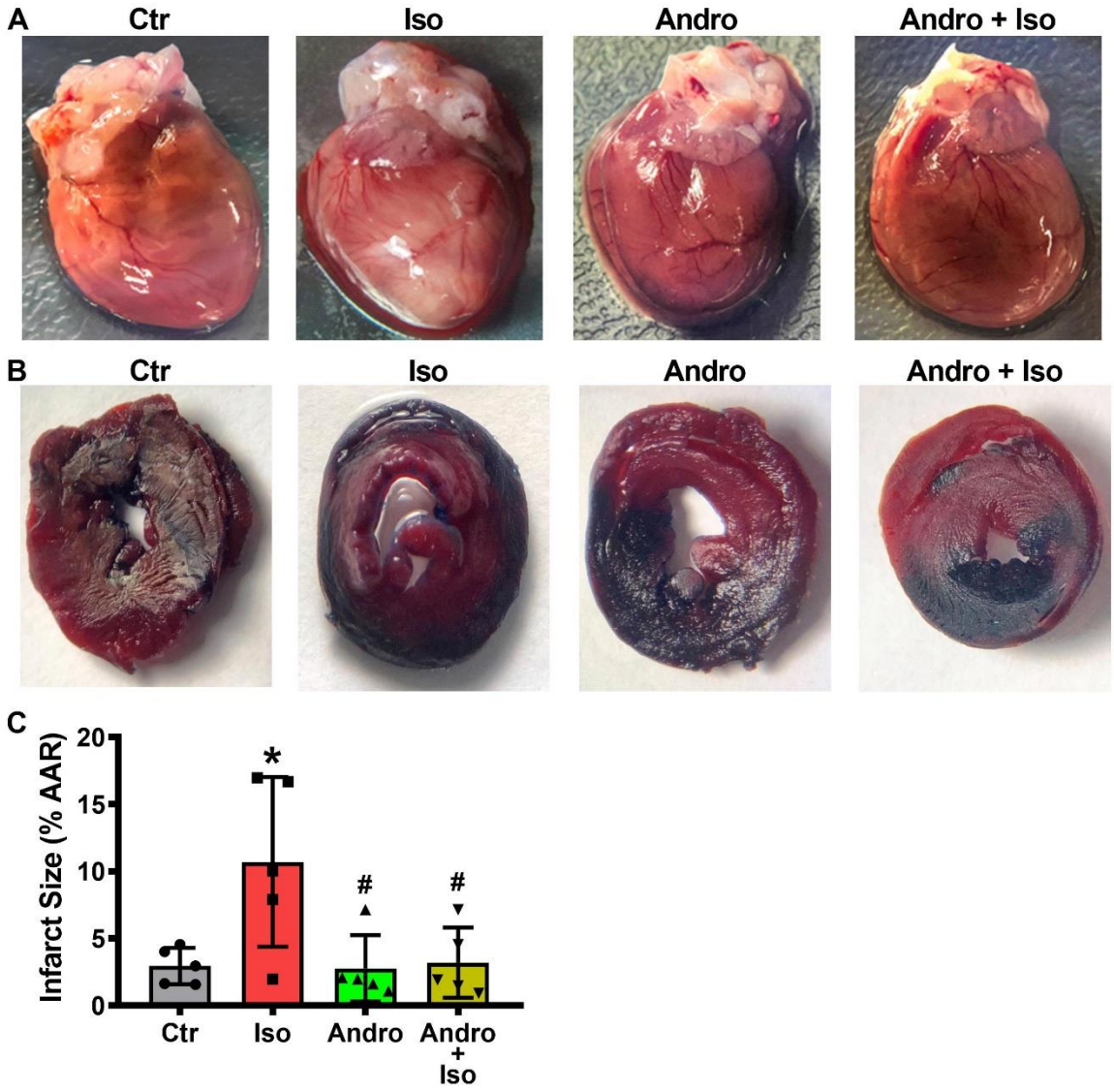

Figure 5.8. Effects of Andrographolide on MI-Associated Cardiac Tissue Necrosis. (A) Representative of whole heart microscopic images of each group. Heart tissues from Ctr, Andro and Andro + Iso groups maintained the normal fresh heart color while that of Iso group appeared mostly pale tan or whitish-brown color. (B) Representative of Evans blue/TTC-stained heart tissue sections of each group. Tissue sections from Ctr, Andro and Andro + Iso groups shows wider areas of positively stained viable myocardial tissue while that of Iso group shows more necrotic area in the ventricular subendocardial region. (C) Impact of andrographolide on infarct size. The infarct size was expressed as a % of areas at risk (AAR). Data are presented as Mean ± SD, n = 5 tissue sections per group and analysed by one-way ANOVA followed by Bonferroni's multiple comparisons test. *$p < 0.05$ vs Ctr and $^{\#}p < 0.05$ vs Iso.

5.8 Andrographolide Pretreatment Minimizes Infarction-like Cardiac Histological Alterations

Impacts of treatments on histological structure of heart tissue of each experimental group are presented in Fig. 5.9 and Fig. 5.10. The Ctr group (Fig. 5.9&5.10A) and Andro group (Fig. 5.9&5.10B) shows normal myocardial histological features, characterized by orderly arranged thin collagen fibers, void of lesions and without interstitial edema and leukocytes infiltrations. In contrast, tissues from Iso group (Fig. 5.9&5.10C), shows apparent myocardial histological alterations including: massive lesions; degeneration, disruption, nuclear enlargement, binucleation and loss of cardiomyocytes; replaced with disorganized fibroblasts and few macrophages. Additionally, was noted edema. Interestingly, these histological alterations were quietly minimized in the Andro + Iso group (Fig. 5.9&5.10D), suggesting myocardial tissue protective ability of andrographolide.

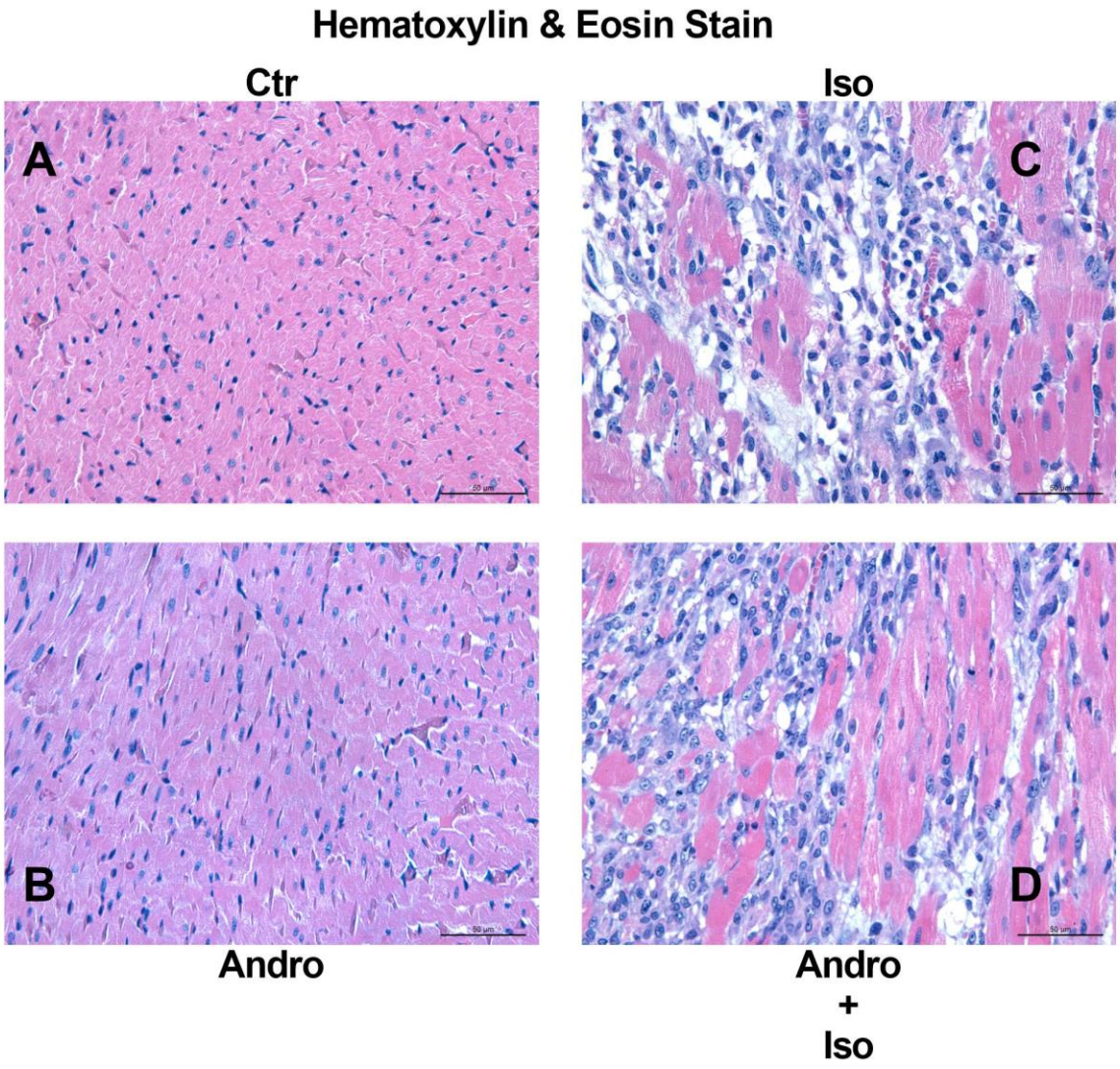

Figure 5.9. Effects of Andrographolide on Histological Structure of Heart Tissue as Revealed by Hematoxylin and Eosin (H&E) Staining. Sections were stained with H&E and visualized under light microscope at magnification of 400x. Micrographs of tissue sections of Ctr (A) and Andro group (B) shows normal heart tissue's histological architecture. In contrast, micrographs of tissue sections of Iso group (C) revealed degeneration, disruption, nuclear enlargement, binucleation and loss of cardiomyocytes, replaced by disorganized fibroblasts and few macrophages which were quietly minimized in the Andro + Iso group (D). Scale = 50 µm.

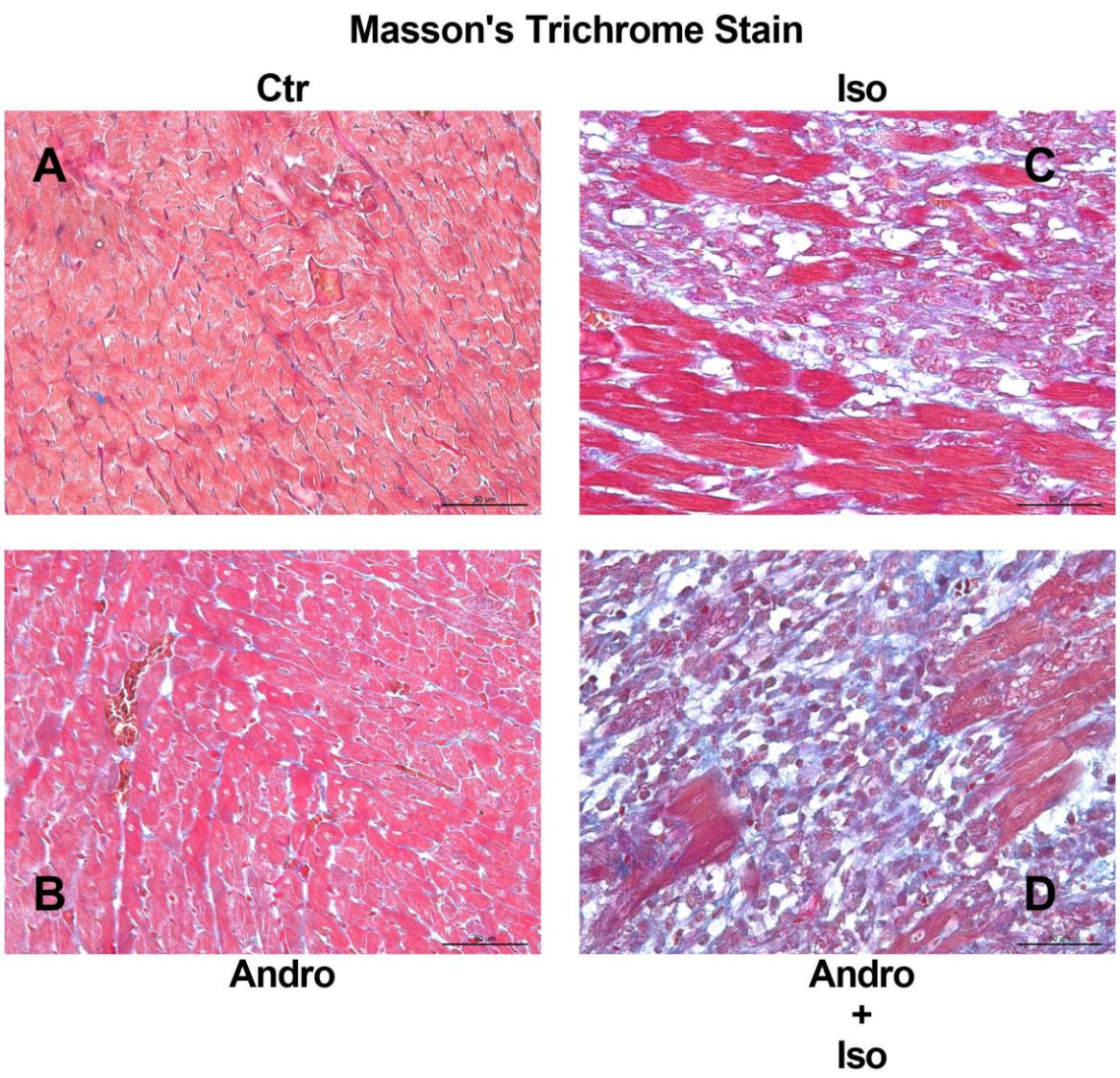

Figure 5.10. Effects of Andrographolide on Histological Structure of Heart Tissue as Revealed by Masson's trichrome Staining. Sections were stained with Masson's trichrome and visualized under light microscope at magnification of 400x. Micrographs of tissue sections of Ctr (A) and Andro group (B) shows normal heart tissue's histological architecture. In contrast, micrographs of tissue sections of Iso group (C) revealed degeneration, disruption, nuclear enlargement, binucleation and loss of cardiomyocytes, replaced by disorganized fibroblasts and few macrophages which were quietly minimized in the Andro + Iso group (D). Scale = 50 µm.

5.9 Andrographolide Pretreatment Averts Uncharacteristic Increases in Myocyte Shortening, Maximal Velocities of Contraction and Relaxation

To determine the effects of andrographolide on the mechanical activities of the heart, cardiomyocytes isolated from each experimental group were subjected to field-stimulation and their contractile properties were recorded using edge motion detection techniques. Results are presented in Fig. 5.11(A-E). Significant ($p < 0.05$) increases were recorded in myocyte shortening (Fig. 5.11A-C), maximal velocity of contraction (+dL/dt) (Fig. 5.11D) and maximal velocity of relaxation (-dL/dt) (Fig. 5.11E) in Iso group compared to the Ctr, suggesting intracellular Ca^{2+} overload and hyper-enhanced intracellular Ca^{2+} cycling respectively. In contrast, the parameters in question were significantly ($p < 0.05$) decreased in Andro group when compared to both the Ctr and Iso group, and were as a result maintained significantly ($p < 0.05$) at the Ctr levels in Andro + Iso group when compared to the Iso group. Thus, our results showed for the first time that, at cellular level, shortening of individual surviving cardiomyocytes increases at the onset of MI and that andrographolide was able to avert the intracellular Ca^{2+} overload and hyper-enhanced intracellular Ca^{2+} cycling insinuated as underlying the phenomenon.

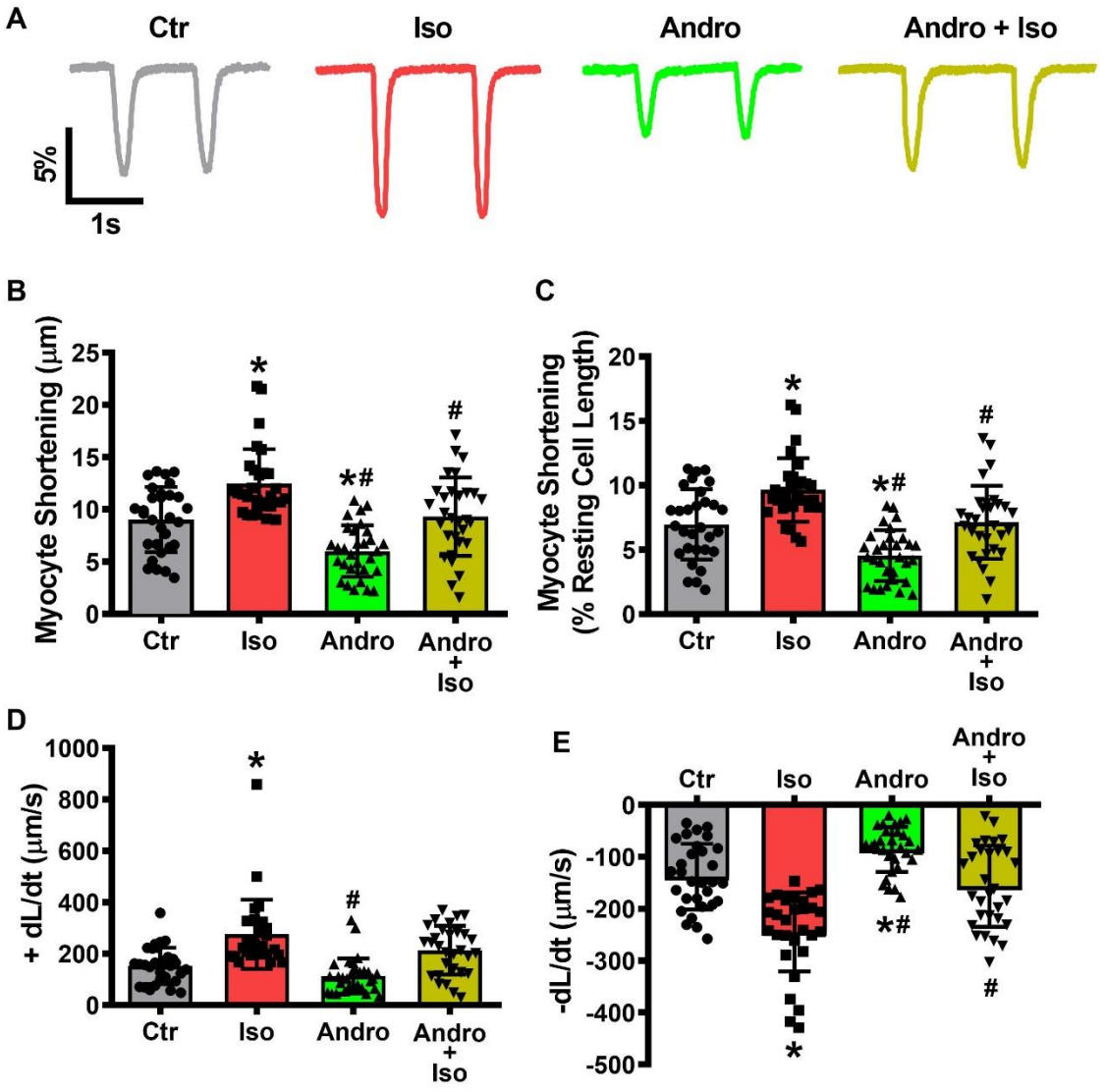

Figure 5.11. Effects of Andrographolide on Cardiac Contractile Properties. (A) Representative contraction traces obtained from cardiomyocytes isolated from each experimental group. (B) Myocyte shortening measured in µm. (C) Myocyte shortening expressed as % of the baseline. (D) Maximal velocity of contraction (+dL/dt). (E) Maximal velocity of relaxation (-dL/dt). Each of these parameters were markedly increased in Iso group, suggesting intracellular Ca^{2+} overload and hyper-enhanced intracellular Ca^{2+} cycling. However, pretreatment with andrographolide maintained them at Ctr levels. Data are presented as Mean ± SD, n = 30 cells per group and analysed by one-way ANOVA followed by Bonferroni's multiple comparisons test. *$p < 0.05$ vs Ctr and $^{\#}p < 0.05$ vs Iso.

5.10 Andrographolide Pretreatment Prevents MI-associated Prolongation of Cardiac Myocytes Action Potential Duration (APD)

To unravel the mode of action of andrographolide, electrical profiles that shapes the functions of the heart were recorded in cardiomyocytes isolated from each experimental group, beginning with action potential (AP). Results shows a clear difference in the AP waveform recorded in Iso group compared to the Ctr and other treatment groups (Fig. 5.12). Despite this difference, we did not find alterations in the resting membrane potential (Fig. 5.13A) and the AP amplitude (Fig. 5.13B) across all the experimental groups. However, the APDs measured at 30 % (APD_{30}), 50 % (APD_{50}) and 90 % (APD_{90}) repolarization (Fig. 5.13C-E) were significantly ($p < 0.05$) prolonged in Iso group compared to the Ctr, suggesting a perturbation of the L-type Ca^{2+} channel in this group which may have facilitated intracellular Ca^{2+} overload and or decreased outward potassium current. Interestingly, the aforementioned parameters were all maintained significantly ($p < 0.05$) at the Ctr levels in Andro as well as Andro + Iso group when compared to the Iso group. Thus, underscoring the ability of andrographolide to prevent MI-associated prolongation of cardiomyocytes APD.

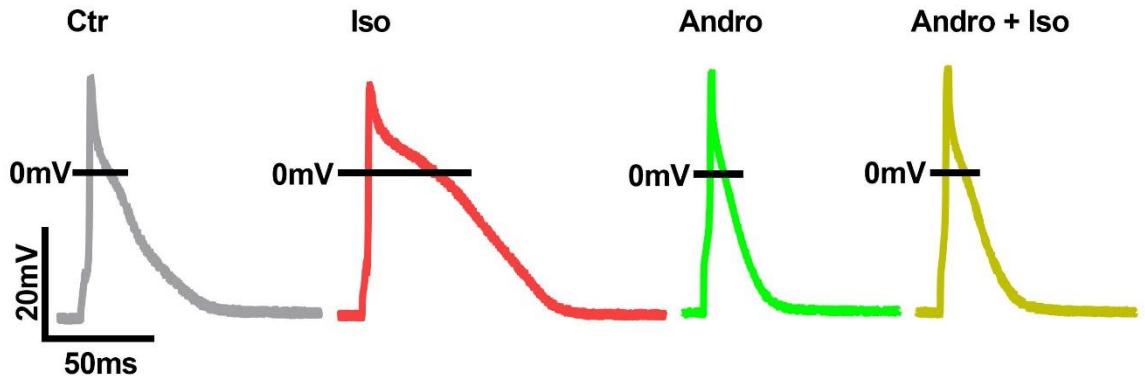

Figure 5.12. Representative AP Traces Obtained from Cardiomyocytes Isolated from Each Experimental Group. APs were elicited by applying test pulse of 1 nA current for duration of 5 ms at frequency of 1 Hz.

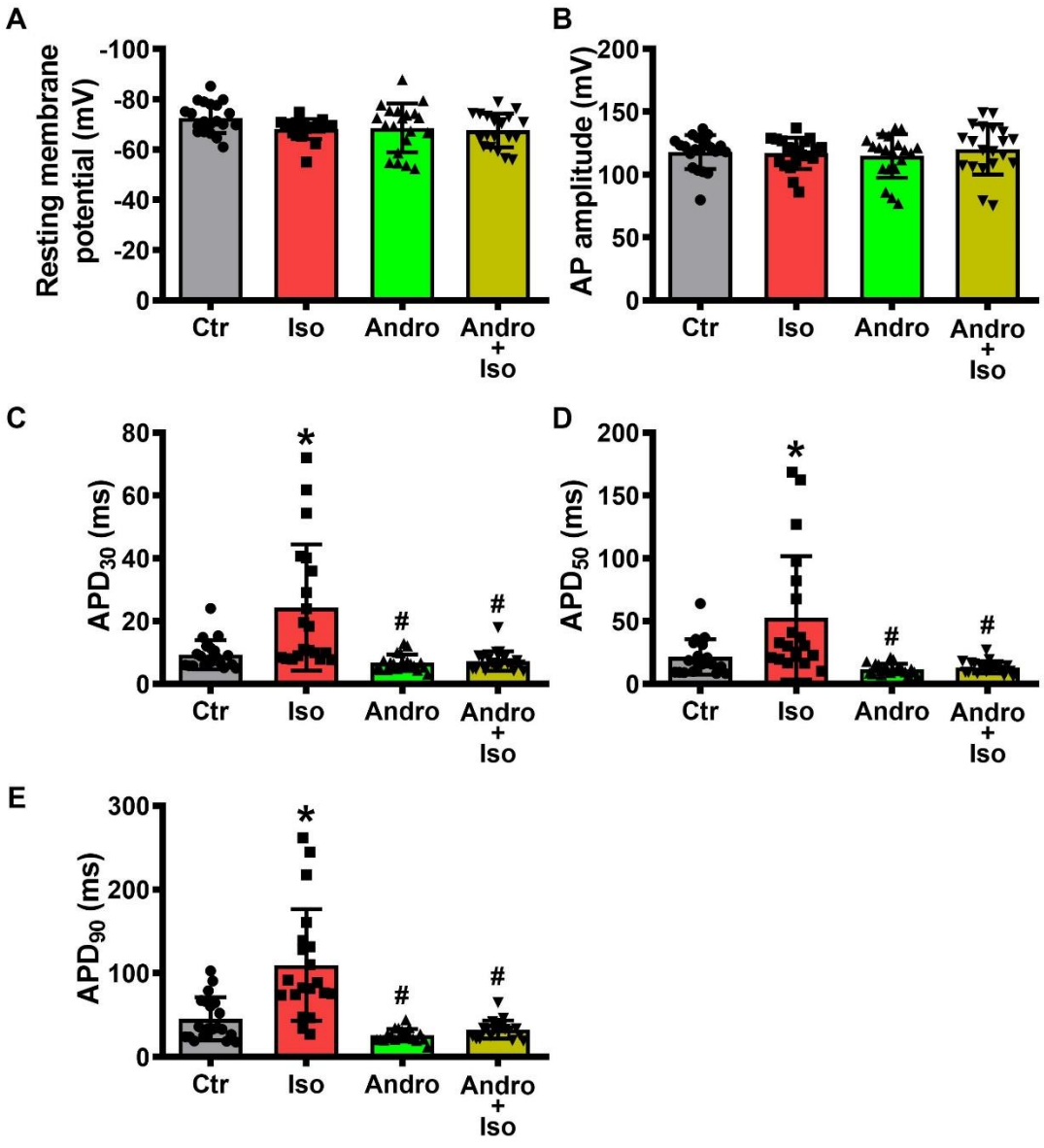

Figure 5.13. Effects of Andrographolide on Cardiac Action Potential (AP). (A) Resting membrane potential and (B) AP amplitude. Both were not significantly altered across all experimental group. (C) AP duration measured at 30 % repolarization (APD_{30}), (D) AP duration measured at 50 % repolarization (APD_{50}), and (E) AP duration measured at 90 % repolarization (APD_{90}). Each of these durations were markedly prolonged in Iso group, whereas, they were all maintained at Ctr levels in Andro and Andro + Iso group. Data are presented as Mean ± SD, n = 20 cells per group and analysed by one-way ANOVA followed by Bonferroni's multiple comparisons test. *$p < 0.05$ vs Ctr and $^{\#}p < 0.05$ vs Iso.

5.11 Andrographolide Pretreatment Prevents Pathological Intracellular Ca^{2+} Overload

To determine if L-type Ca^{2+} channel blockage is in part responsible for the prevention of increases in myocyte shortening and APD by andrographolide reported earlier in this study, we measured $I_{Ca,L}$ in cardiomyocytes isolated from each experimental group in whole-cell mode using patch clamp techniques. Recordings shows a significant ($p < 0.05$) increase in $I_{Ca,L}$ density in Iso group and significant ($p < 0.05$) decrease in $I_{Ca,L}$ density in Andro group compared to the Ctr, and by implication $I_{Ca,L}$ density was maintained nearly at Ctr level in Andro + Iso group (Fig. 5.14A&B). Further analysis of the current density-voltage relationship shows no shift in the voltage at which current maximum, as $I_{Ca,L}$ density was peaked at test potential of 0 mV in all experimental groups, suggesting that voltage-dependence of the channel did not differ grossly in all experimental groups, only permeability did (Fig. 5.14B). In order to substantiate this assertion, maximal conductance (G_{max}) of $I_{Ca,L}$ was determined for all the experimental groups. Our result indicated that Iso caused significant ($p < 0.05$) increase in G_{max}, while Andro administration prevented Iso induce G_{max} increase (Fig. 5.14C). Thus, suggesting andrographolide as a L-type Ca^{2+} channel blocker.

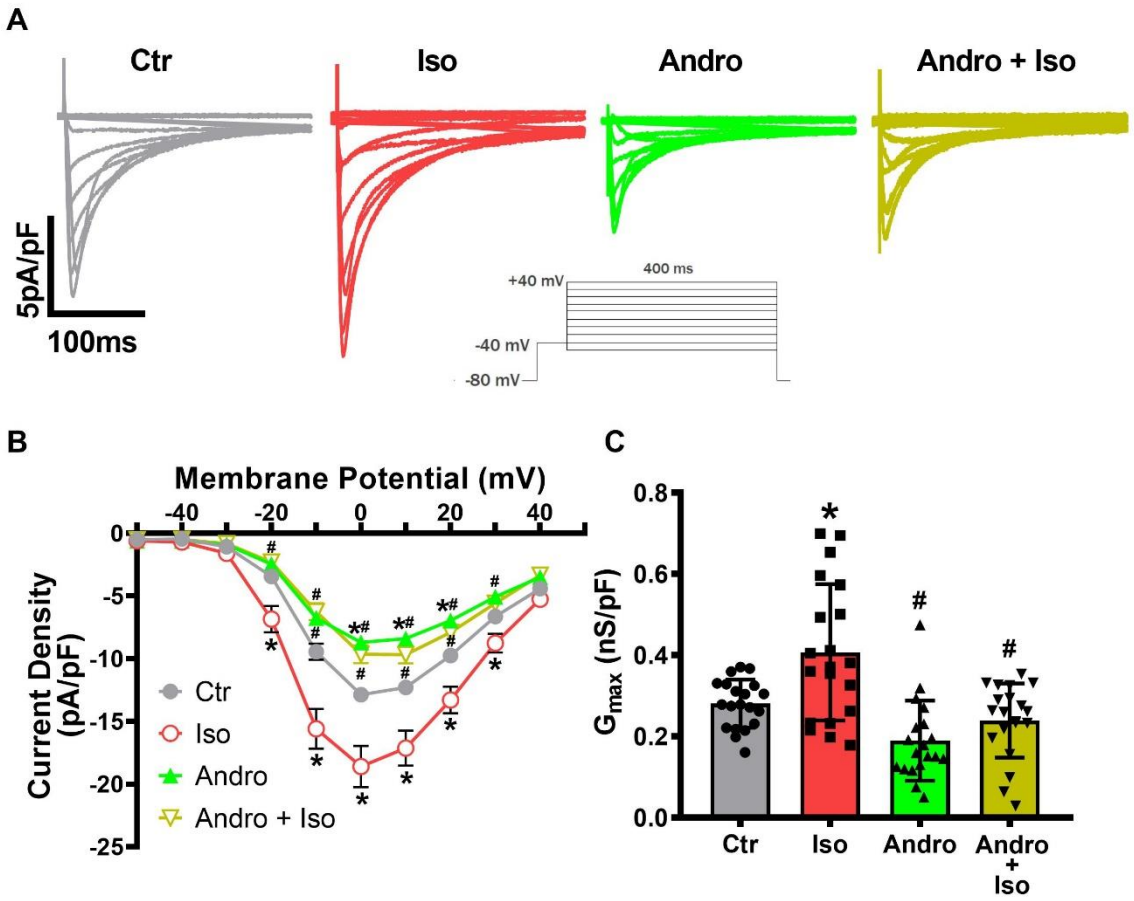

Figure 5.14. Effects of Andrographolide on Cardiac L-type Ca^{2+} Current ($I_{Ca,L}$). (A) Representative $I_{Ca,L}$ Traces Obtained from Cardiomyocytes Isolated from Each Experimental Group. Currents were recorded by applying prepulse from holding potential of -80 mV to -40 mV for 50 ms and pulses from -50 mV to +40 mV in 10 mV increments for 400 ms. (B) Current density-voltage relationship and (C) Maximal conductance (G_{max}) of all experimental groups. $I_{Ca,L}$ density was peaked at test potential of 0 mV in all experimental groups, markedly increased in Iso group, while pretreatment with andrographolide maintains the current density at nearly control levels in Andro + Iso group. Data are presented as Mean ± SD, n = 20 cells per group and analyzed by one-way ANOVA followed by Bonferroni's multiple comparisons test. *$p < 0.05$ vs Ctr and $^{\#}p < 0.05$ vs Iso.

5.12 Andrographolide Pretreatment Increases Transient Outward Potassium Current (I_{to}) in Cardiac Myocytes

To determine whether enhanced conductance of K^+ channel is involved in the ability of andrographolide to prevent MI-associated APD elongation reported earlier in this study, we measured I_{to} in cardiomyocytes isolated from each experimental group using the same protocol, and under the same assay conditions. Presented in Fig. 5.15A are representative I_{to} traces recorded in each experimental group. In Fig. 5.15B, marked differences were observed in I_{to} density among experimental groups beginning from test potential of 0 mV upwards. To this effect, in Fig. 5.15C, I_{to} density peak was significantly ($p < 0.05$) decreased in Iso group compared to the Ctr, whereas, it was significantly ($p < 0.05$) increased in Andro group when compared to either Ctr or Iso group, a development that may have facilitated similar increase of I_{to} density peak observed in Andro + Iso group. Thus, suggesting that andrographolide enhances conductance of cardiac transient outward K^+ channel.

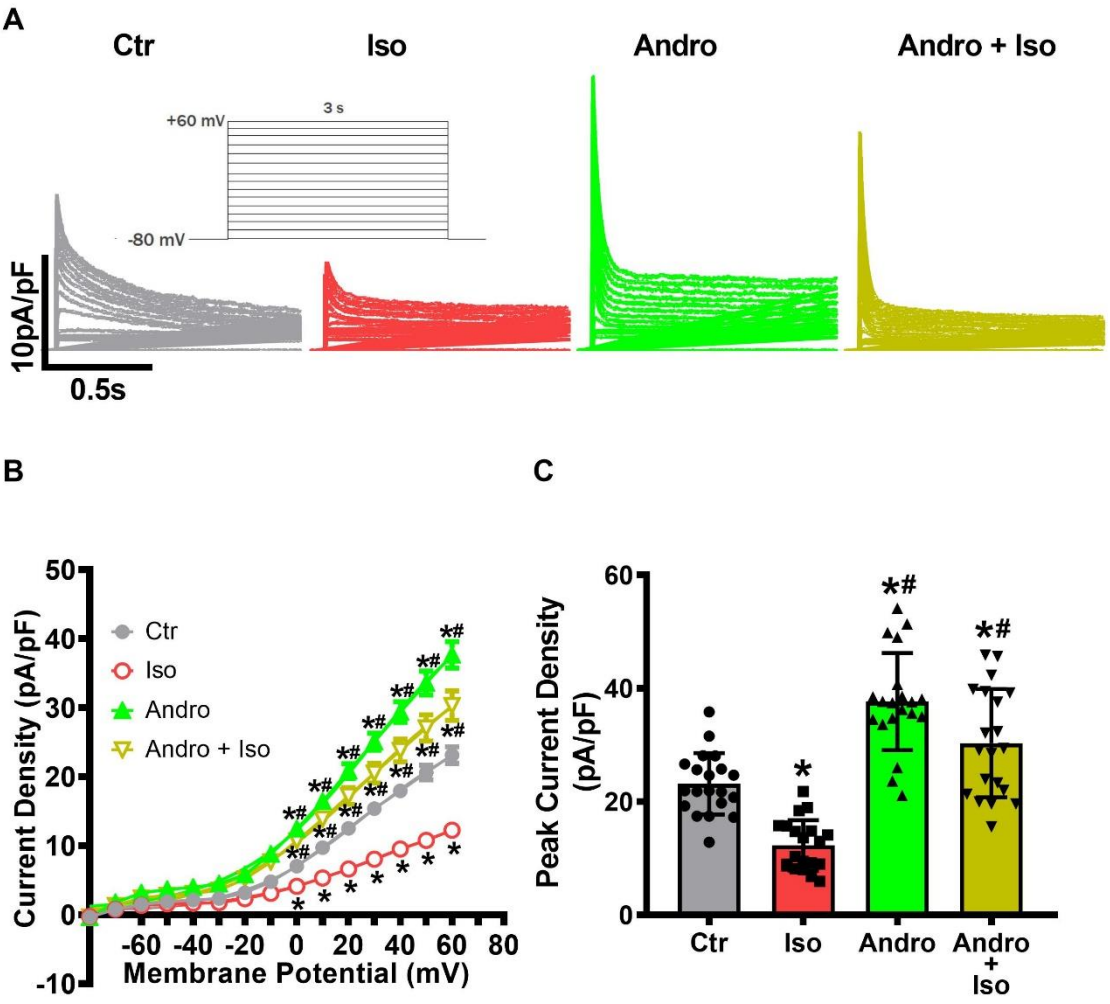

Figure 5.15. Effects of Andrographolide on Cardiac Transient Outward Potassium Current (I_{to}). (A) Representative I_{to} traces recorded from cardiomyocytes isolated from each experimental group. Currents were recorded with the holding potential set at -80 mV and then depolarized to test potential of +60 mV in 10 mV increments for 3 s. (B) Current density-voltage relationship and (C) Peak current density of all experimental groups. I_{to} density was markedly decreased in Iso group as against the Ctr, while pretreatment with Andro remarkably increased I_{to} density. Data are presented as Mean ± SD, n = 20 cells per group and analyzed by one-way ANOVA followed by Bonferroni's multiple comparisons test. *$p < 0.05$ vs Ctr and $^{\#}p < 0.05$ vs Iso.

5.13 Andrographolide Produced Concentration-Dependent Reduction in Myocyte Shortening, +dL/dt and -dL/dt in Isolated Cardiomyocytes

To further substantiate the inferences drawn from the *in-vivo* studies regarding cardioprotective mode of actions of andrographolide, different concentrations of andrographolide were tested on freshly isolated cardiomyocytes (*in-vitro*). The impacts on mechanical and electrical activities were assessed and compared to the control and standard drug. Results indicate that andrographolide had a concentration-dependent effects on key cardiac contractile profiles. Shown in Fig. 5.16 are the representative contraction traces before and after incubation in different concentrations of andrographolide and nicardipine. As anticipated, *in-vitro* application of andrographolide produced concentration-dependent reduction in myocyte shortening (Fig. 5.17A&B), +dL/dt and -dL/dt (Fig. 5.17C&D) similar to the effects of nicardipine and in consistence with *in-vivo* observations.

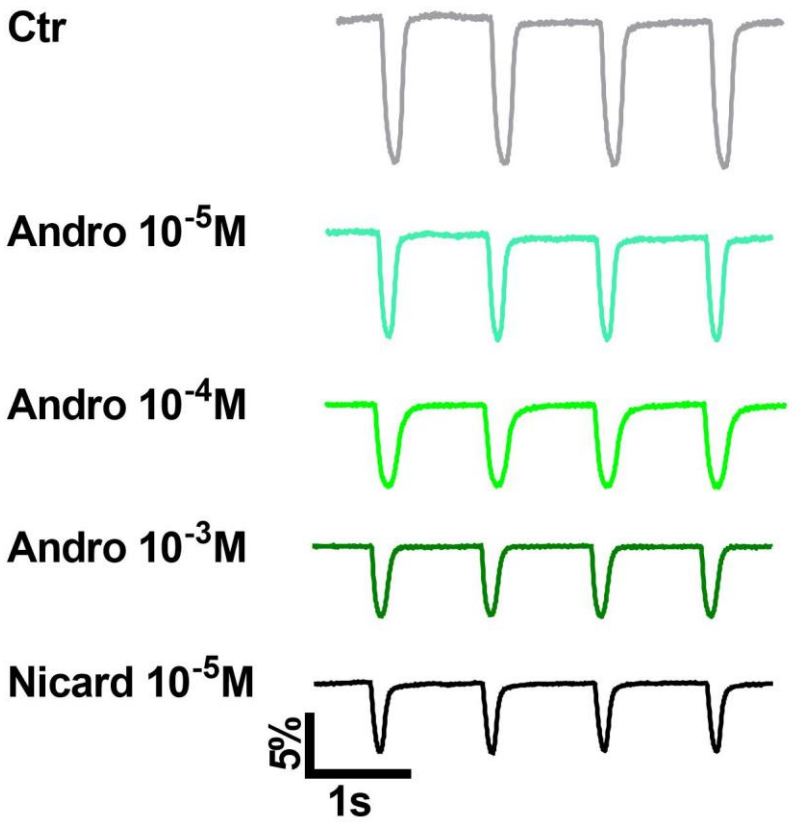

Figure 5.16. Representative Contraction Traces Obtained Before and After Incubation in Different Concentrations of Andrographolide and Nicardipine.

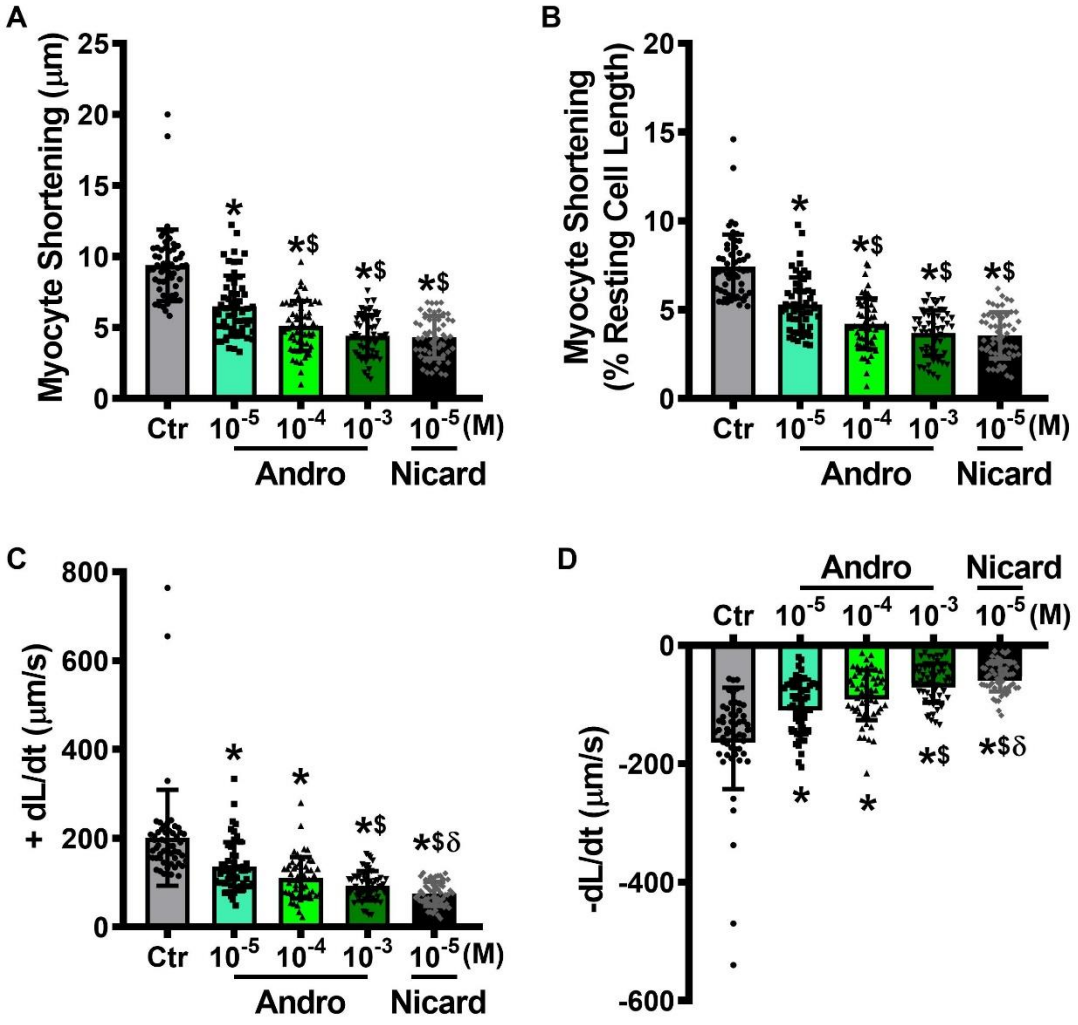

Figure 5.17. Concentration-Response Effects of Andrographolide on Isolated Cardiomyocytes' Contractile Properties. (A) Myocyte shortening measured in μm. (B) Myocyte shortening expressed as % of the baseline. (C) Maximal velocity of contraction (+dL/dt). (D) Maximal velocity of relaxation (-dL/dt). Andrographolide reduced myocyte shortening, +dL/dt and -dL/dt in a concentration-dependent manner. Data are presented as Mean ± SD, n = 55 cells per group and analysed by one-way ANOVA followed by Bonferroni's multiple comparisons test. *$p < 0.05$ vs Ctr, $^{\$}p < 0.05$ vs Andro 10^{-5}M, $^{\delta}p < 0.05$ vs Andro 10^{-4}M, $^{\phi}p < 0.05$ vs Andro 10^{-3}M.

5.14 Andrographolide Produced Concentration-Related Decreases in Action Potential Duration (APD) in Isolated Cardiomyocytes

Results also show that andrographolide had a concentration-dependent effects in reducing APD. As indicated in Fig. 5.18 and Fig. 5.19A-E, different concentrations of andrographolide reduced APD significantly ($p < 0.05$) in similar manner as nicardipine when compared to the control. Furthermore, Fig. 5.19F shows progressive reduction in the APD_{90} with increasing concentration of andrographolide (10^{-5} M = 75.56 ± 3.572%, 10^{-4} M = 65.32 ± 2.793%, and 10^{-3} M = 55.46 ± 6.354%).

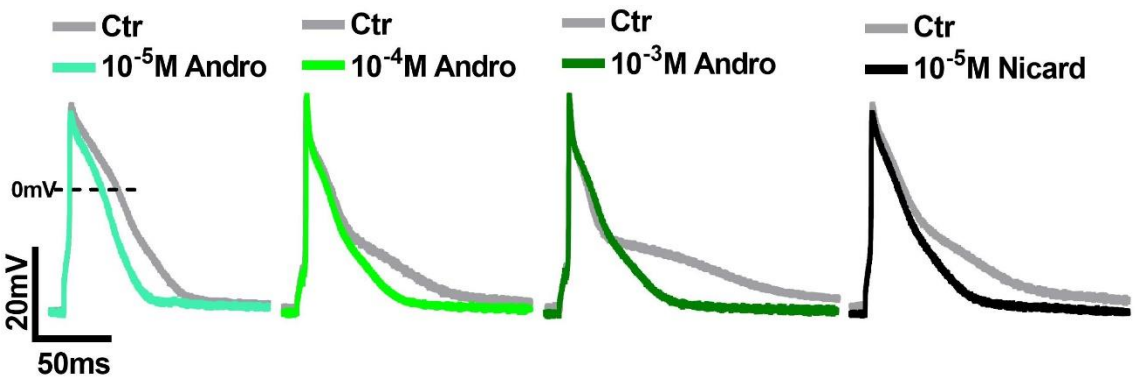

Figure 5.18. Representative AP Traces Obtained Before and After Exposure to Different Concentrations of Andrographolide and Nicardipine. APs were elicited by applying test pulse of 1 nA current for duration of 5 ms at frequency of 1 Hz.

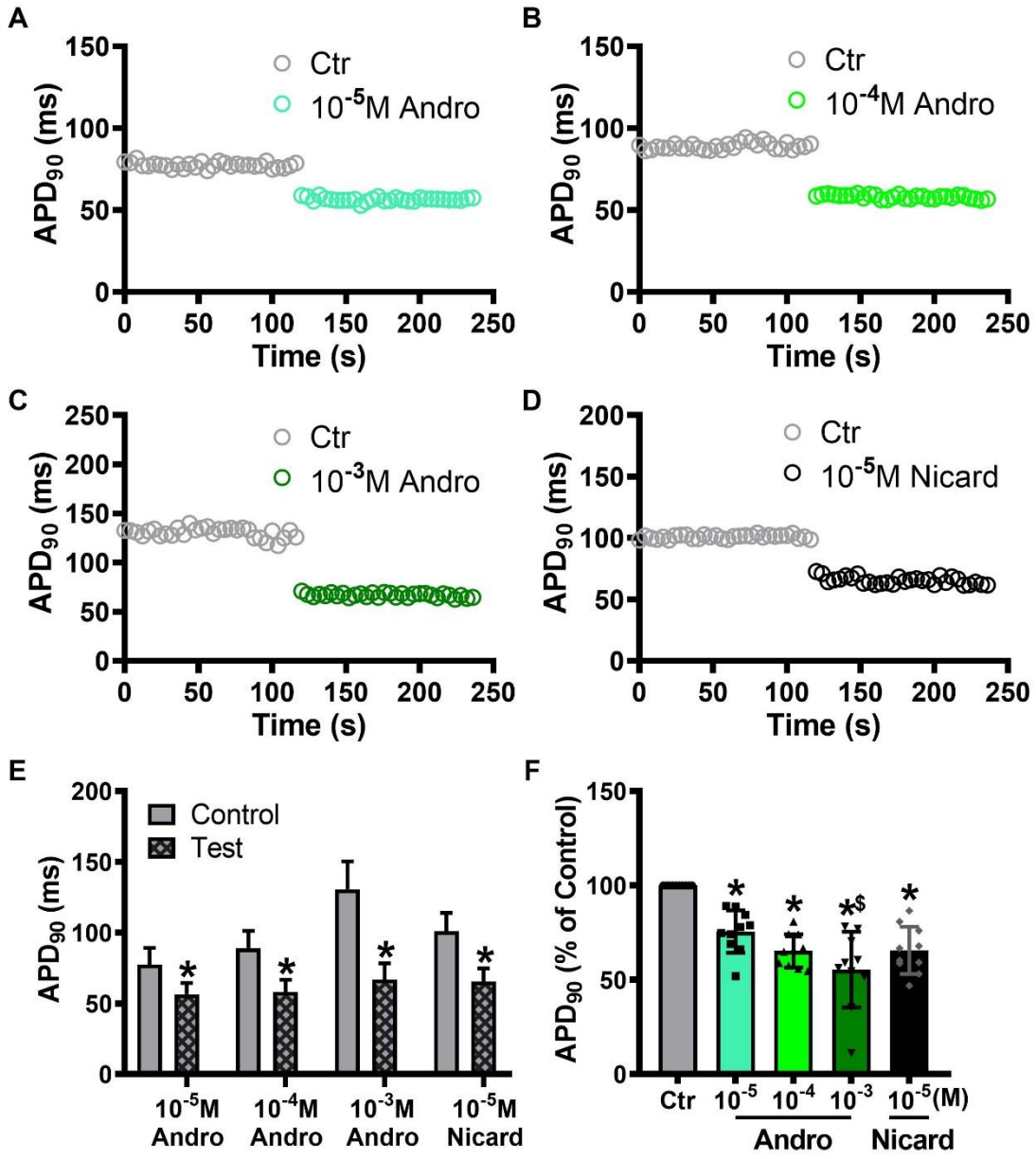

Figure 5.19. Concentration-Response Effects of Andrographolide on Isolated Cardiomyocytes' Action Potential (AP). (A, B, C, D) Time course effects of Andro (10^{-5}, 10^{-4}, 10^{-3}) M and Nicard (10^{-5}M) on APD_{90}. (E) APD_{90} measured in ms. (F) APD_{90} expressed as % of the control. Andrographolide produced concentration-dependent decreases in APD_{90}. Data are presented as Mean ± SD, n = 10 cells per group and analysed by Student's t-test and one-way ANOVA followed by Bonferroni's multiple comparisons test. *$p < 0.05$ vs Ctr, $^{\$}p < 0.05$ vs Andro 10^{-5}M, $^{\delta}p < 0.05$ vs Andro 10^{-4}M, $^{\phi}p < 0.05$ vs Andro 10^{-3}M.

5.15 Andrographolide Produced Concentration-Related Decreases in L-type Calcium Current in Isolated Cardiomyocytes

In what seems like repeat of the *in-vivo* observations, andrographolide also reduced $I_{Ca,L}$ when applied *in-vitro* (Fig. 5.20). Besides, it was noted that the effects progressed with time, and was well correlated with the effects of nicardipine (Fig. 5.21A-E). Also, the $I_{Ca,L}$ density expressed as percentage of the control (Fig. 5.21F) revealed that the inhibition effects of andrographolide on $I_{Ca,L}$ is concentration-dependent (Andro 10^{-5} M = 80.51 ± 4.343%, Andro 10^{-4} M = 72.90 ± 3.578%, Andro 10^{-3} M = 57.95 ± 5.346%, Nicard 10^{-5} M = 72.81 ± 2.553%). Thus, supports our earlier inference that $I_{Ca,L}$ inhibition could be one of the mechanisms by which andrographolide protects cardiac tissue against MI.

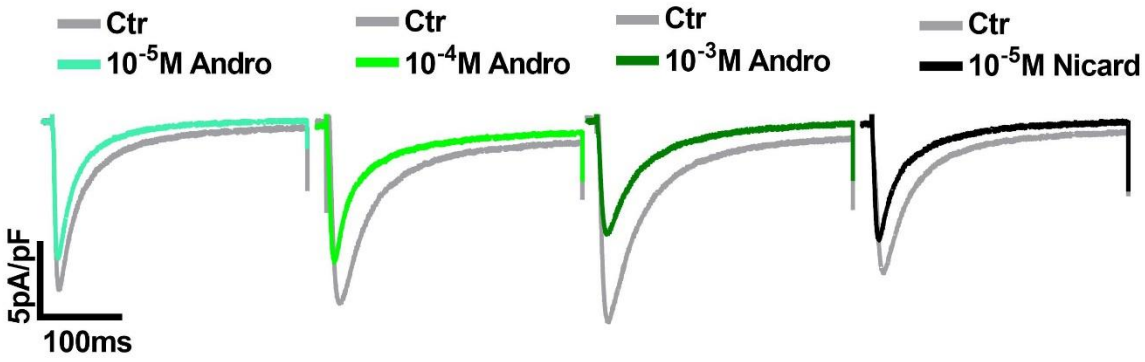

Figure 5.20. Representative $I_{Ca,L}$ Traces Obtained Before and After Exposure to Different Concentrations of Andrographolide and Nicardipine. Currents were recorded by applying prepulse from holding potential of -80 mV to -40 mV for 50 ms from which pulses were applied to raise the membrane potential to 0 mV for 400 ms.

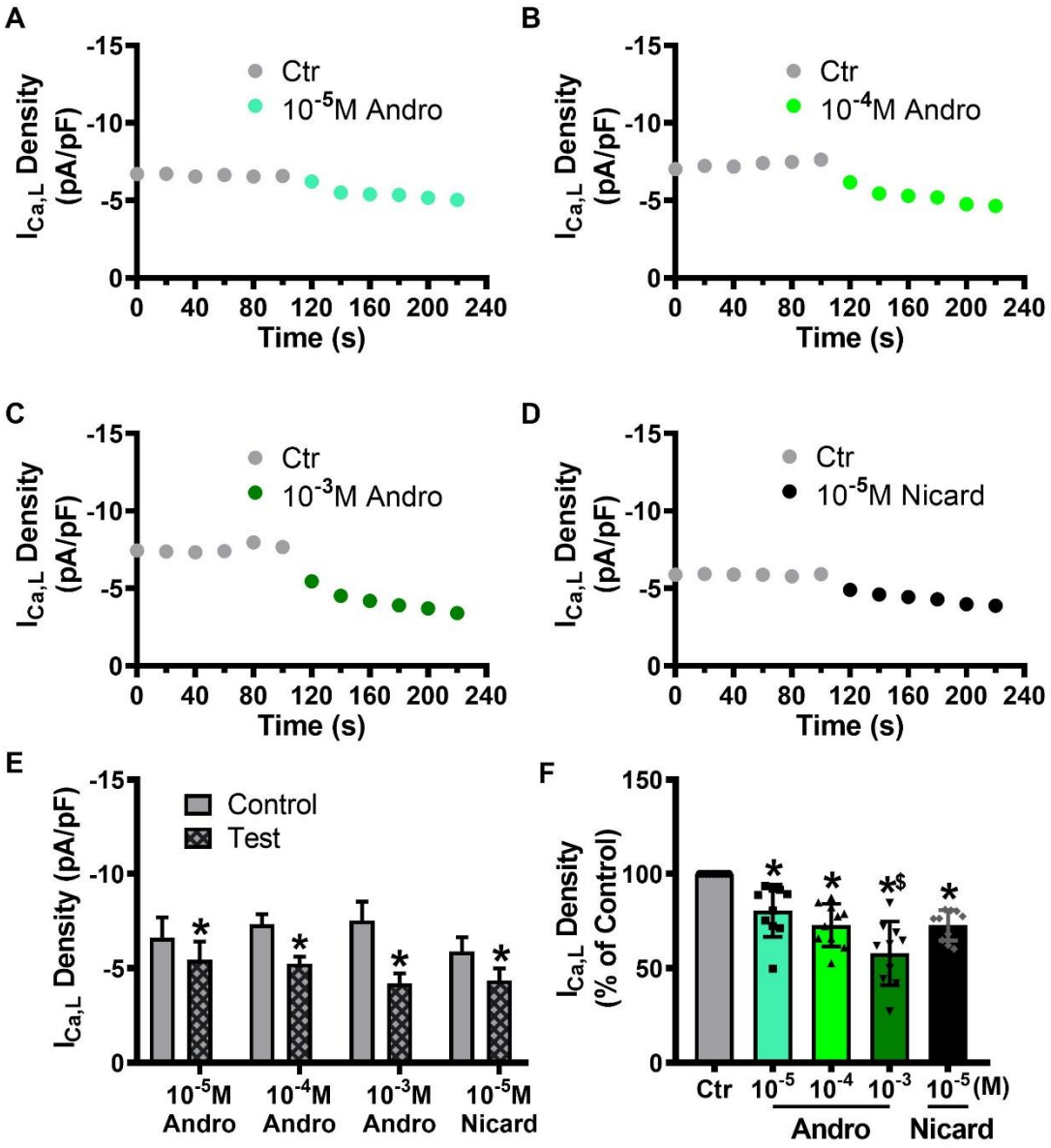

Figure 5.21. Concentration-Response Effects of Andrographolide on Isolated Cardiomyocytes' L-type Ca^{2+} Current ($I_{Ca,L}$). (A, B, C, D) Time course effects of Andro (10^{-5}, 10^{-4}, 10^{-3}) M and Nicard (10^{-5}M) on $I_{Ca,L}$ density. (E) $I_{Ca,L}$ density measured in pA/pF. (F) $I_{Ca,L}$ density expressed as % of the control. Andrographolide produced concentration-related decreases in $I_{Ca,L}$ density. Data are presented as Mean ± SD, n = 10 cells per group and analysed by Student's t-test and one-way ANOVA followed by Bonferroni's multiple comparisons test. *$p < 0.05$ vs Ctr, $^{\$}p < 0.05$ vs Andro 10^{-5}M, $^{\delta}p < 0.05$ vs Andro 10^{-4}M, $^{\phi}p < 0.05$ vs Andro 10^{-3}M.

5.16 Andrographolide Produced Concentration-Related Increases in Transient Outward Potassium Current in Isolated Cardiomyocytes

Fig. 5.22 shows the representative of I_{to} traces obtained before and after exposure to different concentrations of andrographolide and nicardipine. The time course effects are presented in Fig 5.23A-D, results show that the effects of andrographolide on I_{to} progresses with time. Equally, it was observed that andrographolide at various test concentrations increased I_{to} density significantly ($p < 0.05$) when compared to the control, while nicardipine did not (Fig 5.23E). More importantly, the I_{to} density calculated as percentage of the control (Fig. 5.23F), indicated that the I_{to} increase facilitated by andrographolide in isolated cardiomyocytes is concentration-related (Andro 10^{-5} M = 108.2 ± 2.015%, Andro 10^{-4} M = 113.6 ± 2.422%, Andro 10^{-3} M = 125.3 ± 6.547%, Nicard 10^{-5} M = 99.52 ± 2.289%). Hence, corroborates the *in-vivo* interpretation that I_{to} upregulation could be one of the mechanisms by which andrographolide protects cardiac tissue against MI.

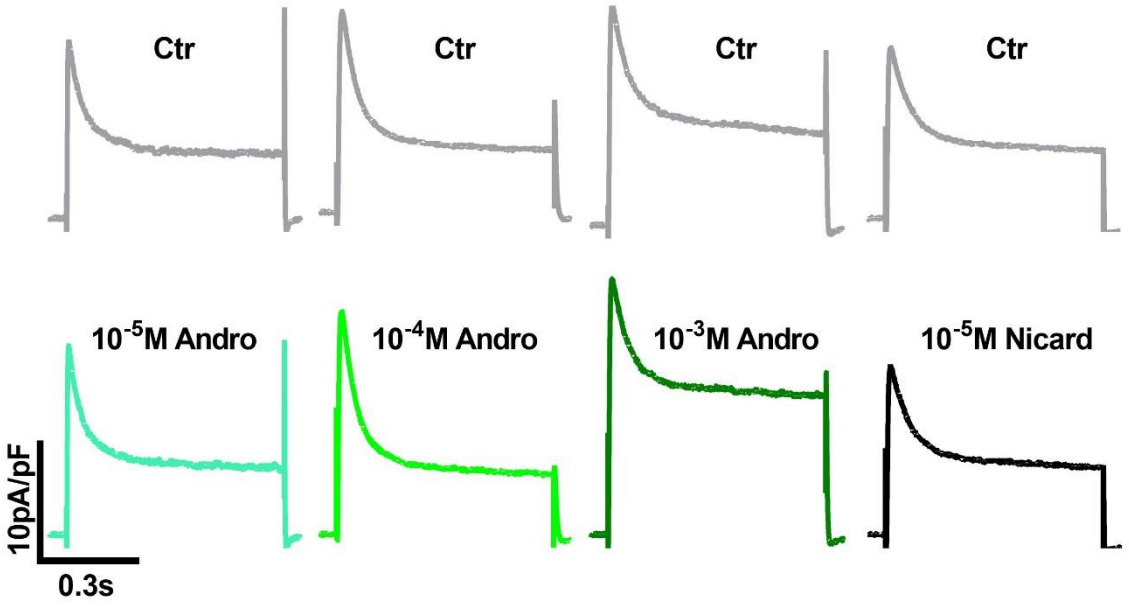

Figure 5.22. Representative I_{to} Traces Recorded Before and After Exposure to Different Concentrations of Andrographolide and Nicardipine. Currents were recorded with the holding potential set at -80 mV and then depolarized to test potential of +60 mV for 600ms.

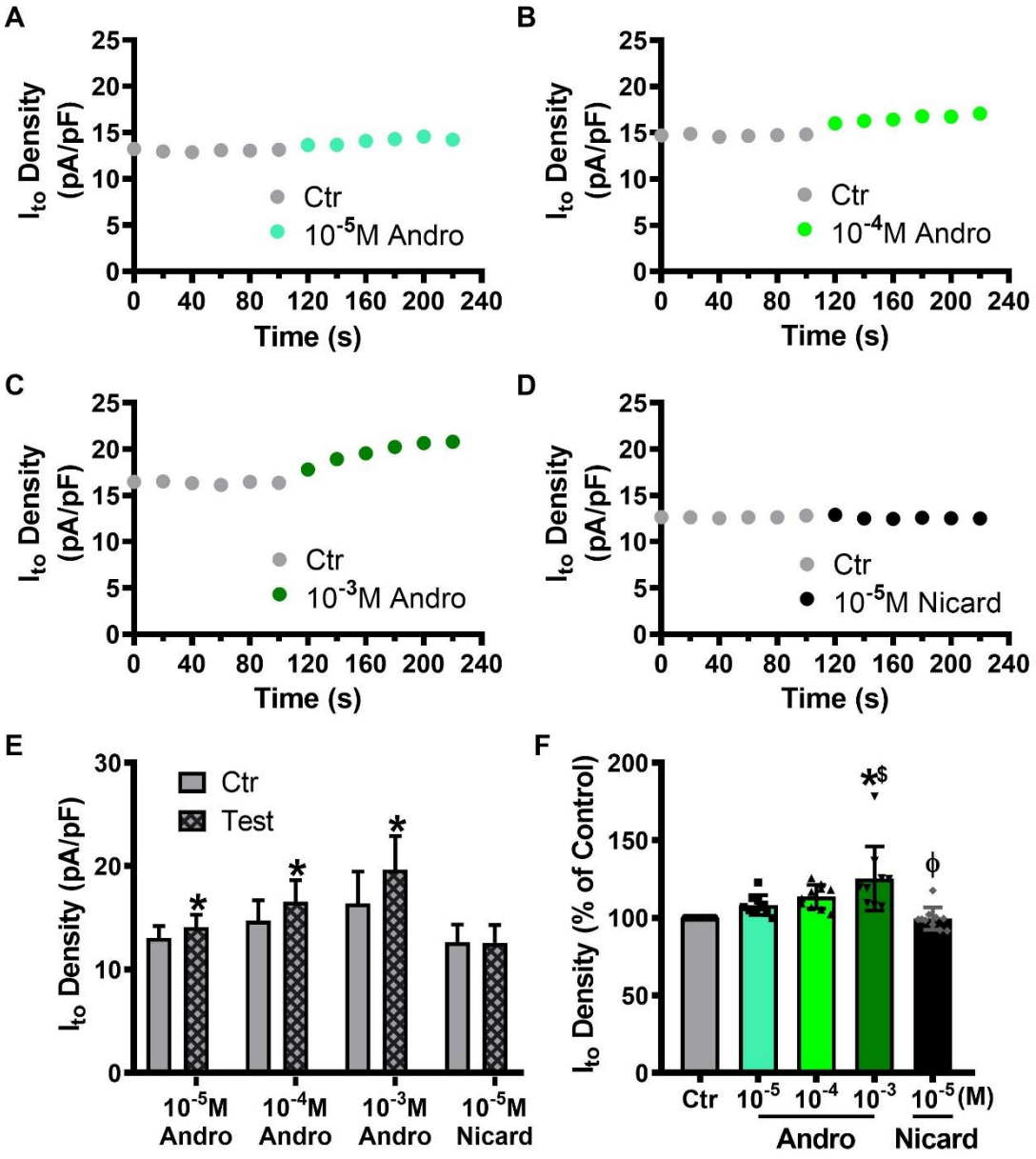

Figure 5.23. Concentration-Response Effects of Andrographolide on Isolated Cardiomyocytes' Transient Outward Potassium Current (I_{to}). (A, B, C, D) Time course effects of Andro (10^{-5}, 10^{-4}, 10^{-3}) M and Nicard (10^{-5}M) on I_{to} density. (E) I_{to} density measured in pA/pF. (F) I_{to} density expressed as % of the control. Andrographolide produced concentration-related increases in I_{to} density. Data are presented as Mean ± SD, n = 10 cells per group and analysed by Student's t-test and one-way ANOVA followed by Bonferroni's multiple comparisons test. *$p < 0.05$ vs Ctr, $^{\$}p < 0.05$ vs Andro 10^{-5}M, $^{\delta}p < 0.05$ vs Andro 10^{-4}M, $^{\phi}p < 0.05$ vs Andro 10^{-3}M.

VI. DISCUSSION

Myocardial infarction is the injury of the myocardium caused by prolonged myocardial ischemia (Thygesen et al., 2012a). The goal to develop interventions against MI has been long sought, with some breakthroughs recorded over decades. However, the increasing number of reported side effects of existing interventions motivates a strong need for new and improved interventions. This study demonstrated for the first time, the protective effects of andrographolide against isoproterenol-induced myocardial infarction in rats. Precisely, the effects of the compound on cardiac-specific parameters that defines MI, and those that shapes cardiac functions were explored using both biophysical and pharmacological assay methods.

Tolerability is the first *in-vivo* safety criteria for new drug candidates. The maximum tolerated dose (MTD) test by dose escalation scheme is a common test used for the dose selection and identification of the dose at which target organ toxicity is likely to be observed (Andrade et al., 2016). To this effect, we found andrographolide to be well tolerated in rats (up to 80 mg/kg/day for 3 weeks) with non-observed adverse effects. In agreement with this, Al-Batran et al reported that andrographolide was well tolerated in rabbits even up to the maximum dose of 500 mg/kg/day for 4 weeks (Al Batran et al., 2014).

Electrocardiography is pivotal in the diagnosis of cardiac ischemia and infarction as it provides information about the health of the electrical system of the heart (Sampson and McGrath, 2015). In this study, we found that andrographolide prevented infarction-like changes in ECG profile. The significant increase recorded in the HR, coupled with unambiguous ST-segment elevation in Iso group are typical of the onset of MI. Previous report on MI indicated that elevated heart rate in susceptible subjects predicts risk of developing MI and that a sustained elevated heart rate after MI is well correlated with higher mortality (Hjalmarson et al., 1990). The stabilization of the HR at the control level in Andro + Iso group can be linked to the ability of andrographolide to reduce HR. This is consistent with the report of others that agents that exclusively reduced heart rate are important as anti-ischemic, antianginal and anti-infarction agents on the basis of their ability to reduce myocardial oxygen consumption (Singh, 2003). The unaltered PR interval among experimental groups, including Iso group, can be interpreted as absence of signalling alterations between the atria and the ventricle. This is because, the PR interval is characterized as the time necessary for the electrical impulse to be conducted from the SA node to the ventricle (Schwarzwald et al., 2009). QRS complex measured on an ECG

signifies ventricular depolarization while the QT and QTc intervals are indicative of action potential duration of ventricular myocyte. Significant prolongation of these parameters, as recorded in Iso group, has since been interpreted to mean ventricular dysfunction in MI patients (Karahan et al., 2016). Nonexistence of such prolongations in Andro and Andro + Iso group underscores the ability of andrographolide to prevent ventricular systolic and diastolic dysfunction.

Pathological hypertrophy and remodelling of cardiac tissue has been frequently linked with MI (Kehat and Molkentin, 2010). It was reported to be characterized by excessive increase in ventricular dimensions (Samak et al., 2016), functional perturbations of cellular Ca^{2+} homeostasis and ionic currents (Frey et al., 2004), which contribute to impaired post-infarction prognosis (Nepper-Christensen et al., 2017). Our results indicate that andrographolide minimized MI-associated cardiac hypertrophy. The unprecedented increases recorded in the HW and cardiac mass indexes (HW/BW and HW/TL ratios) in Iso group undoubtedly signified cardiac hypertrophy, while the ability of andrographolide to maintain the HW and cardiac mass indexes at control levels in Andro group and near control levels in Andro + Iso group signified its efficacy at preventing and or minimizing ventricular wall stress, a major event required for the induction of cardiac hypertrophy in MI. In agreement with our report, Xie et al reported that andrographolide protected against MI-associated adverse cardiac remodelling in mice through enhancing Nrf2 signalling pathway (Xie et al., 2020). Similarly, Wu et al reported that andrographolide protected against pressure overload-induced cardiac hypertrophy in mice by inhibiting MAPKs signalling (Wu et al., 2017).

Systemic elevation of biomarkers of myocardial injury including CK, CK-MB, LDH, AST and cTnI are key diagnostic features of MI (Mythili and Malathi, 2015). In line with this, significant increases were recorded in the levels of CK, CK-MB, AST and cTnI in Iso group. This development can be attributed to destabilization and loss of functional integrity of myocardial membrane sequel to cardiac damage (Panda et al., 2017). Hence, the decreased levels of these biomarkers in Andro group as well as Andro + Iso group implies that andrographolide prevented MI-associated myocardial membrane destabilization and enzyme leakages.

Leukocyte count has long been established as a predictor myocardial infarction (Friedman et al., 1974). The significant elevation of WBC counts recorded in Iso group connotes clear indication of myocardial damage. In agreement with this, others have reported association between leukocyte elevation and impaired epicardial and myocardial perfusion (Sabatine et al., 2002). Likewise, others have found leukocyte levels to be characteristically elevated among patients with myocardial infarction and unstable angina (Avramakis et al., 2007). More specifically, Filho et al reported that MI induction with isoproterenol raised leukocyte and neutrophil counts in Wistar rats (Filho et al., 2011). Thus, the leukocyte level that was maintained at the control level in Andro group and relatively near control level in Andro + Iso group indicate that andrographolide is capable of minimizing MI-associated elevation of systemic leukocytes. In corroboration of this claim, most anti-MI drugs have been reported to reduce leukocyte infiltration after MI (Ertl and Frantz, 2005).

Cardiac oxidative stress occurs when the manifestation of free radicals surpasses the cardiac antioxidant machineries and it has been identified as one of the risk factors of MI (Dhawan et al., 2019). Antioxidant enzymes are important for maintaining cells and tissue integrity against deleterious effects of free radicals (Hassan et al., 2017). Even though, there was no significant difference recorded in the activity of SOD across all the experimental groups, the increases recorded in the activities of catalase and GPx in Andro + Iso group as against the Iso group where the activities of both enzymes were remarkably decreased underscores the ability of andrographolide to boost cardiac antioxidant status and protect cardiac tissue against MI-associated cardiac oxidative stress.

Infarct size is a major determinant of MI prognosis and it depends on the myocardial region supplied by the obstructed coronary artery (McKay et al., 1986). The pale tan appearance of the heart, which others described as pale gray (Jennings and Ganote, 1974), coupled with patches of whitish color in cardiac tissue sections, as well as significant increase in infarct size obtained in Iso group indicates necrosis of significant portion of myocardium in this group. In agreement with this, Panda et al reported similar observations in cardiac tissue slices of Iso treated rats and characterized their observations as areas of necrosis due to non-reduction of tetrazolium salt (Panda et al., 2017). Therefore, the apparently normal appearance of the heart tissue, positively stained cardiac tissue section with Evans blue/TTC

and control level infarct size recorded in Andro group and Andro + Iso group underscored the potency of andrographolide at preventing infarction-like ventricular necrosis.

Similarly, histopathological assessment of myocardial sections of various experimental groups corroborates the biochemical observations reported in this study. Most importantly, the histological alterations, characterized by remarkable degree of lesions, degeneration, disruption, nuclear enlargement, binucleation and loss of cardiomyocytes, replaced by disorganized fibroblasts and few macrophages, as well as edema observed in Iso group is similar to those reported by others in experimental models of MI (Acikel et al., 2005; Filho et al., 2011; Goyal et al., 2015; Panda et al., 2017). Hence, the absence of such alterations in Andro group and the apparent minimization of them in Andro + Iso group could be seen as the ability of andrographolide to abate MI-associated cardiac histological alterations. In support of this, Zhang et al previously informed that andrographolide minimized myocardial histological alterations in an experimental model of autoimmune myocarditis by inhibiting infiltration of inflammatory cells (Q. Zhang et al., 2019).

Cardiomyocytes contractility is the hallmark of cardiac function and is a predictor of healthy or diseased cardiac tissue (Gaitas et al., 2015). Here, andrographolide was found to avert pathological increases in myocyte shortening, maximal velocities of contraction and relaxation. The unprecedented increases in cardiomyocytes shortening, maximal velocities of contraction and relaxation recorded in Iso group was attributed to intracellular Ca^{2+} overload and hyper-enhanced intracellular Ca^{2+} cycling consequent of positive ionotropic effects**.** In agreement with this, Zhang and colleagues reported that myocytes contractility is increased after MI in regions of the heart where blood flow is maintained, through activation of sympathetic reflex responses and that the phenomenon is responsible for the exacerbation of cardiac injury and pump dysfunction that will eventually lead to heart failure (H. Zhang et al., 2010). Therefore, the sustained myocytes shortening, maximal velocities of contraction and relaxation at the control level in Andro + Iso group can be linked to the ability of andrographolide to reduce these parameters when applied singly. This is consistent with the report of Zeng et al that andrographolide reduced maximum upstroke velocity in rabbit left ventricular and left atrial myocytes (Zeng et al., 2017).

Furthermore, results from this study indicated that andrographolide prevented MI-associated cardiac myocytes APD prolongation. The non-significant changes recorded in the resting membrane potential and the AP amplitude across all the experimental groups correlates with the unaltered PR interval of the ECG and suggests that fast sodium current (I_{Na+}) was unaffected in all the groups. This is because, change in membrane potential as well as the upstroke of the AP is dependent on the flow of ion through channels specific for Na^+ and the steepest portion of the AP upstroke occurs at maximal Na^+ ion flow (Berecki et al., 2010; Kleber, 2005; Weidmann, 1955). Also, the prolongation of APD recorded in Iso group correlates with the QT and QTc interval elongation of the ECG and suggestive of perturbation of L-type Ca^{2+} channel and or downregulation of K^+ channel. In agreement with this result, prolongation of action potential duration has been reported in rat left ventricular myocardium following infarction (Qin et al., 1996) and it has been established as a hallmark feature of myocardial infarction (Kaprielian et al., 1999). Besides, these folks and others have also correlated the cause of APD prolongation in cells from infarcted heart with an increased $[Ca^{2+}]_i$ transient amplitude (Kaprielian et al., 1999) and a decreased outward K^+ current (Qin et al., 1996; Rozanski et al., 1998). Therefore, the preserved APDs at the control levels in Andro group and Andro + Iso group could be seen as the ability of andrographolide to prevent perturbation of L-type Ca^{2+} channel and or facilitate upregulation of K^+ channel.

L-type Ca^{2+} channels are the primary pathway for Ca^{2+} influx into cardiac cells (Satin and Schroder, 2009). It has been reported that subtle perturbation of its function may cause intracellular Ca^{2+} overload leading to profound cardiac diseases (Betzenhauser et al., 2015; Nejatbakhsh and Feng, 2011). Results from this study emphasized that andrographolide prevented pathological intracellular Ca^{2+} overload through blockage of L-type Ca^{2+} channels. This is consistent with the findings of Zeng et al who reported that andrographolide inhibited $I_{Ca,L}$ in a concentration-dependent manner in left atrial and ventricular myocytes (Zeng et al., 2017). Another remarkable note taken from these results is that $I_{Ca,L}$ density of each experimental group correlates with their corresponding myocytes shortening results. Interestingly, it has been reported that there is a close correlation between $I_{Ca,L}$ and cardiac myocytes contraction (Bodi et al., 2005). Therefore, inhibition of $I_{Ca,L}$ can be seen as one of the mechanisms by which andrographolide protects cardiac tissue against MI.

In rat cardiac myocytes, I_{to} is the major K^+ current that contributes to the rapid membrane repolarization, and the peak current predominantly reflects I_{to} (Apkon and Nerbonne, 1991). In this study, we stressed that andrographolide increased (I_{to}) in cardiac myocytes. The significant reduction of I_{to} density in Iso group explains, in part, the prolongation of the APD recorded in this group. In agreement with our findings, post-MI myocytes has been reported to exhibit significant reductions in I_{to} and I_{K1} densities (Kaprielian et al., 1999). Therefore, with the I_{to} density being significantly elevated in Andro group, it is conceivable that andrographolide prevented pathological APD prolongation in Andro + Iso group by enhancing conductance of cardiac transient outward K^+ channel. Therefore, increase of I_{to} could also be seen as one of the mechanisms by which andrographolide protects cardiac tissue against MI.

VII. CONCLUSION AND PERSPECTIVES

7.1 CONCLUSION

The results obtained in this study contributed new evidence that andrographolide was well tolerated in-vivo and that:

- Andrographolide pretreatments prevented morphological changes in the heart and attenuated infarction-like ventricular necrosis while preserving ECG profile.

- Andrographolide pretreatments prevented MI-associated increases in systemic cardiac markers.

- Andrographolide pretreatments minimized infarction-like cardiac histological alterations.

- Andrographolide pretreatments preserved excitation-contraction coupling in cardiac myocytes.

- Inhibition of L-type Ca^{2+} Current and increase of transient outward K^{+} current are involved in the mechanism of cardiac protection facilitated by andrographolide against MI.

Therefore, andrographolide could be seen as a promising therapeutic agent capable of making the heart resistant to infarction and it could be used as template for the development of semisynthetic drug(s) for cardiac protection against MI.

7.2 PERSPECTIVES

Finally, the results of this study open perspectives for future investigations of the cardioprotective benefits of andrographolide against other cardiovascular diseases whose pathogenesis are associated with intracellular Ca^{2+} overload. We have as future goal to investigate the signalling cascades activated by andrographolide to facilitate inhibition of L-type Ca^{2+} current and upregulation of cardiac transient outward K^{+} current.

VIII. REFERENCES

Abdulhannan, P., Russell, D. A., and Homer-Vanniasinkam, S. (2012). Peripheral arterial disease: A literature review. *British Medical Bulletin*, *104*(1), 21–39. https://doi.org/10.1093/bmb/lds027

Abu-Ghefreh, A. A., Canatan, H., and Ezeamuzie, C. I. (2009). In vitro and in vivo anti-inflammatory effects of andrographolide. *International Immunopharmacology*, *9*(3), 313–318. https://doi.org/10.1016/j.intimp.2008.12.002

Acikel, M., Buyukokuroglu, M. E., Erdogan, F., Aksoy, H., Bozkurt, E., and Senocak, H. (2005). Protective effects of dantrolene against myocardial injury induced by isoproterenol in rats: Biochemical and histological findings. *International Journal of Cardiology*, *98*(3), 389–394. https://doi.org/10.1016/j.ijcard.2003.10.054

Adeoye, B. O., Ajibade, T. O., Oyagbemi, A. A., Omobowale, T. O., Yakubu, M. A., Adedapo, A. D., Ayodele, A. E., and Adedapo, A. A. (2019). Cardioprotective effects and antioxidant status of Andrographis paniculata in isoproterenol-induced myocardial infarction in rats. *Journal of Medicinal Plants for Economic Development*, *3*(1), 1–12. https://doi.org/10.4102/jomped.v3i1.49

Akbar, S. (2011). Andrographis paniculata: A review of pharmacological activities and clinical effects. *Alternative Medicine Review*, *16*(1), 66–77.

Akbar, S. (2020). Andrographis paniculata (Burm. f.) Nees. (Acanthaceae). In *Handbook of 200 Medicinal Plants* (pp. 267–283). Springer. https://doi.org/10.1007/978-3-030-16807-0_26

Al Batran, R., Al-Bayaty, F., Jamil Al-Obaidi, M. M., Hussain, S. F., and Mulok, T. Z. (2014). Evaluation of the effect of andrographolide on atherosclerotic rabbits induced by Porphyromonas gingivalis. *BioMed Research International*, *2014*, 1–11. https://doi.org/10.1155/2014/724718

Ali, N. S., Nawaz, A., Junaid, M., Kazi, M., and Akhtar, S. (2015). Venous thromboembolism-incidence of deep venous thrombosis and pulmonary embolism in patients with head and neck cancer: A tertiary care experience in Pakistan. *International Archives of Otorhinolaryngology*, *19*(3), 200–204. https://doi.org/10.1055/s-0035-1549153

Alpert, J. S. (1989). The Pathophysiology of Acute Myocardial Infarction. *Cardiology*, *76*(2), 85–95. https://doi.org/DOI:10.1159/000174479

Alves, L., and Polanczyk, C. A. (2020). Hospitalization for Acute Myocardial Infarction: A Population-Based Registry. *Arquivos Brasileiros de Cardiologia*, *[online].a*, 1–8. https://doi.org/10.36660/abc.20190573

Alwan, A., and MacLean, D. R. (2009). A review of non-communicable disease in low- and middle-income countries. *International Health*, *1*(1), 3–9. https://doi.org/10.1016/j.inhe.2009.02.003

Amegah, A. K. (2018). Tackling the Growing Burden of Cardiovascular Diseases in Sub-Saharan Africa: Need for Dietary Guidelines. *Circulation*, *138*(22), 2449–2451. https://doi.org/10.1161/CIRCULATIONAHA.118.037367

Amin, A. S., Tan, H. L., and Wilde, A. A. M. (2010). Cardiac ion channels in health and disease. *Heart Rhythm*, *7*(1), 117–126. https://doi.org/10.1016/j.hrthm.2009.08.005

Amroyan, E., Gabrielian, E., Panossian, A., Wikman, G., and Wagner, H. (1999). Inhibitory effect of andrographolide from Andrographis paniculata on PAF-induced platelet aggregation. *Phytomedicine*, *6*(1), 27–31. https://doi.org/10.1016/S0944-7113(99)80031-2

Anand, S. S., and Yusuf, S. (2011). Stemming the global tsunami of cardiovascular disease. *The Lancet*, *377*(9765), 529–532. https://doi.org/10.1016/S0140-6736(10)62346-X

Andrade, E. L., Bento, A. F., Cavalli, J., Oliveira, S. K., Schwanke, R. C., Siqueira, J. M., Freitas, C. S., Marcon, R., and Calixto, J. B. (2016). Non-clinical studies in the process of new drug development - Part II: Good laboratory practice, metabolism, pharmacokinetics, safety and dose translation to clinical studies. *Brazilian Journal of Medical and Biological Research*, *49*(12), 1–19. https://doi.org/10.1590/1414-431X20165646

Apkon, M., and Nerbonne, J. M. (1991). Characterization of two distinct depolarization-activated K+ currents in isolated adult rat ventricular myocytes. *Journal of General Physiology*, *97*(5), 973–1011. https://doi.org/10.1085/jgp.97.5.973

Arackal, A., and Alsayouri, K. (2020). Histology, Heart. In *StatPearls [Internet]* (p. 1). StatPearls Publishing. https://www.ncbi.nlm.nih.gov/books/NBK545143/

Asghar, O., Al-Sunni, A., Khavandi, K., Khavandi, A., Withers, S., Greenstein, A., Heagerty, A. M., and Malik, R. A. (2009). Diabetic cardiomyopathy. *Clinical Science*, *116*(10), 741–760. https://doi.org/10.1042/CS20080500

Avramakis, G., Papadimitraki, E., Papakonstandinou, D., Liakou, K., Zidianakis, M., Dermitzakis, A., Mikhailidis, D. P., and Ganotakis, E. S. (2007). Platelets and white blood cell subpopulations among patients with myocardial infarction and unstable angina. *Platelets*, *18*(1), 16–23. https://doi.org/10.1080/09537100600800412

Baingana, F. K., and Bos, E. R. (2006). Changing Patterns of Disease and Mortality in Sub-Saharan Africa: An Overview. In D. T. Jamison, R. G. Feachem, M. W. Makgoba, E. R. Bos, F. K. Baingana, K. J. Hofman, and K. O. Rogo (Eds.), *Disease and Mortality in Sub-Saharan Africa* (Second, pp. 1–9). The World Bank.

Baman, J. R., and Ahmad, F. S. (2020). Heart Failure. *JAMA - Journal of the American Medical Association*, *324*(10), 1015. https://doi.org/10.1001/jama.2020.13310

Bao, Z., Guan, S., Cheng, C., Wu, S., Wong, S. H., Michael Kemeny, D., Leung, B. P., and Fred Wong, W. S. (2009). A novel antiinflammatory role for andrographolide in asthma via inhibition of the nuclear factor-κb pathway. *American Journal of Respiratory and Critical Care Medicine*, *179*(8), 657–665. https://doi.org/10.1164/rccm.200809-1516OC

Berecki, G., Wilders, R., de Jonge, B., van Ginneken, A. C. G., and Verkerk, A. O. (2010). Re-Evaluation of the Action Potential Upstroke Velocity as a Measure of the Na+ Current in Cardiac Myocytes at Physiological Conditions. *PLoS ONE*, *5*(12), 1–11. https://doi.org/10.1371/journal.pone.0015772

Bers, D. M. (2002). Cardiac excitation-contraction coupling. *Nature*, *415*, 198–205. https://doi.org/ez27.periodicos.capes.gov.br/10.1038/415198a

Bessman, S. P., and Carpenter, C. L. (1985). The Creatine-Creatine Phosphate Energy Shuttle. *Annual Review of Biochemistry*, *54*(1), 831–862.

https://doi.org/10.1146/annurev.biochem.54.1.831

Betzenhauser, M., Pitt, G., and Antzelevitch, C. (2015). Calcium Channel Mutations in Cardiac Arrhythmia Syndromes. *Current Molecular Pharmacology*, *8*(2), 133–142. https://doi.org/10.2174/1874467208666150518114857

Beutler, J. A. (2009). Natural products as a foundation for drug discovery. *Current Protocols in Pharmacology*, *46*, 9.11.1-9.11.21. https://doi.org/10.1002/0471141755.ph0911s46

Beznak, M. (1962). Hemodynamics During the Acute Phase of Myocardial Damage Caused by Isoproterenol. *Canadian Journal of Biochemistry and Physiology*, *40*(1), 25–30. https://doi.org/10.1139/o62-004

Bodi, I., Akhter, S. A., Schwartz, A., Bodi, I., Mikala, G., Koch, S. E., Akhter, S. A., and Schwartz, A. (2005). The L-type calcium channel in the heart : the beat goes on Find the latest version : The L-type calcium channel in the heart : the beat goes on. *The Journal of Clinical Investigation*, *115*(12), 3306–3317. https://doi.org/10.1172/JCI27167.3306

Bohl, S., Medway, D. J., Schulz-Menger, J., Schneider, J. E., Neubauer, S., and Lygate, C. A. (2009). Refined approach for quantification of in vivo ischemia-reperfusion injury in the mouse heart. *American Journal of Physiology - Heart and Circulatory Physiology*, *297*(6), 2054–2058. https://doi.org/10.1152/ajpheart.00836.2009

Bovet, P., and Paccaud, F. (2011). Cardiovascular Disease and the Changing Face of Global Public Health: A Focus on Low and Middle Income Countries. *Public Health Reviews*, *33*(2), 397–415. https://link.springer.com/content/pdf/10.1007%2FBF03391643.pdf

Brahmachari, G. (2011). Andrographolide: a plant-derived natural molecule of pharmaceutical promise. In G. Brahmachari (Ed.), *Bioactive Natural Products: Opportunities and Challenges in Medicinal Chemistry* (pp. 335–368). World Scientific. https://doi.org/10.1142/9789814335386_0006

Brahmkshatriya, P. P., and Brahmkshatriya, P. S. (2013). Terpenes: Chemistry, Biological

Role, and Therapeutic Applications. In K. Ramawat and J. M. Mérillon (Eds.), *Natural Products* (pp. 2665–2691). Springer. https://doi.org/10.1007/978-3-642-22144-6_120

Breitmaier, E. (2006). Terpenes: Importance, General Structure, and Biosynthesis. In *Terpenes: Flavors, Fragrances, Pharmaca, Pheromones* (pp. 1–9). WILEY-VCH. https://doi.org/10.1002/9783527609949.ch1

Campbell, B. C. V., and Khatri, P. (2020). Stroke. *The Lancet*, *396*(10244), 129–142. https://doi.org/10.1016/S0140-6736(20)31179-X

Carbone, S., Canada, J. M., Billingsley, H. E., Siddiqui, M. S., Elagizi, A., and Lavie, C. J. (2019). Obesity paradox in cardiovascular disease: Where do we stand? *Vascular Health and Risk Management*, *15*, 89–100. https://doi.org/10.2147/VHRM.S168946

Carmena, R., Duriez, P., and Fruchart, J. C. (2004). Atherogenic lipoprotein particles in atherosclerosis. *Circulation*, *109*(23 SUPPL.), 2–7. https://doi.org/10.1161/01.cir.0000131511.50734.44

Carmona, F., and Pereira, A. M. S. (2013). Herbal medicines: Old and new concepts, truths and misunderstandings. *Brazilian Journal of Pharmacognosy*, *23*(2), 379–385. https://doi.org/10.1590/S0102-695X2013005000018

Casas, R., Castro-Barquero, S., Estruch, R., and Sacanella, E. (2018). Nutrition and cardiovascular health. *International Journal of Molecular Sciences*, *19*(12), 1–31. https://doi.org/10.3390/ijms19123988

Chan, S. J., Wong, W. S. F., Wong, P. T. H., and Bian, J. S. (2010). Neuroprotective effects of andrographolide in a rat model of permanent cerebral ischaemia. *British Journal of Pharmacology*, *161*(3), 668–679. https://doi.org/10.1111/j.1476-5381.2010.00906.x

Chao, W. W., and Lin, B. F. (2010). Isolation and identification of bioactive compounds in Andrographis paniculata (Chuanxinlian). *Chinese Medicine*, *5*, 1–15. https://doi.org/10.1186/1749-8546-5-17

Chen, H., Huang, C., Li, C., Lin, A., Huang, Y., Wang, T., Yao, H., and Lii, C. (2014). Bioavailability of andrographolide and protection against carbon tetrachloride-induced oxidative damage in rats. *Toxicology and Applied Pharmacology*, *280*(1), 1–9.

https://doi.org/10.1016/j.taap.2014.07.024

Chen, J. X., Xue, H. J., Ye, W. C., Fang, B. H., Liu, Y. H., Yuan, S. H., Yu, P., and Wang, Y. Q. (2009). Activity of andrographolide and its derivatives against influenza virus in vivo and in vitro. *Biological and Pharmaceutical Bulletin*, *32*(8), 1385–1391. https://doi.org/10.1248/bpb.32.1385

Choi, B. G., Rha, S. W., Park, T., Choi, S. Y., Byun, J. K., Shim, M. S., Xu, S., Li, H., Park, S. H., Park, J. Y., Choi, W. G., Cho, Y. H., Lee, S., Na, J. O., Choi, C. U., Lim, H. E., Kim, J. W., Kim, E. J., Park, C. G., … Oh, D. J. (2016). Impact of cigarette smoking: A 3-Year clinical outcome of vasospastic angina patients. *Korean Circulation Journal*, *46*(5), 632–638. https://doi.org/10.4070/kcj.2016.46.5.632

Conte, S. M., and Vale, P. R. (2018). Peripheral Arterial Disease. *Heart Lung and Circulation*, *27*(4), 427–432. https://doi.org/10.1016/j.hlc.2017.10.014

Costal-Oliveira, F., Guerra-Duarte, C., Oliveira, M. S., Castro, K. L. P. de, Lopes-de-Sousa, L., Lara, A., Gomes, E. R. de M., Bonilla, C., Guatimosim, S., Melo, M. M., and Chávez-Olórtegui, C. (2016). Cardiorespiratory alterations in rodents experimentally envenomed with Hadruroides lunatus scorpion venom. *Journal of Venomous Animals and Toxins Including Tropical Diseases*, *23*(1), 1–9. https://doi.org/10.1186/s40409-016-0076-5

Croteau, R. (1998). The Discovery of Terpenes. In S.-D. Kung and S.-F. Yang (Eds.), *Discoveries in Plant Biology* (Volume 1, pp. 329–343). World Scientific. https://doi.org/10.1142/9789812817563_0020

Cuadrado, I., Fernández-Velasco, M., Boscá, L., and De Las Heras, B. (2011). Labdane diterpenes protect against anoxia/reperfusion injury in cardiomyocytes: Involvement of AKT activation. *Cell Death and Disease*, *2*(11), 1–7. https://doi.org/10.1038/cddis.2011.113

Danese, E., and Montagnana, M. (2016). An historical approach to the diagnostic biomarkers of acute coronary syndrome. *Annals of Translational Medicine*, *4*(10), 194. https://doi.org/10.21037/atm.2016.05.19

de Oliveira, L. F. G., Pereira, B. A. S., Gilbert, B., Corrêa, A. L., Rocha, L., and Alves, C. R. (2017). Natural products and phytotherapy: an innovative perspective in leishmaniasis treatment. *Phytochemistry Reviews*, *16*(2), 219–233. https://doi.org/10.1007/s11101-016-9471-3

Dhawan, V., Bakshi, C., and Rather, R. A. (2019). Molecular Targets and Novel Therapeutics to Target Oxidative Stress in Cardiovascular Diseases. In S. Chakraborti, N. Dhalla, N. Ganguly, and M. Dikshit (Eds.), *Oxidative Stress in Heart Diseases* (pp. 59–82). Springer, Singapore. https://doi.org/10.1007/978-981-13-8273-4_4

Di Gennaro, C., Biggi, A., Barilli, A. L., Fasoli, E., Carra, N., Novarini, A., Delsignore, R., and Montanari, A. (2007). Endothelial dysfunction and cardiovascular risk profile in long-term withdrawing alcoholics. *Journal of Hypertension*, *25*(2), 367–373. https://doi.org/10.1097/HJH.0b013e328010929c

Di Nisio, M., van Es, N., and Büller, H. R. (2016). Deep vein thrombosis and pulmonary embolism. *The Lancet*, *388*(10063), 3060–3073. https://doi.org/10.1016/S0140-6736(16)30514-1

Dieterich, S., Bieligk, U., Beulich, K., Hasenfuss, G., and Prestle, J. (2000). Gene expression of antioxidative enzymes in the human heart: Increased expression of catalase in the end-stage failing heart. *Circulation*, *101*(1), 33–39. https://doi.org/10.1161/01.CIR.101.1.33

Dokken, B. B. (2008). The pathophysiology of cardiovascular disease and diabetes: Beyond blood pressure and lipids. *Diabetes Spectrum*, *21*(3), 160–165. https://doi.org/10.2337/diaspect.21.3.160

Drozd, M., Relton, S., Walker, A. M. N., Slater, T., Gierula, J., Paton, M., Lowry, J., Straw, S., Koshy, A., McGinlay, M., Simms, A., Gatenby, V. K., Sapsford, R., Witte, K., Kearney, M., and Cubbon, R. (2020). Association of heart failure and its comorbidities with loss of life expectancy. *Heart*, 1–5. https://doi.org/10.1101/2020.07.02.20145011

Egri, C., and Ruben, P. C. (2012). Action Potentials: Generation and Propagation. *ELS*, *April*, 1–8. https://doi.org/10.1002/9780470015902.a0000278.pub2

Eisner, D. A., Caldwell, J. L., Kistamás, K., and Trafford, A. W. (2017). Calcium and Excitation-Contraction Coupling in the Heart. *Circulation Research*, *121*(2), 181–195. https://doi.org/10.1161/CIRCRESAHA.117.310230

Ertl, G., and Frantz, S. (2005). Healing after myocardial infarction. *Cardiovascular Research*, *66*(1), 22–32. https://doi.org/10.1016/j.cardiores.2005.01.011

Evans, C. E. (2019). Hypoxia and HIF activation as a possible link between sepsis and thrombosis. *Thrombosis Journal*, *17*(1), 17–20. https://doi.org/10.1186/s12959-019-0205-9

Ferrari, R. (2001). Pathophysiological vs biochemical ischaemia: A key to transition from reversible to irreversible damage. *European Heart Journal, Supplement*, *3*(C), 2–10. https://doi.org/10.1016/S1520-765X(01)90024-0

Filho, H. G. L., Ferreira, N. L., de Sousa, R. B., de Carvalho, E. R., Lobo, P. L. D., and Filho, J. G. L. (2011). Modelo experimental de infarto do miocárdio induzido por isoproterenol em ratos. *Brazilian Journal of Cardiovascular Surgery*, *26*(3), 469–476. https://doi.org/10.5935/1678-9741.20110024

Fishbein, M. C., Maclean, D., and Maroko, P. R. (1978). The Histopathologic Evolution of Myocardial Infarction. *Chest*, *73*(6), 843–849. https://doi.org/10.1378/chest.73.6.843

Frey, N., Katus, H. A., Olson, E. N., and Hill, J. A. (2004). Hypertrophy of the Heart: A New Therapeutic Target? *Circulation*, *109*(13), 1580–1589. https://doi.org/10.1161/01.CIR.0000120390.68287.BB

Friedman, G. D., Klatsky, A. L., and Siegelaub, A. B. (1974). The leukocyte count as a predictor of myocardial infarction. *N. Engl. J. Med*, *290*, 1275–1278.

Gaitas, A., Malhotra, R., Li, T., Herron, T., and Jalife, J. (2015). A device for rapid and quantitative measurement of cardiac myocyte contractility. *Review of Scientific Instruments*, *86*(3), 1–6. https://doi.org/10.1063/1.4915500

Galbraith, L. V., Leung, F. Y., Jablonsky, G., and Henderson, A. R. (1990). Time-related changes in the diagnostic utility of total lactate dehydrogenase, lactate dehydrogenase isoenzyme-1, and two lactate dehydrogenase isoenzyme-1 ratios in serum after

myocardial infarction. *Clinical Chemistry*, *36*(7), 1317–1322. https://doi.org/10.1093/clinchem/36.7.1317

Galson, S. K. (2008). Prevention of Deep Vein Thrombosis and Pulmonary Embolism. *Public Health Reports*, *123*(4), 420–421. https://doi.org/10.1177/003335490812300402

Garcia, F. A. D. O., Tanae, M. M., Torres, L. M. B., Lapa, A. J., De Lima-Landman, M. T. R., and Souccar, C. (2014). A comparative study of two clerodane diterpenes from Baccharis trimera (Less.) DC. on the influx and mobilization of intracellular calcium in rat cardiomyocytes. *Phytomedicine*, *21*(8–9), 1021–1025. https://doi.org/10.1016/j.phymed.2014.04.018

Gavaghan, M. (1999). Biochemical markers in myocardial injury. *AORN Journal*, *70*(5), 840–854. https://doi.org/10.1016/s0001-2092(06)61303-3

Gawaz, M. (2004). Role of platelets in coronary thrombosis and reperfusion of ischemic myocardium. *Cardiovascular Research*, *61*(3), 498–511. https://doi.org/10.1016/j.cardiores.2003.11.036

Gaziano, T. A., Bitton, A., Anand, S., Abrahams-Gessel, S., and Murphy, A. (2010). Growing Epidemic of Coronary Heart Disease in Low- and Middle-Income Countries. *Current Problems in Cardiology*, *35*(2), 72–115. https://doi.org/10.1016/j.cpcardiol.2009.10.002

Genoni, M., Malacrida, R., Maggioni, A., and Moccetti, T. (1996). Kontraindikationen der thrombolytischen Therapie beim akuten Myokardinfarkt [Contraindications of thrombolytic therapy in acute myocardial infarct]. *Z Kardiol*, *85*(6), 397–406.

Gioda, C. R., Barreto, T. D. O., Prímola-Gomes, T. N., De Lima, D. C., Campos, P. P., Capettini, L. D. S. A., Lauton-Santos, S., Vasconcelos, A. C., Coimbra, C. C., Lemos, V. S., Pesquero, J. L., and Cruz, J. S. (2010). Cardiac oxidative stress is involved in heart failure induced by thiamine deprivation in rats. *American Journal of Physiology - Heart and Circulatory Physiology*, *298*(6), 2039–2045. https://doi.org/10.1152/ajpheart.00820.2009

Go, A. S., Mozaffarian, D., Roger, V. L., Benjamin, E. J., Berry, J. D., Blaha, M. J., Dai, S., Ford, E. S., Fox, C. S., Franco, S., Fullerton, H. J., Gillespie, C., Hailpern, S. M., Heit, J. A., Howard, V. J., Huffman, M. D., Judd, S. E., Kissela, B. M., Kittner, S. J., … Turner, M. B. (2014). Heart Disease and Stroke Statistics - 2014 Update: A report from the American Heart Association. *Circulation*, *129*(3), e28–e292. https://doi.org/10.1161/01.cir.0000441139.02102.80

Goldbloom, A. A., and Dumanis, A. A. (1946). Short P-R Interval with Prolongation of QRS Complex And Myocardial Infarction. *Annals of Internal Medicine*, *25*(2), 362–368. https://doi.org/10.7326/0003-4819-25-2-362

Goldman, L., Cook, E. F., Johnson, P. A., Brand, D. A., Rouan, G. W., and Lee, T. H. (1996). Prediction of the need for intensive care in patients who come to emergency departments with acute chest pain. *New England Journal of Medicine*, *334*(23), 1498–1504. https://doi.org/10.1056/NEJM199606063342303

Golomb, B. A., Dang, T. T., and Criqui, M. H. (2006). Peripheral arterial disease: Morbidity and mortality implications. *Circulation*, *114*(7), 688–699. https://doi.org/10.1161/CIRCULATIONAHA.105.593442

Goyal, S. N., Sharma, C., Mahajan, U. B., Patil, C. R., Agrawal, Y. O., Kumari, S., Arya, D. S., and Ojha, S. (2015). Protective effects of cardamom in isoproterenol-induced myocardial infarction in rats. *International Journal of Molecular Sciences*, *16*(11), 27457–27469. https://doi.org/10.3390/ijms161126040

Grant, A. O. (2009). Cardiac ion channels. *Circulation: Arrhythmia and Electrophysiology*, *2*(2), 185–194. https://doi.org/10.1161/CIRCEP.108.789081

Guo, B. Y., Li, Y. J., Han, R., Yang, S. L., Shi, Y. H., Han, D. R., Zhou, H., and Wang, M. (2011). Telmisartan attenuates isoproterenol-induced cardiac remodeling in rats via regulation of cardiac adiponectin expression. *Acta Pharmacologica Sinica*, *32*(4), 449–455. https://doi.org/10.1038/aps.2010.231

Guo, Z., Zhao, H., and Zheng, X. (1995). An Experimental Study of the Mechanism of Andrographis Paniculata Nees (APN) in Alleviating the Ca2 + -overloading in the Process of Myocardial Ischemic Reperfusion. *Journal of Tongji Medical University*,

15(4), 205–208.

Halar, E. M. (1995). Physical Inactivity: A Major Risk Factor for Coronary Heart Disease. *Physical Medicine and Rehabilitation Clinics of North America*, *6*(1), 55–67. https://doi.org/10.1016/S1047-9651(18)30478-9

Hamburg, R. J., Friedman, D. L., and Perryman, M. B. (1991). Metabolic and diagnostic significance of creatine kinase isoenzymes. *Trends in Cardiovascular Medicine*, *1*(5), 195–200. https://doi.org/10.1016/1050-1738(91)90037-F

Handforth, C. P. (1962). Isoproterenol-Induced Myocardial Infarction in Animals. *Arch. Pathol.*, *73*, 161–165.

Hassan, M. Q., Akhtar, M., Ahmed, S., Ahmad, A., and Najmi, A. K. (2017). Nigella sativa protects against isoproterenol-induced myocardial infarction by alleviating oxidative stress, biochemical alterations and histological damage. *Asian Pacific Journal of Tropical Biomedicine*, *7*(4), 294–299. https://doi.org/10.1016/j.apjtb.2016.12.020

Hedayatnia, M., Asadi, Z., Zare-Feyzabadi, R., Yaghooti-Khorasani, M., Ghazizadeh, H., Ghaffarian-Zirak, R., Nosrati-Tirkani, A., Mohammadi-Bajgiran, M., Rohban, M., Sadabadi, F., Rahimi, H. R., Ghalandari, M., Ghaffari, M. S., Yousefi, A., Pouresmaeili, E., Besharatlou, M. R., Moohebati, M., Ferns, G. A., Esmaily, H., and Ghayour-Mobarhan, M. (2020). Dyslipidemia and cardiovascular disease risk among the MASHAD study population. *Lipids in Health and Disease*, *19*(1), 1–11. https://doi.org/10.1186/s12944-020-01204-y

Heinrich, M. (2018). Medicinal Plants. *The International Encyclopedia of Anthropology*, 1–3. https://doi.org/10.1002/9781118924396.wbiea1352

Herrick, J. B. (1912). Clinical Features of Sudden Obstruction of the Coronary Arteries. *The Journal of the American Medical Association*, *LIX*(23), 2015–2022. https://doi.org/10.1001/jama.1912.04270120001001

Hill, R., Howard, A. N., and Gresham, G. A. (1960). The Electrocardiographic Appearances of Myocardial Infarction in the Rat. *British Journal of Experimental Pathology*, *XLI*(6), 633–637.

Hille, B. (2001). *Ion Channels of Excitable Membranes* (Third). Sinauer Associates.

Hinton, R. B., and Yutzey, K. E. (2011). Heart valve structure and function in development and disease. *Annual Review of Physiology*, *73*, 29–46. https://doi.org/10.1146/annurev-physiol-012110-142145

Hjalmarson, Å., Gilpin, E. A., Kjekshus, J., Schieman, G., Nicod, P., Henning, H., and Ross, J. (1990). Influence of heart rate on mortality after acute myocardial infarction. *The American Journal of Cardiology*, *65*(9), 547–553. https://doi.org/10.1016/0002-9149(90)91029-6

Hoffman, B. F., and Cranefield, P. F. (1960). *Electrophysiology of the Heart*. McGraw-Hill Book Company.

Hollenberg, N. K. (2005). The road ahead with β-blockers: Expanding treatment options in cardiovascular disease. *American Journal of Hypertension*, *18*(12 SUPPL.), 163–164. https://doi.org/10.1016/j.amjhyper.2005.09.011

Hossain, M. S., Urbi, Z., Sule, A., and Rahman, K. M. H. (2014). Andrographis paniculata (Burm. f.) Wall. ex Nees: A review of ethnobotany, phytochemistry, and pharmacology. *The Scientific World Journal*, *2014*, 1–28. https://doi.org/10.1155/2014/274905

Ibrahim, A. W., Riddell, T. C., and Devireddy, C. M. (2014). Acute myocardial infarction. *Critical Care Clinics*, *30*(3), 341–364. https://doi.org/10.1016/j.ccc.2014.03.010

Isselbacher, E. M. (2005). Thoracic and abdominal aortic aneurysms. *Circulation*, *111*(6), 816–828. https://doi.org/10.1161/01.CIR.0000154569.08857.7A

Jafri, M. S. (2012). Models of excitation-contraction coupling in cardiac ventricular myocytes. *Methods in Molecular Biology*, *910*, 309–335. https://doi.org/10.1007/978-1-61779-965-5_14

Janero, D. R. (1990). Malondialdehyde and thiobarbituric acid-reactivity as diagnostic indices of lipid peroxidation and peroxidative tissue injury. *Free Radical Biology and Medicine*, *9*(6), 515–540. https://doi.org/10.1016/0891-5849(90)90131-2

Jayakumar, T., Hsieh, C. Y., Lee, J. J., and Sheu, J. R. (2013). Experimental and clinical pharmacology of andrographis paniculata and its major bioactive phytoconstituent andrographolide. *Evidence-Based Complementary and Alternative Medicine*, *2013*, 1–16. https://doi.org/10.1155/2013/846740

Jayaraj, J. C., Davatyan, K., Subramanian, S. S., and Priya, J. (2018). Epidemiology of Myocardial Infarction. In B. Pamukçu (Ed.), *Myocardial Infarction* (pp. 9–19). IntechOpen. https://doi.org/10.5772/intechopen.74768

Jennings, R. B., and Ganote, C. E. (1974). Structural Changes in Myocardium During Acute Ischemia. *Circulation Research*, *34*&*35*(III), 156–172. https://doi.org/10.1161/res.35.3_supplement.iii-156

Jim, M. H., Siu, C. W., Chan, A. O. O., Chan, R. H. W., Lee, S. W. L., and Lau, C. P. (2006). Prognostic implications of PR-segment depression in inferior leads in acute inferior myocardial infarction. *Clinical Cardiology*, *29*(8), 363–368. https://doi.org/10.1002/clc.4960290809

Jin, H. J., and Li, C. G. (2016). Molecular Mechanisms of Cardioprotective Actions of Tanshinones. *Journal of Chemistry*, *2016*, 1–14. https://doi.org/10.1155/2016/9150108

Jockers-Wretou, E., and Pfleiderer, G. (1975). Quantitation of creatine kinase isoenzymes in human tissues and sera by an immunological method. *Clinica Chimica Acta*, *58*(3), 223–232. https://doi.org/10.1016/0009-8981(75)90441-6

Jones, A. W. (2011). Early drug discovery and the rise of pharmaceutical chemistry. *Drug Testing and Analysis*, *3*(6), 337–344. https://doi.org/10.1002/dta.301

Jousilahti, P., Vartiainen, E., Tuomilehto, J., and Puska, P. (1999). Sex, Age, Cardiovascular Risk Factors, and Coronary Heart Disease. *Circulation*, *99*(9), 1165–1172. https://doi.org/10.1161/01.cir.99.9.1165

Kalin, M. F., and Zumoff, B. (1990). Sex hormones and coronary disease: a review of the clinical studies. *Steroids*, *55*(8), 330–352. https://doi.org/10.1016/0039-128X(90)90058-J

Kaprielian, R., Wickenden, A. D., Kassiri, Z., Parker, T. G., Liu, P. P., and Backx, P. H.

(1999). Relationship between K+ channel down-regulation and [Ca2+](i) in rat ventricular myocytes following myocardial infarction. *Journal of Physiology*, *517*(1), 229–245. https://doi.org/10.1111/j.1469-7793.1999.0229z.x

Karahan, Z., Altıntaş, B., Uğurlu, M., Kaya, İ., Uçaman, B., Uluğ, A. V., Altındağ, R., Altaş, Y., Adıyaman, M. Ş., and Öztürk, Ö. (2016). The association between prolongation in QRS duration and presence of coronary collateral circulation in patients with acute myocardial infarction. *JRSM Cardiovascular Disease*, *5*, 1–4. https://doi.org/10.1177/2048004016657475

Karunamoorthi, K., Jegajeevanram, K., Vijayalakshmi, J., and Mengistie, E. (2013). Traditional Medicinal Plants: A Source of Phytotherapeutic Modality in Resource-Constrained Health Care Settings. *Journal of Evidence-Based Complementary and Alternative Medicine*, *18*(1), 67–74. https://doi.org/10.1177/2156587212460241

Katsiari, C. G., Bogdanos, D. P., and Sakkas, L. I. (2019). Inflammation and cardiovascular disease. *World Journal of Translational Medicine*, *8*(1), 1–8. https://doi.org/10.5528/wjtm.v8.i1.1

Kehat, I., and Molkentin, J. D. (2010). Molecular pathways underlying cardiac remodeling during pathophysiological stimulation. *Circulation*, *122*(25), 2727–2735. https://doi.org/10.1161/CIRCULATIONAHA.110.942268

Kemp, M., Donovan, J., Higham, H., and Hooper, J. (2004). Biochemical markers of myocardial injury. *British Journal of Anaesthesia*, *93*(1), 63–73. https://doi.org/10.1093/bja/aeh148

Kjeldsen, S. E. (2018). Hypertension and cardiovascular risk: General aspects. *Pharmacological Research*, *129*, 95–99. https://doi.org/10.1016/j.phrs.2017.11.003

Kleber, A. G. (2005). The shape of the electrical action-potential upstroke: A new aspect from optical measurements on the surface of the heart. *Circulation Research*, *97*(3), 204–206. https://doi.org/10.1161/01.RES.0000177922.62341.f2

Kokubo, Y., and Iwashima, Y. (2015). Higher Blood Pressure as a Risk Factor for Diseases Other Than Stroke and Ischemic Heart Disease. *Hypertension*, *66*(2), 254–259.

https://doi.org/10.1161/HYPERTENSIONAHA.115.03480

Kourkoutas, Y., Chorianopoulos, N., Lazar, V., and Di Ciccio, P. (2018). Bioactive Natural Products 2018. *BioMed Research International*, *2018*, 1–3. https://doi.org/10.1155/2018/5063437

Krause, J., and Tobin, G. (2013). Discovery, Development, and Regulation of Natural Products. In M. Kulka (Ed.), *Using Old Solutions to New Problems - Natural Drug Discovery in the 21st Century* (pp. 3–35). IntechOpen. https://doi.org/10.5772/56424

Kullo, I. J., and Rooke, T. W. (2016). Peripheral Artery Disease. *The New England Journal of Medicine*, *374*(9), 861–871. https://doi.org/10.1056/NEJMcp1507631

Kulyal, P., Tiwari, U. K., Shukla, A., and Gaur, A. K. (2010). Chemical constituents isolated from Andrographis paniculata. *Indian Journal of Chemistry, 49B*, 356–359. https://doi.org/10.1002/chin.201029197

Kumar, M., Kasala, E. R., Bodduluru, L. N., Kumar, V., and Lahkar, M. (2017). Molecular and biochemical evidence on the protective effects of quercetin in isoproterenol-induced acute myocardial injury in rats. *Journal of Biochemical and Molecular Toxicology*, *31*(1), 1–8. https://doi.org/10.1002/jbt.21832

Lawes, C. M., Hoorn, S. Vander, and Rodgers, A. (2008). Global burden of blood-pressure-related disease, 2001. *The Lancet*, *371*(9623), 1513–1518. https://doi.org/10.1016/S0140-6736(08)60655-8

Leon, B. M., and Maddox, T. M. (2015). Diabetes and cardiovascular disease: Epidemiology, biological mechanisms, treatment recommendations and future research. *World Journal of Diabetes*, *6*(13), 1246–1258. https://doi.org/10.4239/wjd.v6.i13.1246

Li, W., Xu, X., Zhang, H., Ma, C., Fong, H., van Breemen, R., and Fitzloff, J. (2007). Secondary Metabolites from Andrographis paniculata. *Chem. Pharm. Bull*, *55*(3), 455–458. https://doi.org/10.1248/cpb.55.455

Liang, E., Liu, X., Du, Z., Yang, R., and Zhao, Y. (2018). Andrographolide Ameliorates Diabetic Cardiomyopathy in Mice by Blockage of Oxidative Damage and NF-κB-

Mediated Inflammation. *Oxidative Medicine and Cellular Longevity*, *2018*, 1–13. https://doi.org/10.1155/2018/9086747

Lomlim, L., Jirayupong, N., and Plubrukarn, A. (2003). Heat-accelerated degradation of solid-state andrographolide. *Chemical and Pharmaceutical Bulletin*, *51*(1), 24–26. https://doi.org/10.1248/cpb.51.24

Lott, J. A., and Abbott, L. B. (1986). Creatine Kinase Isoenzymes. *Clinics in Laboratory Medicine*, *6*(3), 547–576. https://doi.org/10.1016/S0272-2712(18)30800-X

Lowry, O. H., Rosenbrough, H. J., Farra, L., and Randall, R. J. (1951). Protein measurement with folin phenol reagent. *Journal of Biological Chemistry*, *193*(1), 265–275.

Lumen Learning. (2021). *The cardiovascular system*. Anatomy and Physiology. https://courses.lumenlearning.com/nemcc-ap/chapter/heart-anatomy/

Lüscher, T. F. (2018). Inflammation: The new cardiovascular risk factor. *European Heart Journal*, *39*(38), 3483–3487. https://doi.org/10.1093/eurheartj/ehy607

Marijon, E., Mirabel, M., Celermajer, D. S., and Jouven, X. (2012). Rheumatic heart disease. *The Lancet*, *379*(9819), 953–964. https://doi.org/10.1016/S0140-6736(11)61171-9

Mc Namara, K., Alzubaidi, H., and Jackson, J. K. (2019). Cardiovascular disease as a leading cause of death: how are pharmacists getting involved? *Integrated Pharmacy Research and Practice*, *8*, 1–11. https://doi.org/10.2147/iprp.s133088

McKay, R. G., Pfeffer, M. A., Pasternak, R. C., Markis, J. E., Come, P. C., Nakao, S., Alderman, J. D., Ferguson, J. J., Safian, R. D., and Grossman, W. (1986). Left ventricular remodeling after myocardial infarction: A corollary to infarct expansion. *Circulation*, *74*(4), 693–702. https://doi.org/10.1161/01.CIR.74.4.693

mdmedicine. (2011). *Heart Conduction System*. Medical Education for Undergraduate MD Students. https://mdmedicine.wordpress.com/2011/04/24/heart-conduction-system/

Mesotten, L., Maes, A., Hambÿe, A. S., Everaert, H., Van Den Maegdenbergh, V., Franken,

P., and Mortelmans, L. (1998). Nuclear cardiology, Part I: Anatomy and function of the normal heart. *Journal of Nuclear Medicine Technology*, *26*(1), 4–8.

Miller, M. (2009). Dyslipidemia and cardiovascular risk: The importance of early prevention. *Qjm*, *102*(9), 657–667. https://doi.org/10.1093/qjmed/hcp065

Mishra, S. K., Sangwan, N. S., and Sangwan, R. S. (2007). Andrographis paniculata (Kalmegh): A Review. *Pharmacognosy Reviews*, *1*(2), 283–298.

Molnar, C., and Gair, J. (2015). *Mammalian Heart and Blood Vessels*. Concepts of Biology - 1st Canadian Edition. https://opentextbc.ca/biology/chapter/21-3-mammalian-heart-and-blood-vessels/

Monteiro, A. S. E. N., Campos, D. R., Albuquerque, A. A. S., Evora, P. R. B., Ferreira, L. G., and Celotto, A. C. (2020). Effect of diterpene manool on the arterial blood pressure and vascular reactivity in normotensive and hypertensive rats. *Arquivos Brasileiros de Cardiologia*, *115*(4), 669–677. https://doi.org/10.36660/abc.20190198

Morand, J., Arnaud, C., Pepin, J. L., and Godin-Ribuot, Di. (2018). Chronic intermittent hypoxia promotes myocardial ischemia-related ventricular arrhythmias and sudden cardiac death. *Scientific Reports*, *8*(1), 1–8. https://doi.org/10.1038/s41598-018-21064-y

Mythili, S., and Malathi, N. (2015). Diagnostic markers of acute myocardial infarction. *Biomedical Reports*, *3*(6), 743–748. https://doi.org/10.3892/br.2015.500

Nachlas, M. M., and Shnitka, T. K. (1963). Macroscopic identification of early myocardial infarcts by alterations in dehydrogenase activity. *The American Journal of Pathology*, *42*(4), 379–405.

Nejatbakhsh, N., and Feng, Z. P. (2011). Calcium binding protein-mediated regulation of voltage-gated calcium channels linked to human diseases. *Acta Pharmacologica Sinica*, *32*(6), 741–748. https://doi.org/10.1038/aps.2011.64

Nelson, D. P., and Kiesow, L. A. (1972). Enthalpy of decomposition of hydrogen peroxide by catalase at 25° C (with molar extinction coefficients of H2O2 solutions in the UV). *Analytical Biochemistry*, *49*(2), 474–478. https://doi.org/10.1016/0003-

2697(72)90451-4

Nepper-Christensen, L., Lønborg, J., Ahtarovski, K. A., Høfsten, D. E., Kyhl, K., Ghotbi, A. A., Schoos, M. M., Göransson, C., Bertelsen, L., Køber, L., Helqvist, S., Pedersen, F., Saünamaki, K., Jørgensen, E., Kelbæk, H., Holmvang, L., Vejlstrup, N., and Engstrøm, T. (2017). Left ventricular hypertrophy is associated with increased infarct size and decreased myocardial salvage in patients with ST-segment elevation myocardial infarction undergoing primary percutaneous coronary intervention. *Journal of the American Heart Association*, *6*(1), 1–10. https://doi.org/10.1161/JAHA.116.004823

Nerbonne, J. M., and Kass, R. S. (2005). Molecular physiology of cardiac repolarization. *Physiological Reviews*, *85*(4), 1205–1253. https://doi.org/10.1152/physrev.00002.2005

Nishimura, R. A. (2002). Aortic valve disease. *Circulation*, *106*(7), 770–772. https://doi.org/10.1161/01.CIR.0000027621.26167.5E

Ohkawa, H., Ohishi, N., and Yagi, K. (1979). Assay for lipid peroxides in animal tissues by thiobarbituric acid reaction. *Analytical Biochemistry*, *95*(2), 351–358. https://doi.org/10.1016/0003-2697(79)90738-3

Ojha, S. K., Bharti, S., Joshi, S., Kumari, S., and Arya, D. S. (2012). Protective effect of hydroalcoholic extract of Andrographis paniculata on ischaemia-reperfusion induced myocardialinjury in rats. *Indian Journal of Medical Research*, *135*(3), 414–421.

Okhuarobo, A., Ehizogie Falodun, J., Erharuyi, O., Imieje, V., Falodun, A., and Langer, P. (2014). Harnessing the medicinal properties of Andrographis paniculata for diseases and beyond: A review of its phytochemistry and pharmacology. *Asian Pacific Journal of Tropical Disease*, *4*(3), 213–222. https://doi.org/10.1016/S2222-1808(14)60509-0

Olas, B., and Bryś, M. (2018). Is it safe to use Acorus calamus as a source of promising bioactive compounds in prevention and treatment of cardiovascular diseases? *Chemico-Biological Interactions*, *281*(May 2017), 32–36. https://doi.org/10.1016/j.cbi.2017.12.026

Paglia, D. E., and Valentine, W. N. (1967). Studies on the quantitative and qualitative

characterization of erythrocyte glutathione peroxidase. *Journal of Laboratory and Clinical Medicine*, *70*(1), 158–169.

Paloheimo, J. A., and Pitkänen, E. (1964). Elevated lactic dehydrogenase (LDH) activity and the lactic dehydrogenase isoenzyme pattern of serum. *Annales Medicinae Internae Fenniae*, *54*(3), 129–136.

Panda, S., Kar, A., and Biswas, S. (2017). Preventive effect of Agnucastoside C against Isoproterenol-induced myocardial injury. *Scientific Reports*, *7*(1), 1–14. https://doi.org/10.1038/s41598-017-16075-0

Panossian, A., Hovhannisyan, A., Mamikonyan, G., Abrahamian, H., Hambardzumyan, E., Cabrielianl, E., Goukasova, G., Wikman, G., and Wagner, H. (2000). Pharmacokinetic and oral bioavailability of andrographolide from Andrographis paniculata fixed combination Kan Jang in rats and human. *Phytomedicine*, *7*(5), 351–364. https://doi.org/10.1016/S0944-7113(00)80054-9

Passinho, R. S., Sipolatti, W. G. R., Fioresi, M., and Primo, C. C. (2018). Signs , Symptoms and Complications of Acute Myocardial Infarction. *J Nurs UFPE on Line*, *12*(1), 247–264. https://doi.org/10.5205/1981-8963-v12i01a22664p247-264-2018

Pepine, C. J. (1989). New Concepts in the Pathophysiology of Acute Myocardial Infarction. *Am J Cardiol*, *64*(4), 2B-8B. https://doi.org/10.1016/S0002-9149(89)80002-5

Petrovska, B. B. (2012). Historical review of medicinal plants' usage. *Pharmacognosy Reviews*, *6*(11), 1–5. https://doi.org/10.4103/0973-7847.95849

Pham, J. V., Yilma, M. A., Feliz, A., Majid, M. T., Maffetone, N., Walker, J. R., Kim, E., Cho, H. J., Reynolds, J. M., Song, M. C., Park, S. R., and Yoon, Y. J. (2019). A review of the microbial production of bioactive natural products and biologics. *Frontiers in Microbiology*, *10*, 1–27. https://doi.org/10.3389/fmicb.2019.01404

Pholphana, N., Panomvana, D., Rangkadilok, N., Suriyo, T., Puranajoti, P., Ungtrakul, T., Pongpun, W., Thaeopattha, S., Songvut, P., and Satayavivad, J. (2016). Andrographis paniculata: Dissolution investigation and pharmacokinetic studies of four major active diterpenoids after multiple oral dose administration in healthy Thai volunteers.

Journal of Ethnopharmacology, *194*, 513–521. https://doi.org/10.1016/j.jep.2016.09.058

Piano, M. R. (2017). Alcohol's Effects on the Cardiovascular System. *Alcohol Research : Current Reviews*, *38*(2), 219–241.

Piazzesi, G., and Lombardi, V. (1996). Simulation of the rapid regeneration of the actin-myosin working stroke with a tight coupling model of muscle contraction. *Journal of Muscle Research and Cell Motility*, *17*(1), 45–53. https://doi.org/10.1007/BF00140323

Pilote, L. (2014). Chest pain in acute myocardial infarction : Are men from mars andwomen from venus? *JAMA Internal Medicine*, *174*(2), 249–250. https://doi.org/10.1001/jamainternmed.2013.12097

Poirier, P., Giles, T. D., Bray, G. A., Hong, Y., Stern, J. S., Pi-Sunyer, F. X., and Eckel, R. H. (2006). Obesity and cardiovascular disease: Pathophysiology, evaluation, and effect of weight loss: An update of the 1997 American Heart Association Scientific Statement on obesity and heart disease from the Obesity Committee of the Council on Nutrition, Physical. *Circulation*, *113*(6), 898–918. https://doi.org/10.1161/CIRCULATIONAHA.106.171016

Ponikowski, P., Voors, A. A., Anker, S. D., Bueno, H., Cleland, J. G. F., Coats, A. J. S., Falk, V., Gonzalez-Juanatey, J. R., Harjola, V.-P., Jankowska, E. A., Jessup, M., Linde, C., Nihoyannopoulos, P., Parissis, J. T., Pieske, B., Riley, J. P., Rosano, G. M. C., Ruilope, L. M., Ruschitzka, F., … Meer, P. van der. (2017). 2016 Esc guidelines for the diagnosis and treatment of acute and chronic heart failure. *Russian Journal of Cardiology*, *141*(1), 7–81. https://doi.org/10.15829/1560-4071-2017-1-7-81

Qin, D., Zhang, Z. H., Caref, E. B., Boutjdir, M., Jain, P., and El-Sherif, N. (1996). Cellular and ionic basis of arrhythmias in postinfarction remodeled ventricular myocardium. *Circulation Research*, *79*(3), 461–473. https://doi.org/10.1161/01.RES.79.3.461

Rajagopal, S., Kumar, R. A., Deevi, D. S., Satyanarayana, C., and Rajagopalan, R. (2003). Andrographolide, a potential cancer therapeutic agent isolated from Andrographis paniculata. *Journal of Experimental Therapeutics and Oncology*, *3*(3), 147–158. https://doi.org/10.1046/j.1359-4117.2003.01090.x

Rajani, M., Shrivastava, N., and Ravishankara, M. N. (2000). A rapid method for isolation of andrographolide from Andrographis paniculata Nees (Kalmegh). *Pharmaceutical Biology*, *38*(3), 204–209. https://doi.org/10.1076/1388-0209(200007)3831-SFT204

Rao, Y. K., Vimalamma, G., Rao, C. V., and Tzeng, Y.-M. (2004). Flavonoids and andrographolides from Andrographis paniculata. *Phytochemistry*, *65*(16), 2317–2321. https://doi.org/10.1016/j.phytochem.2004.05.008

Roger, V. L. (2007). Epidemiology of Myocardial Infarction. *Medical Clinics of North America*, *91*(4), 537–552. https://doi.org/10.1016/j.mcna.2007.03.007

Roman-Campos, D., Duarte, H. L. L., Sales, P. A., Natali, A. J., Ropert, C., Gazzinelli, R. T., and Cruz, J. S. (2009). Changes in cellular contractility and cytokines profile during Trypanosoma cruzi infection in mice. *Basic Research in Cardiology*, *104*(3), 238–246. https://doi.org/10.1007/s00395-009-0776-x

Rona, G., Chappel, C. I., Balazs, T., and Gaudry, R. (1959). An infarct-like myocardial lesion and other toxic manifestations produced by isoproterenol in the rat. *Arch. Pathol.*, *67*(4), 443–455.

Rona, G., Chappel, C. I., and Kahn, D. S. (1963). The significance of factors modifying the development of isoproterenol-induced myocardial necrosis. *American Heart Journal*, *66*(3), 389–395. https://doi.org/10.1016/0002-8703(63)90271-0

Roth, G. A., Abate, D., Abate, K. H., Abay, S. M., Abbafati, C., Abbasi, N., Abbastabar, H., Abd-Allah, F., Abdela, J., Abdelalim, A., Abdollahpour, I., Abdulkader, R. S., Abebe, H. T., Abebe, M., Abebe, Z., Abejie, A. N., Abera, S. F., Abil, O. Z., Abraha, H. N., … Murray, C. J. L. (2018). Global, regional, and national age-sex-specific mortality for 282 causes of death in 195 countries and territories, 1980–2017: a systematic analysis for the Global Burden of Disease Study 2017. *The Lancet*, *392*(10159), 1736–1788. https://doi.org/10.1016/S0140-6736(18)32203-7

Roy, P., Das, S., Auddy, R. G., and Mukherjee, A. (2014). Engineered andrographolide nanosystems for smart recovery in hepatotoxic conditions. *International Journal of Nanomedicine*, *2014*(9), 4723–4735. https://doi.org/10.2147/IJN.S65262

Rozanski, G. J., Xu, Z., Zhang, K., and Patel, K. P. (1998). Altered K+ current of ventricular myocytes in rats with chronic myocardial infarction. *American Journal of Physiology - Heart and Circulatory Physiology*, *274*(H), 259–265. https://doi.org/10.1152/ajpheart.1998.274.1.h259

Russell, R. P. (1988). Side effects of calcium channel blockers. *Hypertension*, *11*(3), II.42-II.44.

Sabatine, M. S., Morrow, D. A., Cannon, C. P., Murphy, S. A., Demopoulos, L. A., DiBattiste, P. M., McCabe, C. H., Braunwald, E., and Gibson, C. M. (2002). Relationship between baseline white blood cell count and degree of coronary artery disease and mortality in patients with acute coronary syndromes: A TACTICS-TIMI 18 substudy. *Journal of the American College of Cardiology*, *40*(10), 1761–1768. https://doi.org/10.1016/S0735-1097(02)02484-1

Sacco, R. L., Kasner, S. E., Broderick, J. P., Caplan, L. R., Connors, J. J., Culebras, A., Elkind, M. S. V., George, M. G., Hamdan, A. D., Higashida, R. T., Hoh, B. L., Janis, L. S., Kase, C. S., Kleindorfer, D. O., Lee, J. M., Moseley, M. E., Peterson, E. D., Turan, T. N., Valderrama, A. L., and Vinters, H. V. (2013). An updated definition of stroke for the 21st century: A statement for healthcare professionals from the American heart association/American stroke association. *Stroke*, *44*(7), 2064–2089. https://doi.org/10.1161/STR.0b013e318296aeca

Sadasivam, K. (2016). *Structure cardiac muscle cell*. Cardiac Muscle Physiology. https://www.slideshare.net/KanimozhiSadasivam/cardiac-muscle-physiology-68104251

Sah, D. K., and Nagarathana, P. K. M. (2016). Screening of cardioprotective activity of leaves of Andrographis paniculata against isoproterenol induced myocardial infarction in rats. *International Journal of Pharmacological Research*, *6*(1), 23–28. https://doi.org/10.7439/ijpr

Sairazi, N. S. M., and Sirajudeen, K. N. S. (2020). Natural Products and Their Bioactive Compounds: Neuroprotective Potentials against Neurodegenerative Diseases. *Evidence-Based Complementary and Alternative Medicine*, *2020*, 5–7.

https://doi.org/10.1155/2020/6565396

Samak, M., Fatullayev, J., Sabashnikov, A., Zeriouh, M., Schmack, B., Farag, M., Popov, A. F., Dohmen, P. M., Choi, Y. H., Wahlers, T., and Weymann, A. (2016). Cardiac Hypertrophy: An Introduction to Molecular and Cellular Basis. *Medical Science Monitor Basic Research*, *22*, 75–79. https://doi.org/10.12659/MSMBR.900437

Sampson, M., and McGrath, A. (2015). Understanding the ECG. Part 1: Anatomy and physiology. *British Journal of Cardiac Nursing*, *10*(11), 548–554. https://doi.org/10.12968/bjca.2015.10.11.548

Saroff, J., and Wexler, B. C. (1970). Isoproterenol-Induced Myocardial Infarction in Rats. *Circulation Research*, *27*(6), 1101–1109. https://doi.org/10.1161/01.res.27.6.1101

Satin, J., and Schroder, E. A. (2009). Autoregulation of Cardiac L-type calcium channels. *Trends in Cardiovascular Medicine*, *19*(8), 268–271. https://doi.org/10.1016/j.tcm.2010.02.009

Schwarzwald, C. C., Bonagura, J. D., and Muir, W. W. (2009). The Cardiovascular System. In *Equine Anesthesia* (Second, pp. 37–100). Elsevier Inc. https://doi.org/10.1016/B978-1-4160-2326-5.00003-1

Sharma, V. (2019). Congenital Heart Defects. *Insights in Biomedicine*, *4*(1:5), 1–2. https://doi.org/10.36648/2572-5610.4.1.56

Shioya, T. (2007). A simple technique for isolating healthy heart cells from mouse models. *Journal of Physiological Sciences*, *57*(6), 327–335. https://doi.org/10.2170/physiolsci.RP010107

Siddiqui, M. A., Ahmad, U., Khan, A. A., Ahmad, M., Badruddeen, Khalid, M., and Akhtar, J. (2016). Isoprenaline: a Tool for Inducing Myocardial Infarction in Experimental Animals. *International Journal of Pharmacy*, *6*(2), 138–144.

Sika-Paotonu, D., Beaton, A., Raghu, A., Steer, A., and Carapetis, J. (2017). Acute Rheumatic Fever and Rheumatic Heart Disease. In J. J. Ferretti, D. L. Stevens, and V. A. Fischetti (Eds.), *Streptococcus pyogenes : Basic Biology to Clinical Manifestations [Internet]* (pp. 771–826). University of Oklahoma Health Sciences Center.

https://www.ncbi.nlm.nih.gov/books/NBK425394/

Singh, B. N. (2003). Increased heart rate as a risk factor for cardiovascular disease. *European Heart Journal Supplements*, *5*(G), G3–G9. https://doi.org/10.1016/S1520-765X(03)90001-0

Snider, P., and Conway, S. J. (2011). Probing human cardiovascular congenital disease using transgenic mouse models. In *Progress in Molecular Biology and Translational Science* (1st ed., Vol. 100). Elsevier Inc. https://doi.org/10.1016/B978-0-12-384878-9.00003-0

Stevens, B., Pezzullo, L., Verdian, L., Tomlinson, J., George, A., and Bacal, F. (2018). The economic burden of heart conditions in Brazil. *Arquivos Brasileiros de Cardiologia*, *111*(1), 29–36. https://doi.org/10.5935/abc.20180104

Teo, K. K., Ounpuu, S., Hawken, S., Pandey, M. R., Valentin, V., Hunt, D., Diaz, R., Rashed, W., Freeman, R., Jiang, L., Zhang, X., and Yusuf, S. (2006). Tobacco use and risk of myocardial infarction in 52 countries in the INTERHEART study: a case-control study. *The Lancet*, *368*, 647–658.

Thygesen, K., Alpert, J. S., Jaffe, A. S., Chaitman, B. R., Bax, J. J., Morrow, D. A., White, H. D., Mickley, H., Crea, F., Van De Werf, F., Bucciarelli-Ducci, C., Katus, H. A., Pinto, F. J., Antman, E. M., Hamm, C. W., De Caterina, R., Januzzi, J. L., Apple, F. S., Garcia, M. A. A., … Windecker, S. (2019). Fourth universal definition of myocardial infarction (2018). *European Heart Journal*, *40*(3), 237–269. https://doi.org/10.1093/eurheartj/ehy462

Thygesen, K., Alpert, J. S., Jaffe, A. S., Simoons, M. L., Chaitman, B. R., and White, H. D. (2012a). Third universal definition of myocardial infarction. *Journal of the American College of Cardiology*, *60*(16), 1581–1598. https://doi.org/10.1016/j.jacc.2012.08.001

Thygesen, K., Alpert, J. S., Jaffe, A. S., Simoons, M. L., Chaitman, B. R., and White, H. D. (2012b). Third universal definition of myocardial infarction. *Nature Reviews Cardiology*, *9*(11), 620–633. https://doi.org/10.1038/nrcardio.2012.122

Thygesen, K., Alpert, J. S., and White, H. D. (2007). Universal definition of myocardial

infarction. *Circulation*, *116*(22), 2634–2653. https://doi.org/10.1161/CIRCULATIONAHA.107.187397

Timmis, A., Townsend, N., Gale, C. P., Torbica, A., Lettino, M., Petersen, S. E., Mossialos, E. A., Maggioni, A. P., Kazakiewicz, D., May, H. T., De Smedt, D., Flather, M., Zuhlke, L., Beltrame, J. F., Huculeci, R., Tavazzi, L., Hindricks, G., Bax, J., Casadei, B., … Bardinet, I. (2020). European society of cardiology: Cardiovascular disease statistics 2019. *European Heart Journal*, *41*(1), 12–85. https://doi.org/10.1093/eurheartj/ehz859

Tirapelli, C. R., Ambrosio, S. R., da Costa, F. B., and de Oliveira, A. M. (2008). Diterpenes: A therapeutic promise for cardiovascular diseases. *Recent Patents on Cardiovascular Drug Discovery*, *3*(1), 1–8. https://doi.org/10.2174/157489008783331689

Torpy, J. M., Lynm, C., and Glass, R. M. (2008). Myocardial infarction. *Journal of the American Medical Association*, *299*(4), 476. https://doi.org/10.1001/jama.299.4.476

Tran, D. B., Weber, C., and Lopez, R. A. (2020). Anatomy, Thorax, Heart Muscles. In *StatPearls [Internet]* (p. 1). StatPearls Publishing.

Trivedi, N. P., Rawal, U. M., and Patel, B. P. (2007). Hepatoprotective effect of andrographolide against hexachlorocyclohexane- induced oxidative injury. *Integrative Cancer Therapies*, *6*(3), 271–280. https://doi.org/10.1177/1534735407305985

Ueland, K. (1985). Rheumatic Heart Disease. In N. Gleicher (Ed.), *Principles of Medical Therapy in Pregnancy* (pp. 660–665). Springer. https://doi.org/10.1007/978-1-4613-2415-7_104

Van Neste, E. G., Verbruggen, W., and Leysen, M. (2009). Deep venous thrombosis and pulmonary embolism in psychiatric settings. *European Journal of Psychiatry*, *23*(1), 19–30. https://doi.org/10.4321/S0213-61632009000100002

Van Oeffelen, A. A. M., Vaartjes, I., Stronks, K., Bots, M. L., and Agyemang, C. (2015). Sex disparities in acute myocardial infarction incidence: Do ethnic minority groups differ from the majority population? *European Journal of Preventive Cardiology*,

22(2), 180–188. https://doi.org/10.1177/2047487313503618

Vargas, G., Akhtar, M., and Damato, A. N. (1975). Electrophysiologic effects of isoproterenol on cardiac conduction system in man. *American Heart Journal*, *90*(1), 25–34. https://doi.org/10.1016/0002-8703(75)90253-7

Varma, A., Padh, H., and Shrivastava, N. (2011). Andrographolide: A new plant-derived antineoplastic entity on horizon. *Evidence-Based Complementary and Alternative Medicine*, *2011*, 1–9. https://doi.org/10.1093/ecam/nep135

Velu, G., Palanichamy, V., and Rajan, A. P. (2018). Phytochemical and Pharmacological Importance of Plant Secondary Metabolites in Modern Medicine. In S. M. Roopan and G. Madhumitha (Eds.), *Bioorganic Phase in Natural Food: An Overview* (pp. 135–156). Springer International Publishing. https://doi.org/10.1007/978-3-319-74210-6_8

Virani, S. S., Alonso, A., Benjamin, E. J., Bittencourt, M. S., Callaway, C. W., Carson, A. P., Chamberlain, A. M., Chang, A. R., Cheng, S., Delling, F. N., Djousse, L., Elkind, M. S. V., Ferguson, J. F., Fornage, M., Khan, S. S., Kissela, B. M., Knutson, K. L., Kwan, T. W., Lackland, D. T., … Heard, D. G. (2020). Heart disease and stroke statistics—2020 update: A report from the American Heart Association. *Circulation*, E139–E596. https://doi.org/10.1161/CIR.0000000000000757

Virmani, R., Forman, M. B., and Kolodgie, F. D. (1990). Myocardial reperfusion injury. Histopathological effects of perfluorochemical. *Circulation*, *81*(3 Suppl), IV57-68.

Walker, C. A., and Spinale, F. G. (1999). The structure and function of the cardiac myocyte: A review of fundamental concepts. *Journal of Thoracic and Cardiovascular Surgery*, *118*(2), 375–382. https://doi.org/10.1016/S0022-5223(99)70233-3

Wang, S. C., Meng, D., Yang, H., Wang, X., Jia, S., Wang, P., and Wang, Y.-F. (2018). Pathological basis of cardiac arrhythmias: vicious cycle of immune-metabolic dysregulation. *Cardiovascular Disorders and Medicine*, *3*(1), 1–7. https://doi.org/10.15761/cdm.1000158

Wang, W., Wang, J., Dong, S. F., Liu, C. H., Italiani, P., Sun, S. H., Xu, J., Boraschi, D., Ma, S. P., and Qu, D. (2010). Immunomodulatory activity of andrographolide on

macrophage activation and specific antibody response. *Acta Pharmacologica Sinica*, *31*(2), 191–201. https://doi.org/10.1038/aps.2009.205

Wang, Y., Xu, Y., Guth, K., and Kerrick, W. G. L. (1999). Troponin C regulates the rate constant for the dissociation of force-generating myosin cross-bridges in cardiac muscle. *Journal of Muscle Research and Cell Motility*, *20*(7), 645–653. https://doi.org/10.1023/A:1005559613516

Weidmann, S. (1955). The effect of the cardiac membrane potential on the rapid availability of the sodium-carrying system. *The Journal of Physiology*, *127*(1), 213–224. https://doi.org/10.1113/jphysiol.1955.sp005250

Weinhaus, A. J., and Roberts, K. P. (2009). Anatomy of the human heart. In P. A. Iaizzo (Ed.), *Handbook of Cardiac Anatomy, Physiology, and Devices* (Third, pp. 51–79). Humana Press. https://doi.org/10.1007/978-1-60327-372-5

Wilkins, E., Wilson, L., Wickramasinghe, K., and Bhatnagar, P. (2017). European Cardiovascular Disease Statistics 2017. *European Heart Network*, 94–100. www.ehnheart.org

Wilson, P. W. F., D'Agostino, R. B., Sullivan, L., Parise, H., and Kannel, W. B. (2002). Overweight and obesity as determinants of cardiovascular risk: The Framingham experience. *Archives of Internal Medicine*, *162*(16), 1867–1872. https://doi.org/10.1001/archinte.162.16.1867

Wintachai, P., Kaur, P., Lee, R. C. H., Ramphan, S., Kuadkitkan, A., Wikan, N., Ubol, S., Roytrakul, S., Chu, J. J. H., and Smith, D. R. (2015). Activity of andrographolide against chikungunya virus infection. *Scientific Reports*, *5*, 1–14. https://doi.org/10.1038/srep14179

Woo, A. Y. H., Waye, M. M. Y., Tsui, S. K. W., Yeung, S. T. W., and Cheng, C. H. K. (2008). Andrographolide up-regulates cellular-reduced glutathione level and protects cardiomyocytes against hypoxia/reoxygenation injury. *Journal of Pharmacology and Experimental Therapeutics*, *325*(1), 226–235. https://doi.org/10.1124/jpet.107.133918

Woodcock, E. A., and Matkovich, S. J. (2005). Cardiomyocytes structure, function and

associated pathologies. *International Journal of Biochemistry and Cell Biology*, *37*(9), 1746–1751. https://doi.org/10.1016/j.biocel.2005.04.011

World Health Organization. (2011). From Burden to " Best Buys ": Reducing the Economic Impact of Non-Communicable Diseases in Low- and Middle-Income Countries. *World Economic Forum*, 1–12.

Wu, Q. Q., Ni, J., Zhang, N., Liao, H. H., Tang, Q. Z., and Deng, W. (2017). Andrographolide protects against aortic banding-induced experimental cardiac hypertrophy by inhibiting MAPKs Signaling. *Frontiers in Pharmacology*, *8*(NOV), 1–17. https://doi.org/10.3389/fphar.2017.00808

Xie, S., Deng, W., Chen, J., Wu, Q. Q., Li, H., Wang, J., Wei, L., Liu, C., Duan, M., Cai, Z., Xie, Q., Hu, T., Zeng, X., and Tang, Q. (2020). Andrographolide protects against adverse cardiac remodeling after myocardial infarction through enhancing Nrf2 signaling pathway. *International Journal of Biological Sciences*, *16*(1), 12–26. https://doi.org/10.7150/ijbs.37269

Ye, J. F., Zhu, H., Zhou, Z. F., Xiong, R. B., Wang, X. W., Su, L. X., and Luo, B. De. (2011). Protective mechanism of andrographolide against carbon tetrachloride-induced acute liver injury in mice. *Biological and Pharmaceutical Bulletin*, *34*(11), 1666–1670. https://doi.org/10.1248/bpb.34.1666

Yin, F. C. P., Spurgeon, H. A., and Rakusan, K. (1982). Use of tibial length to quantify cardiac hypertrophy: Application in the aging rat. *American Journal of Physiology - Heart and Circulatory Physiology*, *12*(6), H941–H947. https://doi.org/10.1152/ajpheart.1982.243.6.h941

Yokoi, T., Yoshimura, Y., Nozaki, K., Saito, M., and Tsuji, K. (2015). Cerebral aneurysms and inflammation. *Neuroimmunology and Neuroinflammation*, *2*(2), 55. https://doi.org/10.4103/2347-8659.153977

Yu, B., Hung, C., Chen, W., and Cheng, J. (2003). Antihyperglycemic Effect of Andrographolide in Streptozotocin-Induced Diabetic Rats. *Planta Medica*, *69*(12), 1075–1079. https://doi.org/10.1055/s-2003-45185

Yuyun, M. F., Sliwa, K., Kengne, A. P., Mocumbi, A. O., and Bukhman, G. (2020). Cardiovascular Diseases in Sub-Saharan Africa Compared to High-Income Countries: An Epidemiological Perspective. *Global Heart*, *15*(1), 15. https://doi.org/10.5334/gh.403

Zähner, H. (1979). What are secondary metabolites? *Folia Microbiol*, *24*, 435–443. https://doi.org/10.1007/BF02927127

Zakynthinos, E., and Pappa, N. (2009). Inflammatory biomarkers in coronary artery disease. *Journal of Cardiology*, *53*(3), 317–333. https://doi.org/10.1016/j.jjcc.2008.12.007

Zamorano, J., Lancellotti, P., Pierard, L., and Pibarot, P. (2020). *Heart Valve Disease: State of the Art*. Springer, Cham. https://doi.org/10.1007/978-3-030-23104-0

Zeng, M., Jiang, W., Tian, Y., Hao, J., Cao, Z., Liu, Z., Fu, C., Zhang, P., and Ma, J. (2017). Andrographolide inhibits arrhythmias and is cardioprotective in rabbits. *Oncotarget*, *8*(37), 61226–61238. https://doi.org/10.18632/oncotarget.18051

Zhang, C. Y., and Tan, B. (1996). Hypotensive activity of aqueous extract of Andrographis paniculata in rats. *Clinical and Experimental Pharmacology and Physiology*, *23*(8), 675–678. https://doi.org/10.1111/j.1440-1681.1996.tb01756.x

Zhang, C. Y., and Tan, B. K. H. (1997). Mechanisms of cardiovascular activity of Andrographis paniculata in the anaesthetized rat. *Journal of Ethnopharmacology*, *56*(2), 97–101. https://doi.org/10.1016/S0378-8741(97)01509-2

Zhang, H., Chen, X., Gao, E., MacDonnell, S. M., Wang, W., Kolpakov, M., Nakayama, H., Zhang, X., Jaleel, N., Harris, D. M., Li, Y., Tang, M., Berretta, R., Leri, A., Kajstura, J., Sabri, A., Koch, W. J., Molkentin, J. D., and Houser, S. R. (2010). Increasing cardiac contractility after myocardial infarction exacerbates cardiac injury and pump dysfunction. *Circulation Research*, *107*(6), 800–809. https://doi.org/10.1161/CIRCRESAHA.110.219220

Zhang, Q., Hu, L. qun, Li, H. qi, Wu, J., Na-Na-Bian, and Yan, G. (2019). Beneficial effects of andrographolide in a rat model of autoimmune myocarditis and its effects on

PI3K/Akt pathway. *Korean Journal of Physiology and Pharmacology*, *23*(2), 103–111. https://doi.org/10.4196/kjpp.2019.23.2.103

Zhi-Tao, Z., Xue-Song, J., Bai-Chun, W., Wei-Xin, M., Hong-Yu, L., and Ye, T. (2011). Andrographolide Inhibits Intimal Hyperplasia in a Rat Model of Autogenous Vein Grafts. *Cell Biochemistry and Biophysics*, *60*(3), 231–239. https://doi.org/10.1007/s12013-010-9144-6